University of Alberta

TWO MODELS FOR INDIRECTLY TRANSMITTED DISEASES: CHOLERA

by

William Davis

A thesis submitted to the Faculty of Graduate Studies and Research
in partial fulfillment of the requirements for the degree of

Master of Science

in

Applied Mathematics

Department of Mathematical and Statistical Sciences

© William Davis
Fall 2012
Edmonton, Alberta

Permission is hereby granted to the University of Alberta Libraries to reproduce single copies of this thesis and to lend or sell such copies for private, scholarly, or scientific research purposes only. Where the thesis is converted to, or otherwise made available in digital form, the University of Alberta will advise potential users of the thesis of these terms.

The author reserves all other publication and other rights in association with the copyright in the thesis and, except as herein before provided, neither the thesis nor any substantial portion thereof may be printed or otherwise reproduced in any material form whatsoever without the author's prior written permission.

This thesis is dedicated to Brian Moyer and Steve Browne for putting up with me. And to my parents, Dennis and Sharon, for their constant support in everything that I have ever done.

Abstract

Cholera remains epidemic and endemic in the world, causing thousands of deaths annually in locations lacking adequate sanitation and water infrastructure. Yet its dynamics are still not fully understood. An indirectly transmitted infectious disease model, called an iSIR model, was recently proposed for cholera. This model includes a new incidence term for indirect transmission. The analysis of the iSIR model was preliminary and here we present a thorough stability and sensitivity analysis. We introduce a new disease model, called an iSIBP model, using the new incidence term, and including bacteriophage. Our findings highlight the importance of the relationship among the water contamination parameter and the carrying capacity and minimum infectious dose of the pathogen, relating to the partial global results for the iSIR model, and the existence of limit cycles in the iSIBP model. This thesis provides a theoretical basis for further mathematical and experimental work.

Acknowledgements

I would like to acknowledge the support of my family and friends over these last three years. My supervisor, Dr. Hao Wang, for his support and patience, as well as Dr. Michael Li, Dr. Paul Tian and Dr. Xiong Li, for help with the models. I am thankful for the financial support from the Natural Sciences and Engineering Research Council of Canada (NSERC), the University of Alberta and the Department of Mathematical and Statistical Sciences.

Table of Contents

List of Tables

List of Figures

Chapter 1

Introduction

1.A Background Information

1.A.1 Biology and motivation

The study of diseases spreading through human populations has received attention from mathematicians since the seminal papers of Kermack and McKendrick in the 1920s [39]. However, such attention has mostly been confined to diseases which spread directly, meaning that the primary mode of transmission is from person to person. Diseases can be classified as existing exclusively or partially within humans [79], and those that have a significant portion of their life cycles outside of human hosts tend to have multiple routes of transmission and more complicated epidemiological dynamics. We will be focusing on this second type of disease in this thesis. Such diseases can be viral in nature, like rotavirus disease or hantavirus pulmonary syndrome [19, 82]; bacterial, such as cholera or legionellosis [23]; or parasitic, such as schistosomiasis, cryptosporidiosis or giardiasis [11, 63, 78]. The main complicating issue is that ecological factors coming from the nonhuman portion of

the life cycles of the pathogens need to considered.

Cholera and Background

Cholera is an example of a disease where the pathogen causing it has a significant portion of its life cycle outside of human hosts, and that spreads indirectly or in some cases directly. It has garnered particular attention, especially lately, from a mathematical point of view. Cholera is a diarrhoeal disease caused by the serogroups O1 and O139 of the bacterium *Vibrio cholerae* (*V.cholerae*). When this bacteria is consumed by humans, it produces an enterotoxin (called cholera toxin) in the small intestine [56, 80]. This causes severe diarrhea, which if untreated by antibiotics or rehydration therapy, can cause death. Historically, the mortality rate was 20% or higher [4, 60] but, if proper treatments are available, the mortality rate in modern times is less than 1% [75].

Since 2007 there have been outbreaks in India, Bangladesh, Congo, Iraq, Zimbabwe, Vietnam, Nigeria and Haiti [73], leading to several million cases per year [65]. The bacteria *Vibrio cholerae* exists in coastal waters almost everywhere in the world [44] and in areas such as the Ganges Delta, which includes Bangladesh and India, the disease is endemic. While it has not been a real problem in developed nations with modern sanitation and water treatment since the 19th century, including countries in North America and Europe, in 1991 it returned to South America after a 100-year absence [44]. This highlights the importance of understanding the dynamics of *V.cholerae* and cholera. Another reason why it is important to study *V.cholerae* is that because it exists naturally in the aquatic environment of so many places, when natural disasters or political turmoil lead to compromised water utilities, the disease can make a quick return. In countries lacking resources to deal with such outbreaks, it is obviously essential to understand the most efficient and effective way to quell

outbreaks, and it is often precisely in such countries that cholera tends to be an issue. As a result of the continuing problem of cholera, large sets of data dating back many decades have been amassed, which helps any type of research effort, and provides a fruitful background for mathematical and statistical modeling [62].

Much work has been done focusing on the area of Bangladesh where the disease is endemic and research institutes like the International Center for Diarrhoeal Disease Research (ICDDR) collect a lot data and have performed many studies. In an endemic area, the question of infection-caused immunity naturally arises. Most adults in such regions have a partial immunity to *V.cholerae* O1, which leaves children as the primary susceptible category [55]. However, this immunity does not transfer to the newer O139 serogroup [12]. It has been proposed that such partial immunities to the different serogroups, may explain the somewhat cyclical outbreaks of cholera [40].

As mentioned above, the serogroups O1 and O139 of *V.cholerae* are the causative agents of cholera. In addition to these two toxigenic serogroups, there are more than 200 others which are not toxic to humans [44]. The O1 serogroup can be further divided into *V.cholerae* O1 Classic and *V.cholerae* O1 El Tor. There have been 7 pandemics that have swept the world since the 19th century, with O1 Classic being the cause of the 5^{th} and 6^{th}, and O1 El Tor responsible for the 7^{th} pandemic which originated in Indonesia [20]. El Tor has mostly replaced O1 Classic as the cause of outbreaks. In 1992, O139 Bengal first emerged and looked to be replacing El Tor in turn [76]. It is known now that both O1 El Tor and O139 Bengal cause outbreaks in the Ganges Delta region [20]; within this region, in some places one or the other dominates but they have also been known to cause outbreaks in the same place at the same time [68]. The fact that there are two types of *V.cholerae* which cause cholera outbreaks is significant because they are similar but not identical in important physical ways (size and shape) [37, 77], which would have consequences for

antibody resistance and methods of treating the two types. Furthermore, the temporal dynamics are known to be different (timing of outbreaks and relationship with rainfall, etc.) [6, 51], which would need to be considered when evaluating methods of intervention in preventing and dealing with outbreaks.

The aquatic reservoir

In 1854, Pacini first discovered the link between cholera as a disease and bacteria in the water. However, his results were not accepted at the time because it was not believed that cholera was contagious [44, 59]. In 1884, one year after Pacini's death, Koch rediscovered the link between cholera and the bacteria which he named *Vibrio cholerae* [44]. At the same time as Pacini's work, when the 2^{nd} pandemic reached England, physician John Snow famously connected a cholera outbreak in Soho to a single shallow well [64]. Despite this long awareness and association with water, there has historically been much debate between 'localists' and 'contagionists' as to whether environmental factors or human activities respectively are more important to the epidemiology of cholera. In 1977 Colwell et al. [14] were the first to find that *V.cholerae* could exist independently of humans in acquatic environments. Prior to this, the bacteria was not thought to be capable of surviving for long periods in the water, assumed to be sustained only through human contamination. However, *V.cholerae* was not found in the environment at levels that could account for outbreaks, and also not found during inter-epidemic times. Following new methods for detecting the bacteria in samples [31], the long standing idea that *V.cholerae* can survive naturally in aquatic environments is now accepted [38]. Whether naturally existing aquatic bacteria are the driving cause behind outbreaks in endemic areas is however still debated.

The exact mechanism behind *V.cholerae* living in aquatic ecosystems was and re-

mains cause for further study. It has been found to live in conjunction with zooplankton [1, 16, 72], phytoplankton [27, 67] and other biotic and abiotic detritus [3].

Providing further difficulties in detecting *V.cholerae* in the water is its ability to change physiologically and morphologically in different situations. In times of low nutrient concentration, it is able to change its production of fatty acids and its shape [5, 26, 29, 57]. This complicates the detection methods used in trying to determine its natural densities. It is also able to enter a viable but not culturable form (VNC or VBNC), the exact reason for which is unclear [15, 20, 32, 33, 58]. In this form, bacterial cells are more difficult to detect, and so this form could also explain why *V.cholerae* is usually found at lower levels than expected. Recently, it has been discovered that *V.cholerae* enters this form after passing through the digestive system of human hosts and entering the aquatic reservoir [55], whereas earlier experiments demonstrated that the human digestive tract could in fact reverse this transition [17]. Whether or not *V.cholerae* is always able to revert back from this form is not clear, nor whether they remain infectious. This raises questions to the exact role of human contamination of the aquatic reservoir during epidemics.

Uncertainty regarding the exact role of the aquatic component in the lifecycle of *V.cholerae* has in the past helped fuel the debate between 'contagionists' and 'localists'. Empirically it has been demonstrated that there is a correlation between increases in aquatic *V.cholerae* preceeding outbreaks of cholera [24, 45, 47]. Furthermore, the primary mode of transmission is now thought to be indirect through water or contaminated food, and not person to person [38], although person to person transmission is possible. Also, in a study by Alam et al. [2] on outbreaks of cholera in Mathbaria, Bangladesh, it was found that despite two years of outbreaks caused by *V.cholerae* O1 El Tor, in 2005 the outbreaks were caused by *V.cholerae* O139. As O139 was found in the environment in 2004 but it was O1 El Tor causing outbreaks, the significance of aquatic reservoirs in cholera outbreaks is supported.

These ideas suggest the importance of explicitly including aquatic bacterial levels in models for cholera outbreaks, which most modern models do in some form.

Minimum Infectious Dose

Also relevant to include in any model of cholera epidemiology is the idea of a minimum infectious dose (MID). Unlike viral diseases, bacteria have to enter the human body in higher concentrations to overwhelm the natural immune response [52]. In 1974, Cash et al. [10] performed an experiment using healthy North American males, to try to determine an exact number for this minimum infectious dose. They found that between 10^8 and 10^{11} bacterial cells were required when issued in saline solution, but only 10^4 to 10^8 cells were required when administered with a buffer to neutralize stomach acid. It should be noted however, that as the volunteers were from North America where the disease is not endemic, they would have lacked any sort of natural immunity which is thought to be present where cholera outbreaks regularly occur. There is disagreement on the actual level of this MID, but the existence of one is accepted [17, 30, 38, 41, 75]. Thus cholera models should include a minimal infectious dose in some way.

Multiple outbreaks and periodicity

In the Ganges Delta area, it is well documented that there are multiple outbreaks every year. The pattern has been described heuristically as having 2 main peaks. The first occurs between September and December following the monsoon rains, and the second smaller outbreak occurs in the dry season between March and June [20, 33, 46, 62].

The existence of this bimodal pattern has lead some to associate the differences in

the seasons in terms of weather and other conditions with outbreaks. Some have linked it with surface sea temperatures and height [8, 45] and others have gone further and found correlations between outbreaks and ENSO patterns- that is the Southern Oscillation weather pattern which has a period of 4 years [62]. The thought is that such abiotic factors could cause plankton blooms, which would in turn increase levels of *V.cholerae* attached to the plankton and then cause outbreaks. While there certainly seems to be a correlation between these factors and outbreaks, one notable objection is that the different serogroups O1 and O139 are not synchronized in their responses to these factors [20, 21]. This would suggest that either the different serogroups react differently to the same seasonal influences, or that seasonality cannot fully explain the nature of the outbreaks.

While it is typically said that there are two outbreaks a year in Bangladesh, the data is not strongly periodic in the exact timing of the peaks and there are considerable differences in the timing and strength of outbreaks year to year [8, 40]. Precisely when the September-December outbreak begins after the monsoon rains is nonconstant [25]. The model I present in Chapter 3 has a region in the parameter space which leads to chaotic behaviour. This could explain the irregularity in the seasonal patterns and the different patters of outbreak amongst different countries, especially if the positive relationship between bacterial proliferation and temperature is considered [69].

Hyperinfectivity

Further contributing to the complicated epidemiology of cholera is the existence of a hyper-infectious state of *V.cholerae* O1 El Tor, found in laboratory settings [49]. Hartely et al. [28] found that for up to 5 hours after passing through a human host, the bacteria was many times more infectious than otherwise. This was quantified in

that the dose which caused infections on average 50% of the time (the ID_{50}), was much lower for *V.cholerae* in this hyperinfectious state than normally. Incorporating this idea into models has been found to better fit the explosive nature of cholera outbreaks [46] but whether these laboratory findings are relevant to natural conditions is not clear [55]. Also as mentioned previously, the tendency for *V.cholerae* to enter a VBNC state after exiting human hosts, would seem to complicate this matter.

The role of bacteriophage

It has been proposed that bacteriophage might be another important aspect of the ecology of *V.cholerae* that needs to be included in models of cholera outbreaks [47, 71]. Bacteriophage are viruses that prey on bacteria, so the two exist in a predator-prey relationship. Just as there are different subgroupings of *V.cholerae*, there are corresponding different types of bacteriophage (phage) which consume them. It has been found that humans, in addition to contaminating the water supply with bacteria when infected, also contaminate the water supply with phage, sometimes of matching type [54, 81]. When both bacteria and matching phage are present within a single human host, the phage do not, or are unable to, completely remove the bacteria. They do, however, appear to increase the required infectious dose of bacteria [81]. The presence of phage in the aquatic reservoir has been inversely correlated to cholera outbreaks, suggesting that phage are responsible for ending epidemics [21, 22].

1.A.2 Mathematical models

The main mathematical models that make use of ordinary differential equations are those built upon the Capasso and Paveri-Fontana model [9] and the Codeço

Holling I (aBS)	Holling II $\left(a\frac{B}{B+H}S\right)$	Holling III $\left(a\frac{B^n}{B^n+H^n}S\right)$ $n=2,3,...$
Tien (2010) [74]	Codeco (2001) [13]	
Mukandavire (2011) [50]	Mukandavire (2011) [50]	
	Bertuzzo (2008) [7]	
	Hartley (2006) [28]	Jensen (2006) [35]

Table 1.1: Summary of the incidence terms in other cholera models.

model [13]. Hartley et al. [28] incorporated a hyperinfectious route of transmission to the Codeço model and Joh et al. [36],Tian et al. [73], Jensen et al. [35] and Mukanvire et al. [50] have further built on and branched off from these models. Most models use a Holling I (or mass action) incidence term, which is perhaps unsuitable for non-viral diseases, or a Holling II incidence term, which can overestimate the infectivity of low levels of bacteria. Table 1.1 groups the main cholera models according to incidence term type. Joh et al. [36] first proposed a threshold infection term which will be used in Chapters 2 and 3, and it is unique to all other models listed previously. Below is a summary of the main mathematical models for cholera.

Codeço Model

The first modern cholera ODE model was created in 2001 by Codeço [13]. While the Capasso and Paveri-Fontana model [9] consisted of two equations, with one for the infected compartment and the other for the aquatic bacterial community, Codeço included the susceptible population and recovered population in the model as well. Denote S, I and R as the susceptible, infected and recovered compartments from standard SIR models. The recovered compartment is not stated explicitly, as the population is assumed to be of constant size and so the dynamics of the recovered compartment follow directly from the rest of the system noting that $H = S + I + R$,

where H is the total population. The model is written

$$\dot{S} = n(H - S) - a\lambda(B)S,$$
$$\dot{I} = a\lambda(B)S - rI,$$
$$\dot{B} = B(n_b - m_b) + eI.$$

The birth and death rate are the same and denoted n. The parameter r represents recovery rate, and include natural recovery and death. Bacteria have a net growth rate of proliferation n_b minus mortality m_b, and human contamination increases bacteria levels at a rate e proportional to the size of the infected class. The infective term consists of the maximum rate of exposure to contaminated water, a, multiplied by $\lambda(B) = \frac{B}{K+B}$ which is a Holling II response curve. The use of such a term would overestimate the infectivity of low levels of bacteria, contrary to the idea of a minimum infectious dose, which we think is important.

Key features of the model are that the aquatic reservoir is represented very simply with a linear growth term and linear shedding contribution. This was because the ecological dynamics of *V.cholerae* were not well understood at the time (they are still not completely understood), so Codeço started with the simplest way to model the bacteria population. Unless net growth is naturally zero ($n_b = m_b$), the bacterial population will die out exponentially in the absence of human shedding if $n_b < m_B$, or tend to infinity if $n_b > m_b$.

The oscillations in this system die out over time, so in order to simulate the periodic behaviour of outbreaks observed in some endemic areas, periodic contact rates, shedding rates and net growth rates of bacteria were also included. In reality, all three are likely periodic at the same time, but not necessarily with the same period. In chapter 3, we will demonstrate periodic behaviour with a system that is still autonomous.

Hyperinfection model

To account for the laboratory findings of a hyperinfectious state, Hartley et al. [28] added an additional bacterial compartment to the Codeço model, and also explicitly included the recovered class in the model (although this doesn't change anything as this category was implied previously). The human population is assumed to be of constant size and there is assumed to be no disease-induced mortality, as in the previous model. Removal of susceptibles to the infected class occurred with the same Holling II response curve as in the Codeço model, but infections were caused either by hyperinfectious bacteria B_H or normal bacteria B_L. The half saturation constant for the hyperinfectious class was smaller to represent a lower MID leading to greater infectivity, and the contact rate could also be varied independently.

All human shedding contributed to the hyperinfectious bacteria only, which transformed to normal bacteria linearly. Normal bacteria then had a linear death term, meaning that in the absence of human shedding, bacteria of either form would die out exponentially. This captures the idea that only bacteria that have recently entered the aquatic environment are relevant to outbreaks, a modeling choice which we do not agree with. Also, as before, the use of a Holling II infection term would overestimate the infectivity of very low levels of bacteria, going against the idea of a minimum infectious dose which is an idea we think is important to include.

Model for nonendemic regions

In 2011, Mukandavire et al. [50] extended the model of Hartley et al. [28] to model outbreaks in Zimbabwe, where the disease is not endemic. As Zimbabwe is not a coastal nation, *V.cholerae* are not thought to naturally exist in the aquatic reservoir, meaning that the emphasis should be placed on the human causes of epidemics.

Unlike in Hartley et al. [28], there is only one category of bacteria, which increases proportionally to the infected class and dies out linearly. Hyperinfectivity is accounted for with a Holling I (or mass action) term, $\beta_h SI$, and infections from non-hyperinfectious bacteria are caused through the reservoir with a Holling II term, $\beta_e S\frac{B}{K+B}$. Here the linear terms for the bacteria compartment are perhaps more realistic because *V.cholerae* is not thought to live naturally in the aquatic environment of Zimbabwe, so exponential decay in the absence of human shedding is likely. The models we will present in Chapter 2 and 3 are intended for endemic areas, where bacteria exist naturally without humans, so this difference is justified. However, the Holling I infection term for hyperinfectious cases, and Holling II for environmental infection both would overestimate infectivity when bacteria exist at low levels.

Bacteriophage model

To include the role of bacteriophage which has been suggested by experimentalists as important, Jensen et al. [35] further modified the Codeço model to include a phage compartment, P, and divided infectives into bacteria infected (I_1) and bacteria and phage infected (I_2) individuals. Bacterial shedding thus comes from both classes of infectives, but phage shedding is from I_2 only. Phage infection is proportional to bacteria infection, and the phage dependent term has a 50% infectious dose (or 'half saturation constant') of l. Bacteria (V) are assumed to experience logistic growth with carrying capacity K_v, and predation by phage occurs via a Holling I response

$(\beta\gamma BP)$.

$$\begin{aligned}
\dot{S} &= -\pi\left(\frac{V}{C(\alpha)K+V}\right)^a S - \delta S + \delta N \\
\dot{I}_1 &= \pi\left(\frac{l}{l+P}\right)\left(\frac{V}{C(\alpha)\kappa+V}\right)^a S - (\mu_1+\delta)I_1 \\
\dot{I}_2 &= \pi\left(\frac{P}{l+P}\right)\left(\frac{V}{C(\alpha)\kappa+V}\right)^a S - (\mu_2+\delta)I_2 \\
\dot{R} &= \mu_1 I_1 + \mu_2 I_2 - \delta R \\
\dot{V} &= \left[m\left(1-\frac{B}{K_v}\right) - \delta P\right]B + c(I_1+I_2) \\
\dot{P} &= (\beta\gamma B - \delta)P + \alpha c I_2
\end{aligned}$$

The infection term $-\pi\left(\frac{V}{C(\alpha)K+V}\right)^a S$ is Holling III in form as $a = 7$ in their analysis. The sigmoidal shape is intended to capture the low infectivity at low levels of bacteria, but there are still infections at very small levels which could overestimate the number of infections in the long run.

The focus of this model was to determine the ability of phage to end outbreaks or indirectly cause outbreaks by being reduced in number. Both of these abilities were demonstrated in the analysis. However, they did not examine the role, or existence, of limit cycles caused by the predator-prey relationship of phage and bacteria, which is something we will pay attention to in Chapter 3.

1.A.3 Outline

In chapter 2, we will present a modified SIR model with aquatic reservoir for bacteria. This model was first proposed by Joh et al. [36], but we will offer a more complete stability and sensitivity analysis. The main difference from other SIR models which incorporate an aquatic reservoir is a new 'indirect' infection term which explicitly includes a minimum infectious dose. This infection term is a piecewise continuous

function which is zero below the minimum infectious dose (MID) threshold and a Holling II response curve above the threshold. Similar to Jensen et al. [35], we also allow bacteria to exist naturally under logistic growth. We will demonstrate the existence of a unique endemic equilibrium which can be globally asymptotically stable given a certain relationship between the minimum infectious dose and the bacterial carrying capacity. Also, a sensitivity analysis is presented which reveals a stronger association between the carrying capacity and peak outbreak times and the magnitude of outbreaks, than the shedding rate and peak times and magnitudes. This has implications in the importance of control strategies focusing either on limiting human contamination and access to water supplies or lowering the natural levels of environmental bacteria.

In chapter 3, this new indirect infection term is included in a model, that following Jensen et al. [35], includes phage levels and phage predation of bacteria, through an additional compartment. The existence of limit cycles in the absence of any human shedding demonstrates that cycles in the bacteria-phage community can cause cyclical outbreaks in the human population. These cycles can match the period of the observed dynamics and do not require time-dependent seasonal forcing. Additionally, the existence of a chaotic region in the parameter space is demonstrated. This region could account for the inexact periodicity of cholera outbreaks in certain endemic regions, and the noncyclic behaviour in other regions where outbreaks lack an exact pattern.

Chapter 2

The iSIR Model

2.A Introduction

Cholera is a disease of the intestinal tract that can cause severe diarrhoea, leading to dehydration and death if left untreated. It is caused by the bacteria *Vibrio cholerae* and is treatable if caught within 1-2 days of symptoms first appearing. Historically, the mortality rate was greater than 20% [4, 60]. With modern methods of treatment (antibiotics and rehyrdation therapy) the mortality rate is less than 1% if treated quickly enough [75]. Thus in places with adequate health care and access to antibiotics, cholera is not much of a problem. However, in countries where such health services are lacking in a permanent sense or because of natural disasters reducing their availability, cholera outbreaks are still a concern with several million cases per year [65]. Dhaka, the capital of Bangladesh, for example has two outbreaks of cholera per year [34] that occur with the changes in seasons and the amount of rainfall, both of which affect the quality of the water supply.

However, the dynamics of cholera are not completely understood. Recently a new

indirect transmission model, called an iSIR model (meaning *indirect* SIR model), was proposed by Joh et al. [36]. The iSIR model has a threshold in the incidence term, representing a minimum infectious dose (MID). If bacterial levels are below the threshold, they cannot overcome the natural immune response of the average person and no infections are caused. Above the threshold infections occur according to a Holling II response curve, which is a more accurate reflection of cholera transmission. This chapter continues the analysis of the iSIR model, first presented by Joh et al. [36]. The model is derived, and a forwardly invariant domain is determined. Then a local stability analysis is performed and some global stability results are obtained. Lastly, a sensitivity analysis and discussion of the results are presented.

2.B Derivation of the iSIR Model

One of the key differences of the iSIR model, proposed in Joh et al. [36], compared to standard SIR models is the incidence term. The rough idea is that humans consume bacteria constantly but do not always get sick. Unlike with viruses where only a small amount of exposure is required, for certain types of bacteria a significant amount of bacterial cells need to be ingested in order to override the body's immune response [52]. This threshold has been measured by the likes of Cash et al. [10] and others [30, 38, 41] to be at least 10^4 cells. Simply using Holling I (or mass action) infection terms or Holling II terms overestimates the infectivity of low levels of bacteria.

The incidence term that will be used in this thesis is $\alpha(B)S$ where $\alpha(B)$ is the bacterial density dependent component, and the S term is present for the same reasons as with standard SIR models. The indirect part of the incidence term is defined as

$$\alpha(B) = \begin{cases} 0, & B < c \\ \frac{a(B-c)}{(B-c)+H}, & B \geq c. \end{cases}$$

When the bacterial density is below the threshold c, there will be no infections even with a nonzero amount of susceptibles, and after the bacterial density is above that threshold, infections will occur via a Holling II response, as shown in Figure 2.1.

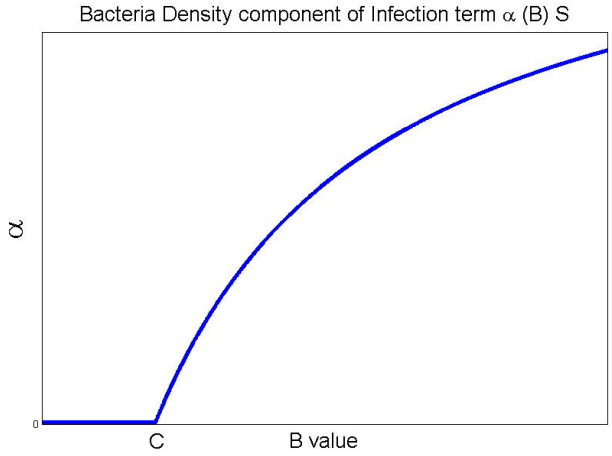

Figure 2.1: If bacteria levels are beneath the threshold c, $\alpha(B)$ is zero (no infections). If bacteria levels are above c, then $\alpha(B)$ is a Holling II curve.

The value of the minimum infectious dose c depends on the type of disease and the immune system of the patient, but here we use it to represent the average immune capability of a population. As *V.cholerae* exist naturally in the aquatic environment, the iSIR model uses logistic bacterial growth in the absence of any infected people, in contrast to most other models which have linear terms for the bacterial growth and death [13, 28, 74]. The latter leads to exponential decay in the absence of infectives, which is consistent as many of those models assume that the aquatic reservoir of *V.cholerae* is not relevant to the cause of outbreaks, and so only the short term dynamics of freshly shed *V.cholerae* are considered. In nonendemic areas, where *V.cholerae* does not naturally exist in the environment, this form of bacterial

growth makes more sense than logistic growth, as used by Mukandavire et al. [50] in a study on recent outbreaks in Zimbabwe. However, most other models are intended for endemic areas, and so linear growth terms are perhaps too simple.

The iSIR model has a positive contribution to the bacteria level when there are sick people shedding bacteria back to the reservoir. This occurs biologically with infected individuals contaminating the water supply through their *V.cholerae* laden feces. The dynamics are summarized in Figure 2.2.

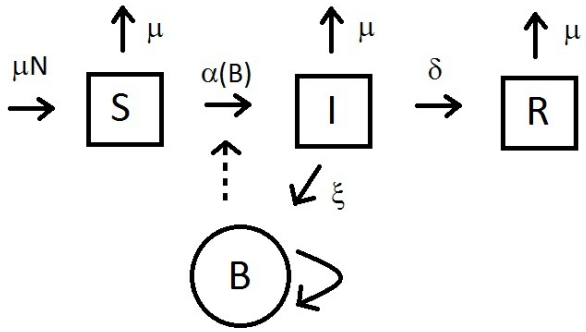

Figure 2.2: A flow diagram demonstrating the relationship between Susceptibles (S), Infectives (I), Recovered (R) and Bacteria (B). Humans have death rate μ, contribute to the bacterial reservoir at rate ξ, recover at rate δ and are infected at rate $\alpha(B)$.

The variables S, I and R in Figure 2.2, are defined in the usual way as susceptible, infected and recovered categories of the human population. The variable B represents the density of bacteria in the aquatic reservoir. The first three equations sum to zero, thus the human population is of constant size. The equations for the model are as

follows:

$$\frac{dS}{dt} = -\alpha(B)S - \mu S + \mu N, \tag{2.1a}$$
$$\frac{dI}{dt} = \alpha(B)S - \mu I - \delta I, \tag{2.1b}$$
$$\frac{dR}{dt} = \delta I - \mu R, \tag{2.1c}$$
$$\frac{dB}{dt} = rB\left(1 - \frac{B}{K}\right) + \xi I, \tag{2.1d}$$
$$N = S + I + R. \tag{2.1e}$$

This model was first proposed in Joh et al. [36], though the analysis was preliminary and here we will present a thorough examination of its dynamics. The parameters are described in Table 2.1, which also states the range of their values for use in numerical simulations, taken from Jensen et al. [35], with the MID range taken from Cash et al. [10].

Parameter	Values	Description	Units
r	0.3-14.3	Maximum per capita pathogen growth efficiency	day $^{-1}$
K	10^6	Pathogen carrying capacity	cell litre $^{-1}$
H	$10^6 - 10^8$	Half-saturation pathogen density	cell litre $^{-1}$
a	0.1	Maximum rate of infection	day $^{-1}$
δ	0.1	Recovery rate	day $^{-1}$
ξ	10 - 100	Pathogen shed rate	cell litre $^{-1}$ day $^{-1}$
μ	$5 \times 10^{-5} - 5 \times 10^{-4}$	Per capita human birth/death rate	day $^{-1}$
N	10^6	Total Population	persons
c	$\approx 10^6$ [10]	MID	cell litre $^{-1}$

Table 2.1: Parameter values from Jensen et al. [35]

2.C Mathematical Results

We can nondimensionalize the system as follows:

$$\mathbf{S} = \frac{S}{N}, \mathbf{I} = \frac{I}{N}, \mathbf{B} = \frac{B}{K},$$
$$\tau = \mu t, \mathbf{A} = \frac{a}{\mu}, \mathbf{C} = \frac{c}{K}, \mathbf{p} = \frac{\mu + \delta}{\mu}, \mathbf{q} = \frac{\xi N}{\mu K}, \boldsymbol{\mathcal{R}} = \frac{r}{\mu}, \boldsymbol{\lambda} = \frac{H}{K}.$$

We redefine the per capita infection rate α accordingly as

$$\overline{\alpha}(\mathbf{B}) = \begin{cases} 0, & \mathbf{B} < \mathbf{C}, \\ \frac{\mathbf{A}(\mathbf{B}-\mathbf{C})}{(\mathbf{B}-\mathbf{C})+\lambda}, & \mathbf{B} \geq \mathbf{C}. \end{cases}$$

The boldface is now dropped and we arrive at the following nondimensionalized iSIR system:

$$\frac{dS}{d\tau} = -\overline{\alpha}(B)S - S + 1, \tag{2.2a}$$
$$\frac{dI}{d\tau} = \overline{\alpha}(B)S - pI, \tag{2.2b}$$
$$\frac{dB}{d\tau} = \mathcal{R}B(1 - B) + qI. \tag{2.2c}$$

2.C.1 Forward invariance

First note that in dimensional terms, if $S = 0$, then $\dot{S} = N > 0$ and so $S(t) > 0$ for $t > 0$. If $I = 0$, then $\dot{I} = \alpha(B)S$ and because $\alpha(B) \geq 0$ by definition, then $I \geq 0$ as well. The third equation of (2.1) gives us that $\dot{R} = \delta I$ when $R = 0$, thus $R(t) \geq 0$. As $S + I + R = N$, we get that $S, I, R \leq N$ in the usual way. This transfers over to the nondimensional quantities of $\mathbf{S}, \mathbf{I}$ and $\mathbf{R}$, the last of which we typically exclude.

We have that $0 \leq \mathbf{S} + \mathbf{I} \leq 1$ in particular.

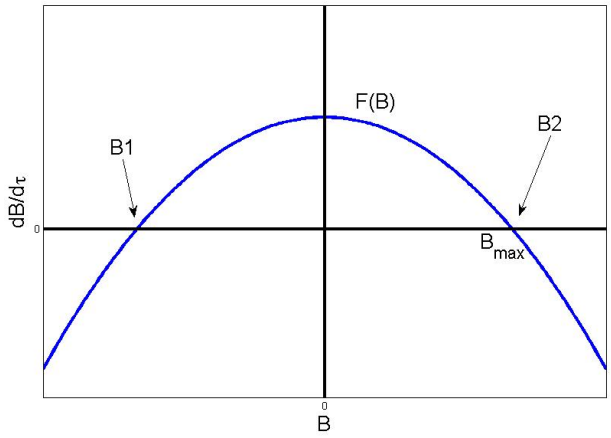

Figure 2.3: The derivative of the Bacteria vs. Bacteria Population. When above B_{max}, the derivative becomes negative. When B is zero, the derivative is positive.

Once again we drop the boldface for convenience. Looking at the third equation of the nondimensional system we can make note that $\mathcal{R}B(1-B)+qI \leq \mathcal{R}B(1-B)+q$ as $I \leq 1$. Define $F(B) := \mathcal{R}B(1-B)+q$ which has roots $B_{1,2} = \frac{\mathcal{R} \pm \sqrt{\mathcal{R}^2+4\mathcal{R}q}}{2\mathcal{R}}$ and note the smaller root $B_1 = \frac{\mathcal{R}-\sqrt{\mathcal{R}^2+4\mathcal{R}q}}{2\mathcal{R}} < 0$ because of the positivity of the parameters. The other root B_2 is clearly positive and is denoted as $B_{max} = \frac{\mathcal{R}+\sqrt{\mathcal{R}^2+4\mathcal{R}q}}{2\mathcal{R}} > 1$. The graph of $F(B)$ is pictured in Figure 2.3.

When $B = 0$, we see that $\dot{B} = qI$ and thus $B(\tau) \geq 0$ for $\tau > 0$. If $B(0) \in [0, B_{max})$ then $B(\tau) \in [0, B_{max})$ for any $\tau > 0$. The invariant region is pictured in Figure 2.4 and we summarize with a proposition.

Proposition 1 (Feasible Region): The set

$$\Omega = \{(S, I, B) : 0 \leq S + I \leq 1, 0 \leq B \leq B_{max}\}$$

defines a forward invariant region of system (2.2).

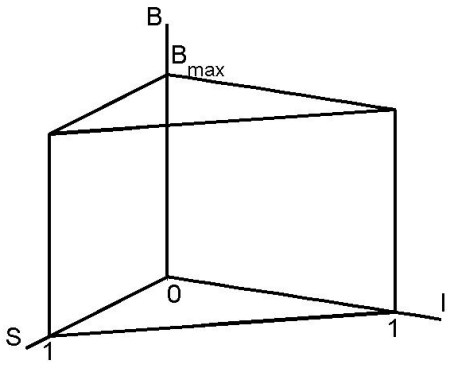

Figure 2.4: The forward invariant region of system (2.2).

2.C.2 Equilibria of the system

Clearly $E_0 = (1, 0, 0)$ is a steady state of (2.2) and biologically it corresponds to a disease-free and bacteria-free population. When $C \geq 1$, this means $\bar{\alpha}(1) = 0$ and $E_1 = (1, 0, 1)$ is an equilibrium corresponding to a disease-free state with bacteria at carrying capacity. When $C < 1$ we get that $\bar{\alpha}(1) \neq 0$ and so $E_1 = (1, 0, 1)$ is not an equilibrium and (2.2) has no equilibrium (S^*, I^*, B^*) with $B^* \leq C$ except E_0. The more complicated steady state $E^* = (S^*, I^*, B^*)$ arises when $B^* > C$ which causes $\bar{\alpha}(B^*) \neq 0$. Thus, system (2.2) implies that

$$S^* = \frac{B^* - C + \lambda}{(A+1)(B^* - C) + \lambda},$$
$$I^* = \frac{1}{p}\left(\frac{A(B^* - C)}{(A+1)(B^* - C) + \lambda}\right) = \frac{\mathcal{R}}{q} B^*(B^* - 1).$$

The expressions for I^* can be combined to form the equation

$$B^*(B^* - 1)\left(B^* - \left(C - \frac{\lambda}{A+1}\right)\right) = \frac{q}{p\mathcal{R}} \frac{A}{A+1}(B^* - C). \tag{2.3}$$

Define $F_1(B) = f(B) - g(B)$ where $f(B) = B(B-1)\left(B - C + \frac{\lambda}{A+1}\right)$ and $g(B) = \frac{q}{p\mathcal{R}}\frac{A}{A+1}(B-C)$. Denote $B_3 = C - \frac{\lambda}{A+1}$ so that if $C < 1$ we see that

$$\begin{aligned} F_1(B_3) &= \frac{q}{p\mathcal{R}}\frac{A}{A+1}\frac{\lambda}{A+1} > 0, \\ F_1(C) &= C(C-1)\left(\frac{\lambda}{A+1}\right) - 0 < 0. \end{aligned}$$

Therefore there exists a root $\overline{B_1} \in (B_3, C)$. However, as $\overline{B_1} < C$ then $\bar{\alpha}(\overline{B_1}) = 0$ and equation (2.3) does not apply. As $f(B)$ is a cubic with positive coefficient on the cubic term, and $g(B)$ is a line with positive slope, there also exists a root $\overline{B}_2 < 0$, which obviously is not biologically relevant as it is negative and it is not within the feasible region Ω. Lastly,

$$\begin{aligned} F_1(1) =& -\frac{q}{p\mathcal{R}}\frac{A}{A+1}(1-C) < 0, \\ F_1(B_{max}) =& (B_{max} - C)\left[\frac{q}{\mathcal{R}} - \frac{q}{\mathcal{R}}\frac{1}{p}\frac{A}{A+1}\right] + \frac{q}{\mathcal{R}}\frac{\lambda}{A+1} > 0. \end{aligned}$$

The latter is true as $p > 1, B_{max} > 1$, and thus we conclude that there exists $B^* \in (1, B_{max})$ when $C < 1$ and it is the unique positive solution to (2.3), giving us a unique interior equilibrium $E^* = (S^*, I^*, B^*)$.

Note that $\lim_{C \to 1^-} B^*(C) = 1$, as the x-intercept of $g(B)$ is 1 when $C \to 1^-$ and $f(1) = 0$. As C increases over the value 1, E^* becomes E_1 or vice versa if C is decreased.

We conclude that when $C \geq 1$, $f(B)$ and $g(B)$ are as in Figure 2.5 and there are $0, 1$ or 2 roots of Equation (2.3) with bacteria values greater than the minimum infectious dose (C). For these values $B^+_{1,2}$, we find S^+_i and I^+_i in the same way as with E^*, leading us to two distinct equilibria $E^+_{1,2}$.

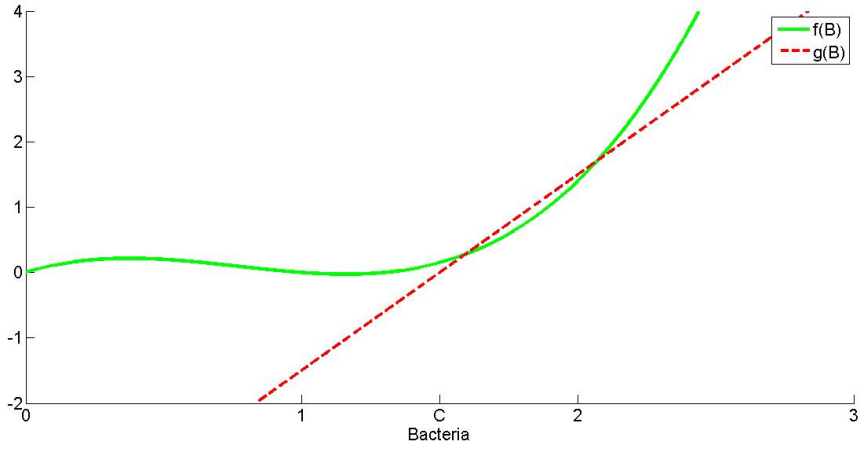

Figure 2.5: The left and right hand sides of Equation **??** when $C \geq 1$. There can be 0, 1 or 2 intersections with bacteria values above the MID.

As C is greater than 1, it is larger than all of the roots of $f(B)$. Thus, $f(B)$ is concave up on $[C, \infty)$ and $f'(B) \geq f'(C) > 0$ for $B \in [C, \infty)$. If the slope of $g(B)$ is less than $f'(C)$, there will be no endemic equilibria, as $g(B)$ will always be below $f(B)$ and there will be no intersections. Defining $\zeta = \frac{q}{p\mathcal{R}}$ and working backwards, we see that

$$\begin{aligned} \zeta &< f'(C), \\ \implies \zeta \frac{A}{A+1} &< f'(C), \\ \implies g'(B) &< f'(C), \end{aligned}$$

meaning that

$$\zeta < f'(C) \tag{2.4}$$

is a sufficient condition for there being no internal equilibria when $C \geq 1$. In dimensional parameters, $\zeta = \left(\frac{\xi N}{\mu+\delta}\right)\left(\frac{\mu}{rK}\right)$, and so ζ is proportional to the shedding rate ξ. This motivates the definition of the condition for no internal steady states, as we

shall see later. We summarize with a proposition.

Proposition 2 (Existence of equilibria): The equilibrium $E_0 = (1, 0, 0)$ always exists in Ω.

- When $C < 1$ (equivalently $c < K$), there exist two equilibria, E_0 on $\partial\Omega$ and a unique endemic equilibrium E^* in $\mathring{\Omega}$.
- When $C \geq 1$ (equivalently $c \geq K$), then $E_1 = (1, 0, 1)$ is also an equilibrium and there can be up to two internal equilibria $E^+_{1,2}$.
  - If $\zeta < f'(C)$, there are no internal equilibria, and only E_1 and E_0 exist.

2.C.3 Local stability of E_0, E_1 and E^*

We calculate the jacobian to analyze the local stability of each of the equilibria. For the simpler case of $B \leq C$,

$$J_1(S, I, B) = \begin{pmatrix} -1 & 0 & 0 \\ 0 & -p & 0 \\ 0 & q & R - 2\mathcal{R}B \end{pmatrix},$$

and for $B > C$,

$$J_2(S, I, B) = \begin{pmatrix} \frac{-A(B-C)}{(B-C)+\lambda} - 1 & 0 & \frac{-A\lambda}{[(B-C)+\lambda]^2} S \\ \frac{A(B-C)}{(B-C)+\lambda} & -p & \frac{A\lambda}{[(B-C)+\lambda]^2} S \\ 0 & q & \mathcal{R} - 2\mathcal{R}B \end{pmatrix}.$$

When $C \geq 1$, the equilibria are $E_0 = (1, 0, 0), E_1 = (1, 0, 1)$ and up to two $E_i^+ = (S_i^+, I_i^+, B_i^+)$. For $C \geq 1$, we use J_1 and find that E_0 has eigenvalues $-1, -p$ and $\mathcal{R}$, which indicates that E_0 is a saddle point equilibrium, as all parameter values are

assumed positive. E_1 in this case has eigenvalues $-1, -p$ and $-\mathcal{R}$ and thus we can conclude that when $C \geq 1$, the equilibrium $(1, 0, 1)$ is locally asymptotically stable: that is, the disease-free equilibrium is locally asymptotically stable. Also, for $C < 1$, E_0 is a saddle point equilibrium for the same reasons.

Now considering E^* and using the nondimensionalized system (2.2), we obtain

$$\begin{aligned} S^* =& \frac{B^* - C + \lambda}{(A+1)\left(B^* - C + \frac{\lambda}{A+1}\right)} = \frac{B^* - C + \lambda}{(A+1)\left(\frac{q}{p\mathcal{R}}\frac{A}{A+1}(B^* - C)\frac{1}{B^*(B^*-1)}\right)} \\ S^* =& \frac{p\mathcal{R}}{Aq}\frac{B^*}{B^* - C}(B^* - 1)(B^* - C + \lambda). \end{aligned}$$

We will use γ for eigenvalues as the traditional λ is already used elsewhere. We can compute

$$\det(\gamma I - J_{E^*}) = \det \begin{pmatrix} \gamma + \frac{A(B^*-C)}{(B^*-C)+\lambda} + 1 & 0 & \frac{A\lambda}{[(B^*-C)+\lambda]^2}S^* \\ \frac{-A(B^*-C)}{(B^*-C)+\lambda} & \gamma + p & \frac{-A\lambda}{[(B^*-C)+\lambda]^2}S^* \\ 0 & -q & \gamma + \mathcal{R}(2B^* - 1) \end{pmatrix}$$

$$\begin{aligned} =& \left(\gamma + \frac{A(B^* - C)}{B^* - C + \lambda} + 1\right)\left[(\gamma + p)(\gamma + \mathcal{R}(2B^* - 1)) - \frac{A\lambda q}{(B^* - C + \lambda)^2}S^*\right] \\ &+ \frac{A^2\lambda q}{(B^* - C + \lambda)^3}(B^* - C)S^*. \end{aligned}$$

Define $F_2(\gamma) := \det(\gamma I - J_{E^*})$, $h := A\frac{B^*-C}{B^*-C+\lambda} + 1$ and $m := \frac{A\lambda q}{(B^*-C+\lambda)^2}S^*$. Later we will make use of the following alternate forms of these definitions:

$$h = A\left(\frac{B^* - C}{B^* - C + \lambda} + \frac{1}{A}\right) = \frac{(A+1)(B^* - C) + \lambda}{B * -C + \lambda} > 1$$

and

$$m = \frac{A\lambda q}{(B^* - C + \lambda)^2}\frac{p\mathcal{R}}{Aq}\frac{B^*}{B^* - C}(B^* - 1)(B^* - C + \lambda) = p\mathcal{R}\frac{\lambda}{B^* - C + \lambda}\frac{B^* - 1}{B^* - C}B^*.$$

We can rewrite the characteristic equation with these new expressions taken into account as follows

$$\begin{aligned}
F_2(\gamma) =&(\gamma + h)[(\gamma + p)(\gamma + \mathcal{R}(2B^* - 1)) - m] + \frac{A^2\lambda q}{(B^* - C + \lambda)^3}(B^* - C)S^* \\
=&(\gamma + h)[\gamma^2 + (\mathcal{R}(2B^* - 1) + p)\gamma + p\mathcal{R}(2B^* - 1) - m] + \frac{A^2\lambda q}{(B^* - C + \lambda)^3}(B^* - C)S^* \\
=&\{\gamma^3 + \mathcal{R}(2B^* - 1 + p)\gamma^2 + [p\mathcal{R}(2B^* - 1) - m]\gamma + h\gamma^2 + h(\mathcal{R}(2B^* - 1) + p)\gamma \\
&+ [p\mathcal{R}(2B^* - 1) - m]h\} + \frac{A^2\lambda q}{(B^* - C + \lambda)^3}(B^* - C)S^*.
\end{aligned}$$

The Routh-Hurwitz coefficients of the above expression are

$$\begin{aligned}
b_3 =& \quad 1, \\
b_2 =& \quad \mathcal{R}(2B^* - 1) + p + h, \\
b_1 =& \quad p\mathcal{R}(2B^* - 1) - b + h(\mathcal{R}(2B^* - 1) + p), \\
b_0 =& \quad [p\mathcal{R}(2B^* - 1) - b]h + \tfrac{A^2\lambda q}{(B^* - C + \lambda)^3}(B^* - C)S^*,
\end{aligned}$$

and note that the Routh-Hurwitz stability criterion requires

$$b_1, b_2, b_3 > 0 \quad \text{and} \quad b_2 b_1 > b_3 b_0$$

as a sufficient condition for stability of the equilibrium. Clearly b_2 and b_3 are positive, and if $p\mathcal{R}(2B^* - 1) - m > 0$ then $b_1, b_0 > 0$. As $C < 1$ for the internal equilibrium E^* to exist, $B^* - 1 < B^* - C$ so that $\frac{B^* - 1}{B^* - C} < 1$.

Thus

$$m = p\mathcal{R}\frac{\lambda}{B^* - C + \lambda}\frac{B^* - 1}{B^* - C}B^* < p\mathcal{R}B^*$$

and so

$$p\mathcal{R}(2B^* - 1) - m > p\mathcal{R}(2B^* - 1) - p\mathcal{R}B^* = p\mathcal{R}(B^* - 1) > 0,$$

which means $b_1, b_0 > 0$.

As for the second condition $b_2 b_1 > b_3 b_0$, we have the following expression

$$\begin{aligned} b_1 b_2 =& [(h+p)\mathcal{R}(2B^* - 1) + hp - m][\mathcal{R}(2B^* - 1) + (p+h)] \\ =& (h+p)\mathcal{R}^2(2B^* - 1)^2 + (h+p)^2\mathcal{R}(2B^* - 1) + (hp - m)\mathcal{R}(2B^* - 1) \\ &+ (h+p)(hp - m). \end{aligned}$$

We can define

$$\begin{aligned} B_1 &= 2hp\mathcal{R}(2B^* - 1) - hm, \\ B_2 &= p\mathcal{R}^2(2B^* - 1)^2 - m\mathcal{R}(2B^* - 1), \\ B_3 &= p^2\mathcal{R}(2B^* - 1) - pm, \\ B_4 &= h\mathcal{R}^2(2B^* - 1)^2 + h^2\mathcal{R}(2B^* - 1) + h^2 p + hp^2 + hp\mathcal{R}(2B^* - 1). \end{aligned}$$

Using the definition of S^*, we can express

$$\begin{aligned} b_3 b_0 &= b_0 \\ &= [p\mathcal{R}(2B^* - 1) - m]h + \frac{A^2\lambda q}{(B^* - C + \lambda)^3}(B^* - C)\frac{p\mathcal{R}}{Aq}\frac{B^*}{B^* - C}(B^* - 1)(B^* - C + \lambda) \\ &= [p\mathcal{R}(2B^* - 1) - m]h + A\lambda p\mathcal{R}\frac{B^*}{(B^* - C + \lambda)^2}(B^* - 1). \end{aligned}$$

Now we check to see if the inequality $b_1 b_2 > b_0$ is satisfied by noting that

$$\begin{aligned}
&(B^* - C)(2B^* - 1) > (B^* - 1)B^* \\
\Rightarrow &\frac{B^* - C}{B^* - C + \lambda}(2B^* - 1) + \frac{1}{A}(2B^* - 1) > (B^* - 1)\frac{B^*}{B^* - C + \lambda} \\
\Rightarrow &Ap\mathcal{R}\left(\frac{B^* - C}{B^* - C + \lambda} + \frac{1}{A}\right)(2B^* - 1) > Ap\mathcal{R}(B^* - 1)\frac{B^*}{B^* - C + \lambda} \\
&\Rightarrow hp\mathcal{R}(2B^* - 1) > Ap\mathcal{R}\lambda(B^* - 1)\frac{B^*}{(B^* - C + \lambda)^2} \\
\Rightarrow &2hp\mathcal{R}(2B^* - 1) - hm > hp\mathcal{R}(2B^* - 1) + Ap\mathcal{R}\lambda\frac{B^*}{(B^* - C + \lambda)^2}(B^* - 1) - hm.
\end{aligned}$$

The left-hand side of the above inequality is precisely B_1 and the right-hand side is b_0. Recall that $m < p\mathcal{R}B^*$, and so

$$p\mathcal{R}^2(2B^* - 1)^2 - m\mathcal{R}(2B^* - C) > p\mathcal{R}^2(2B^* - 1)^2 - p\mathcal{R}^2 B^*(2B^* - 1) > 0$$

and

$$p^2\mathcal{R}(2B^* - 1) - pm > p^2\mathcal{R}(2B^* - 1) - p^2\mathcal{R}B^* = p^2\mathcal{R}(B^* - 1) > 0.$$

Thus $B_2, B_3 > 0$ and clearly $B_4 > 0$. Lastly,

$$b_1 b_2 = \sum_1^4 B_i > B_1 > b_0.$$

Thus the Routh-Hurwitz conditions are satisfied and E^* is locally asymptotically stable.

2.C.4 Local stability of $E^+_{1,2}$

When E_i^+ exist things are more complicated as we lack exact expressions for the equilibrium quantities, and so the local stability is difficult to find analytically.

Numerically it can be demonstrated that E_1^+ (with $B_1^+ < B_2^+$) is often a saddlenode equilibrium, and E_2^+ is often a stable spiral. For example, this can be seen with parameters $A = 1e3, C = 1.1, p = 1112, q = 1e7, \mathcal{R} = 3e3$ and $\lambda = 1$, which leads to $B_{1,2}^+ = 1.1001, 2.301$ and $E_{1,2}^+$ have eigenvalues $\gamma_1 = 10^4 * (-0.0001, 9.2989, -9.7702)$ and $\gamma_2 = 10^4 * (-0.0633 \pm 0.0432i, -1.1200)$. These nondimensional parameters correspond to reasonable dimensional parameters as given previously in Table 2.1.

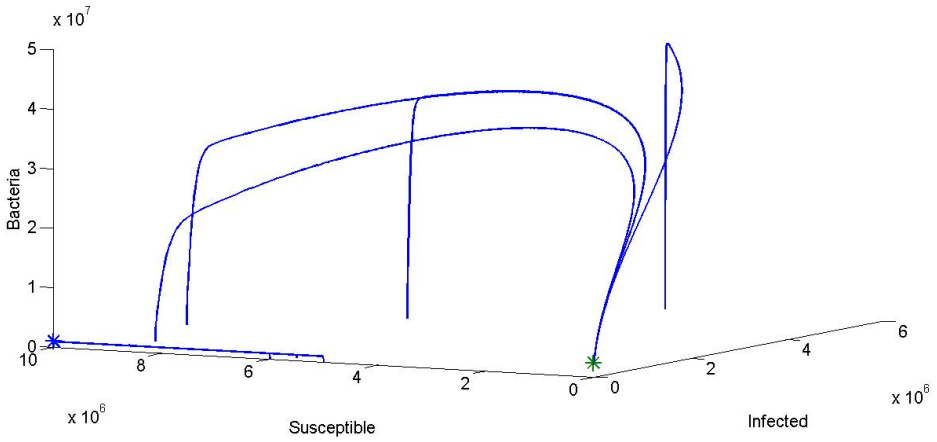

Figure 2.6: Phase diagram of the bistability of (2.1) with parameters $\delta = 0.0999$, K=1e6, a=0.09, H=1e6, c=1.5e6, N=1e7, r=0.27, $\mu = 9e-5$, $\xi = 90$. The dimensional internal and boundary equilibria E_2^+ and E_1 are locally stable and marked with asterisks. In this case, the basin of attraction for E_2^+ is much larger than that of E_1.

This means that there can exist solutions spaces where the equilibria E_1 and E_2^+ are both locally stable and a situation of bistability occurs, as observed in Figure 2.6. Almost every solution will approach either the endemic equilibrium or the disease-free equilibrium, depending on initial conditions. Numerically we observe that the basin of attraction is much larger for the endemic equilibrium E_2^+, meaning that a greater range of initial conditions will lead to an endemic steady state rather than a disease free-one. So, E_0 is always locally stable, E_1 and E^* are locally stable when they exist, and numerically we see that E_1^+ is often unstable and E_2^+ is often locally stable. We summarize the preceding local stability results with a theorem.

Theorem 1 (Local Stability): System (2.2) has between two and four equilibria.

- When $C < 1$ (equivalently $c < K$), $E_0 = (1, 0, 0)$ is unstable and a unique endemic equilibrium E^* exists and is locally asymptotically stable.
- When $C \geq 1$ (equivalently $c \geq K$), then $E_0 = (1, 0, 0)$ is unstable and $E_1 = (1, 0, 1)$ is an equilibrium and is locally asymptotically stable. Up to two internal equilibria, $E^+_{1,2}$, can also exist.

2.C.5 Global stability of E_1 and E^*

We wish to invoke a theorem of Hal Smith in regards to monotone dynamical systems and global stability. Because of the threshold parameter, the jacobian of (2.2) will have two different forms with $\alpha(B) = 0$ or not. Either way, the jacobian is of the form

$$J(S, I, B) = \begin{pmatrix} * & + & - \\ + & * & + \\ - & + & * \end{pmatrix},$$

which is sign stable and sign symmetric in the off-diagonal entries. As demonstrated in Figure 2.7, every closed loop has an even number of edges with + signs and so the system is *monotone* as defined in Smith [70] in Ω with respect to the partial ordering

$$K_m = \{(S, I, B) : S \geq 0, I \leq 0, B \geq 0\}. \tag{2.5}$$

Our argument is as follows: an application of monotone dynamical system theory states that if system (2.2) has a positive periodic orbit in domain Ω, then there exists an unstable equilibrium in Ω (Prop. 4.3 [70]). When $C \geq 1$ and condition (2.4) is satisfied ($\zeta < f'(C)$), then there are only E_0 and E_1, neither of which is

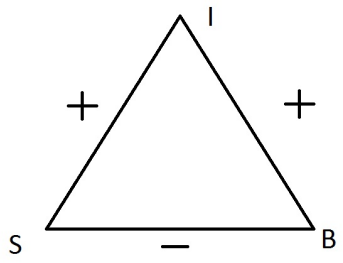

Figure 2.7: The relationship between the three main compartments in the model.

an interior equilibrium. Hence system (2.2) will not have any periodic orbits in Ω. As (2.2) is competitive, it reduces to a two-dimensional system [70]. Because of the absence of limit cycles and by the Poincare-Bendixson theory, the local stability of E_1 implies that E_1 is globally asymptotically stable.

Define

$$H_1 = \{(S, I, B) : B \leq C, 0 < S + I \leq 1\},$$

$$H_2 = \{(S, I, B) : C < B < B_{max}, 0 < S + I \leq 1\},$$

and note that $H_1 \subset \Omega, H_2 \subset \Omega$ with $\Omega = H_1 \bigcup H_2$. We will show that when $C \geq 1$ and $\zeta < f'(C)$, after some τ_0 all solutions will stay entirely in H_1 and we can apply our argument about the global asymptotic stability of E_1.

First we require a result from Hal Smith [70] about competitive systems noting first that $\ll_m$ and $\leq_m$ are order relations with respect to K_m defined in (2.5).

Lemma 1 (Prop 4.3 p.44 Smith [70]): Let γ be a non-trivial periodic orbit of a competitive system in $D \subset \mathbb{R}^3$ and suppose there exists $p, q \in D$ such that $p \ll_m q$ and $[p, q] = \{y \in D : p \leq_m y \leq_m q\} \subset D$. Then W is an open subset of $\mathbb{R}^3$ consisting of two connected components, one bounded and one unbounded. The bounded component, $W(\gamma)$, is homeomorphic to the open ball in $\mathbb{R}^3$. $W(\gamma) \subset [p, q]$, is positively invariant and its closure contains an equilibrium.

Now we require some results about the behaviour of solutions of (2.2) with respect to H_1 and H_2.

Lemma 2: If $C \geq 1$ and $\zeta < f'(C)$, then for all solutions $x(\tau) = (S(\tau), I(\tau), B(\tau))$ of (2.2), if there exists some τ_0 such that $x(\tau_0) \in H_2$, then there exists some $\tau_1 > \tau_0$ such that $x(\tau_1) \in H_1$.

Proof. Assume $x(\tau) \in H_2$ for some $\tau = \tau_1$. Assume for contradiction that $x(\tau) \in H_2$ for all $\tau > \tau_1$. Then by Monotone Dynamical Systems (MDS) Theory we can reduce this 3d system to a 2d system, as it is competitive, and by the Poincare-Bendixson Theorem we can conclude all omega limit sets are limit cycles or equilibria.

As there is not an interior equilibria in H_2, we can conclude by Lemma 1 that there are not any limit cycles in H_2. As there are also no equilibria of any type in H_2, we conclude that $x(\tau)$ exits H_2 at some $\tau_2 > \tau_1$. This contradicts our assumption that $x(\tau) \in H_2$ for all $\tau > \tau_1$ and our Lemma is proven. □

Lemma 3: If $C \geq 1$ and $\zeta < f'(C)$, then for all solutions $x(\tau)$ of (2.2), if there exists s_0, s_1 such that $s_1 > s_0$ where $x(s_0) \in H_2$ and $x(s_1) \in H_1$, then $x(\tau) \in H_1$ for $\tau > s_1$.

Proof. Suppose there exists s_0 and $s_1, 0 < s_0 < s_1$ such that $x(s_0) \in H_2$ and $x(s_1) \in H_1$. There exists $\tau_0 \in (s_0, s_1)$ such that $B(\tau_0) = C$ and $\dot{B}(\tau_0) < 0$. Suppose there exists $\tau_1 > \tau_0$ where $B(\tau_1) = C, \dot{B}(\tau_1) > 0$, meaning that x(t) is re-entering H_2. Choose the first such time τ_1 and note

$$\dot{B}(\tau_1) = \mathcal{R}C(1 - C) + qI(\tau_1) > 0,$$

$$\dot{B}(\tau_0) = \mathcal{R}C(1 - C) + qI(\tau_0) < 0.$$

This means that $I(\tau_1) > I(\tau_0)$ but $B(\tau) \leq C$ on $\tau_0 < \tau < \tau_1$ and so $\dot{I} = -pI < 0$.

This is a contradiction, so there can be no such τ_1 as supposed and the Lemma is proven. □

Thus no solutions can stay in H_2 as $\tau \to \infty$ and once H_1 is entered from H_2, H_1 is forward invariant. This captures the behaviour of all solutions $x(\tau)$.

We can now conclude that E_1 is globally asymptotically stable.

Proposition 3 (Global Stability of E_1): When $C \geq 1$ and $\zeta < f'(C)$, $E_1 = (1, 0, 1)$ is an equilibrium of (2.2) and it is globally asymptotically stable.

Proof. When $C \geq 1$ and $\zeta < f'(C)$, by Lemmas 2 and 3, all solutions eventually exist entirely in H_1 and as there are no interior equilibria (because $\zeta < f'(C)$), by Lemma 1 there are no limit cycles in H_1. Monotone Dynamical Systems theory says that (2.2) reduces to a 2-dimensional system, and so by the Poincare-Bendixson theorem all omega-limit sets are limit cycles or equilibria. As there are no limit cycles in H_1 and no interior equilibria, by the local stability of E_1, we conclude that it is globally asymptotically stable. □

Now we consider the global stability of E^*. As (2.2) is monotone, it verifies the Poincare-Bendixson property: every compact omega-limit set without equilibria is a closed orbit. For systems with this property, a criterion on global stability has been developed by Li, Wang and Muldowney [43] [42]. Note that the *second additive compound* of a 3×3 matrix, $A = [a_{ij}]$, is denoted $A^{[2]}$ and defined

$$A^{[2]} = \begin{bmatrix} a_{11} + a_{22} & a_{23} & -a_{13} \\ a_{32} & a_{11} + a_{33} & a_{12} \\ -a_{31} & a_{21} & a_{22} + a_{33} \end{bmatrix}.$$

Lemma 4 (Theorem 2.5 [43]): Let $\dot{x} = F(x) (F \in C^1)$ be a system defined on an

open convex subset $G \subset \mathbb{R}^3$ having a compact global attractor in G. Assume that

1) The Poincare-Bendixson property holds.

2) There is a unique equilibrium in G which is locally asymptotically stable.

3) For each periodic orbit $p(t)$ in G, the linear system

$$\dot{Y} = \frac{\partial F^{[2]}}{\partial x}(p(t))Y$$

is asymptotically stable.

Then the equilibrium is globally asymptotically stable in G.

In order to apply this result, we have to study the asymptotic stability of the linear equation

$$\dot{Y} = J^{[2]}(p(t))Y \tag{2.4}$$

where $p(t)$ is any periodic solution of (2.2) in Ω. Given our definition of J_{E^*}, the second additive compound of J_{E^*} is

$$J^{[2]} = \begin{pmatrix} -f_0(B) - 1 - p & f_0'(B)S & f_0'(B)S \\ q & -f_0(B) - f_1'(B) - 1 & 0 \\ 0 & f_0(B) & -p - f_1'(B) \end{pmatrix},$$

where $f_0(B) = \frac{A(B-C)}{B-C+\lambda}$ and $f_1'(B) = 2\mathcal{R}B - \mathcal{R}$.

Typically verifying the stability of such a system is nontrivial, but for (2.4) we have a linear, periodic, cooperative, irreducible system with respect to the cone

$$K_1 = \{(S, I, B) : S \geq 0, I \geq 0, B \geq 0\}$$

which suggests we use a comparison result.

Lemma 5: (Proposition 3 [66]) Let $\dot{Y} = A_i(t)Y$ for $i = 1, 2$ be two linear, periodic, cooperative and irreducible systems (with the same period) such that $A_2(t) - A_1(t)$ has nonnegative coefficients. If $\dot{Y} = A_2(t)Y$ is asymptotically stable, then $\dot{Y} = A_1(t)Y$ is too.

For our case, obviously$A_1 = J^{[2]}(p(t))$ and for A_2 we choose a constant matrix whose entries bound those of A_1 independently of the periodic orbit and denote the matrix $\bar{J}$ where

$$\bar{J} = \begin{pmatrix} -1 - p - f_0(1) & f_0'(1) & f_0'(1) \\ q & -f_0(1) - f_1'(1) - 1 & 0 \\ 0 & f_0(B_{max}) & -p - f_1'(1) \end{pmatrix}.$$

The characteristic equation, $P(\gamma)$, of $\bar{J}$ is

$$P(\gamma) = [\gamma+1+p+f_0(1)][\gamma+1+f_0(1)+f_1'(1)][\gamma+p+f_1'(1)]-qf_0'(1)[\gamma+p+f_1'(1)+f_0(B_{max})].$$

Expanding this out we can write

$$P(\gamma) = a_3\gamma^2 + a_2\gamma^2 + a_1\gamma + a_0,$$

with coefficients

$$\begin{aligned} a_3 &= 1, \\ a_2 &= 2(1 + p + f_0(1) + f_1'(1)), \\ a_1 &= [2 + 2f_0(1) + p + f_1'(1)](p + f_1'(1)) + [1 + p + f_0(1)](1 + f_0(1) + f_1'(1)) - qf_0'(1), \\ a_0 &= [1 + p + f_0(1)](1 + f_0(1) + f_1'(1))[p + f_1'(1)] - qf_0'(1)[p + f_1' + f_0(B_{max})]. \end{aligned}$$

To use the Routh-Hurwitz conditions, we require that $a_i > 0$ and that $a_1 a_2 > a_3 a_0$. First consider the positivity of the coefficients. We make the assumption that

$$(p+1)^2 > qA\lambda^{-1}(p+A). \tag{2.5}$$

Only the positivity of a_1 and a_0 require checking.

$$\begin{aligned} a_0 >& p + pf_1'(1) + p^2 f_1'(1) + pf_1'(1) + pf_1'(1)f_1'(1) + f_1'(1)f_1'(1) \\ & - qA\lambda^{-1}(p + f_1'(1) + A)) \\ =& (p+1)^2 f_1'(1) + p^2 + p + pR^2 + R^2 - qA\lambda^{-1}(p + f_1'(1) + A)). \end{aligned}$$

Noting that $f_1'(1) = \mathcal{R} = \frac{r}{\mu}$ it is reasonable to assume that $\mathcal{R} > 1$ as μ is the human birth/date rate and will be very small. Also r, the maximum bacterial growth rate, is often greater than 1. Finally, by definition $p > 1$ thus

$$\begin{aligned} a_0 >& (p+1)^2\mathcal{R} + p^2 + p + p\mathcal{R}^2 + \mathcal{R}^2 - qA\lambda^{-1}(p + \mathcal{R} + A)) \\ >& (p+1)^2\mathcal{R} + (p+1)^2 - qA\lambda^{-1}(p+A) - qA\lambda^{-1}\mathcal{R} \end{aligned}$$

and so $a_0 > 0$ by assumption (2.5). The positivity of a_1 follows similarly,

$$a_1 > (2+p)p + (1+p) - qA\lambda^{-1} > (1+p)^2 - qA\lambda^{-1}.$$

and by (2.5), $a_1 > 0$ too. Now we can consider $\triangle = a_1a_2 - a_3a_0$,

$$\begin{aligned}
\triangle =& 2(1+p+f_0(1)+f_1'(1))\{(1+f_0(1)+p)(p+f_1'(1)) \\
&+ [1+p+f_0(1)][1+f_0(1)+f_1'(1)]\} + [1+p+f_0(1)](1+f_0(1)+f_1'(1))[p+f_1'(1)] \\
&+ 2f_1'(1)[1+f_0(1)+f_1'(1)](p+f_1'(1)) + qf_0'(1)[-2-p-2f_0(1)-f_1'(1)+f_0(B_{max})], \\
\triangle >& 2(1+p+f_0(1)+f_1'(1))(1+p)p + (1+p) - qf_0'(1)[2+2p+f_0(1)+2f_1'(1)] \\
&= 2(1+p+f_0(1)+f_1'(1))\Big[(1+p)^2 - qf_0'(1)\Big].
\end{aligned}$$

Note that $(1+p)^2 - qf_0'(1) > (1+p)^2 - qA\lambda^{-1}$ and so by our assumption (2.5) we have that $a_2a_1 > a_3a_0$. Lastly considering H_1 and H_2 as before, note that if $C < 1$ then $\dot{B}(B = C) = \mathcal{R}C(1-C) + qI > 0$, so eventually all trajectories exist entirely in H_2. In particular, any attracting limit cycles are contained in H_2. We restate the previous results in a proposition.

Proposition 4 (Behaviour of limit cycles and Global Stability of E^*): When $C < 1$, E^* is an equilibrium of (2.2). Any limit cycle, if it exists, should be entirely in H_2, and if $(p+1)^2 > qA\lambda^{-1}(p+A)$, then E^* is globally asymptotically stable.

Recalling that $C = \frac{c}{K}$, we can summarize our results about the equilibria in this section with the following theorem.

Theorem 2 (Global Stability): System (2.2) always has at least two equilibria.

- If $C < 1$ (equivalently $c < K$), the equilibria are $E_0 = (1,0,0)$ which is unstable and $E^* = (S^*, I^*, B^*)$ which is locally asymptotically stable. Furthermore, if $(p+1)^2 > qA\lambda^{-1}(p+A)$, then E^* is globally asymptotically stable.
- If $C \geq 1$ (equivalently $c \geq K$), the equilibria are $E_0 = (1,0,0)$ which is unstable, $E_1 = (1,0,1)$ which is locally asymptotically stable and up to two internal equilibria $E_{1,2}^+$.

–Further, if $\zeta < f'(C)$ only E_0 and E_1 exist, and E_1 is globally asymptotically stable.

Note that if the MID is greater than K and ζ is low enough to satsify condition (2.4), the disease-free equilibrium E_1 is globally asymptotically stable. As nondimensional ζ and the shedding parameter ξ are proportional, this means that with a nonzero but sufficiently small shedding rate, the disease-free equilibrium is inevitable. This is in contrast to the case where the MID is less than the carrying capacity of bacteria, and the bacteria exist at levels which naturally cause new infections. In this case, if other parameters agree, the endemic steady state E^* is globally asymptotically stable for any nonzero shedding rate ξ. Thus if efforts are taken to decrease K and ξ in conjunction, a disease-free globally stable steady state can be attained with a shedding rate that could otherwise lead to an endemic steady state.

2.D Numerical Simulations

Stability was discussed nondimensionally previously but numerical examples are presented in the following diagrams in dimensional parameters. In Figure 2.8, where $\mathbf{C} < 1$, the endemic equilibrium is stable. Bacteria are existing above their carrying capacity of $10^6 \frac{cells}{L}$ and there is a nonnegligible infected population at a level of 1235 out of 10^6 individuals.

In Figure 2.9, we see that if $c \geq K$ ($\mathbf{C} > 1$) with a small ξ value, meaning the minimum infectious dose is larger than the carrying capacity, then there is no endemic equilibrium. Thus the system moves towards the disease free state. Intuitively, this means that it takes more than the 'natural level' of bacterial density in the water supply to make anyone sick and shedding is low, so no one becomes sick.

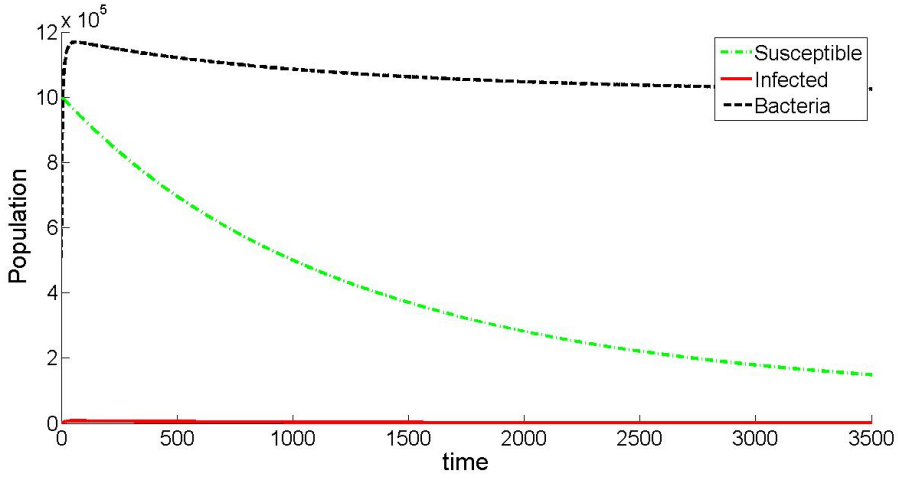

Figure 2.8: An endemic trajectory of (2.1), where an epidemic dies down and then approaches an endemic equilibrium. Parameters are $\delta = 0.1, K = 1e6, a = 0.1, H = 1e8, c = 4e5, N = 1e6, r = 0.3704, \mu = 5e-5, \xi = 10$ with $I^* = 790$ and $B^* = 1,020,886 > K = 1e6$.

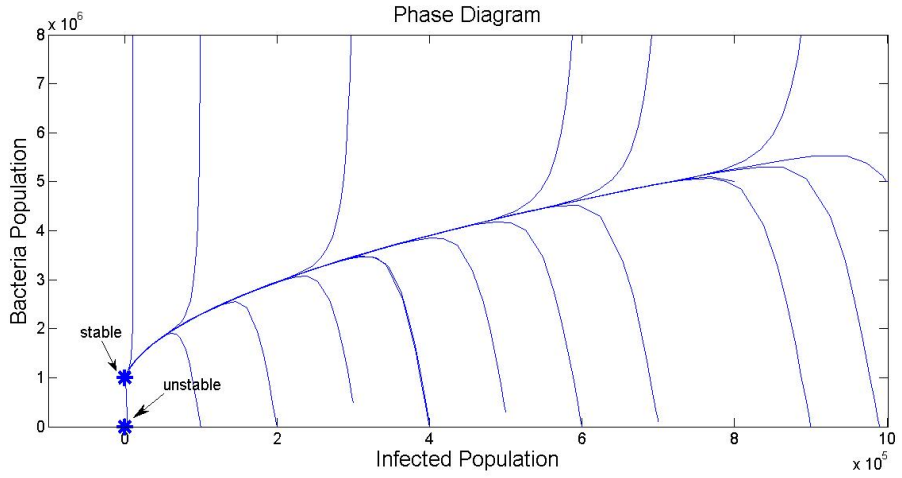

Figure 2.9: A phase diagram of dimensional (2.1), with $\mathbf{C} > 1$, showing trajectories with different inital conditions converging to the disease free steady state E_1. Parameter values $\delta = 0.1, K = 1e6, a = 0.1, H = 1e8, c = 2e6, N = 1e6, r = 0.3704, \mu = 5e-5, \xi = 10$.

Figure 2.10 demonstrates that when the minimum infectious dose is less than the carrying capacity, $c < K$, then the internal endemic steady state is attracting. In it, a wide range of initial conditions all follow a similar path towards the endemic steady

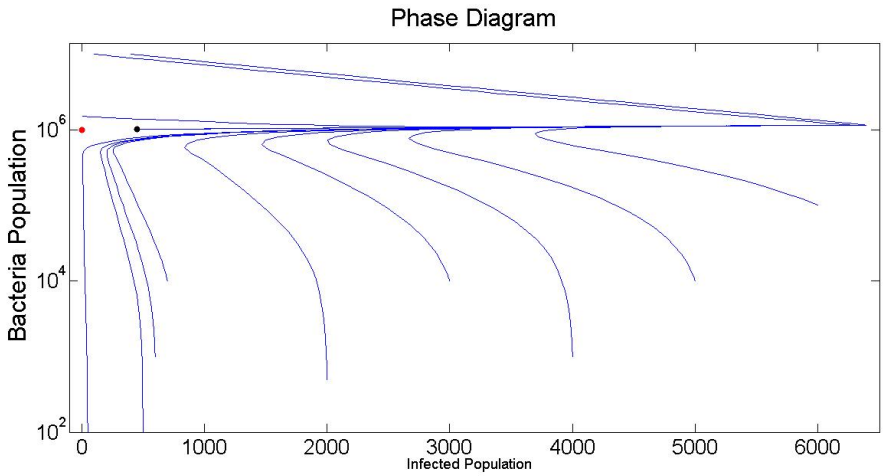

Figure 2.10: A phase diagram of the dimensional system (2.1), with $\mathbf{C} < 1$, showing many different trajectories approaching the endemic steady state, marked with a solid circle. The disease free steady state $(0, 0)$ is not shown. Parameters used $\delta = 0.1, K = 1e6, a = 0.1, H = 1e8, c = 5e5, N = 1e6, r = 0.3704, \mu = 5e - 5, \xi = 10$.

state after each trajectory first experiences an outbreak. This means that if the MID is small enough that a normal bacterial density can make any individual sick, then the disease will persist in the community if only at a low level. As mentioned, a strong epidemic always occurs with a high outbreak peak.

2.E Sensitivity Analysis

In this section, we compute and analyze the normalized forward sensitivity indices of different quantities to the parameters of the system by computing

$$S.I. = \frac{\partial x^*}{\partial p} \frac{p}{x^*}$$

where x^* is the quantity being considered, and p is some parameter which x^* depends upon. Sensitivity indices can be positive or negative which indicates the nature of the relationship, and it is the magnitude that ranks the strength of the relationship

as compared to the other parameters.

2.E.1 Sensitivity of the outbreak peak

The sensitivity indices of the amplitude of the outbreak peak show how the first epidemic depends on the parameters as seen in Table 2.2. This table has three columns because there is a noticeable difference in the sensitivity indices when the bacteria started out above or below the carrying capacity.

Parameter	Sensitivity B(0)< K	Sensitivity B(0)>K	
δ	-1.2024	-0.5296	Recovery rate
K	1.8773	1.1334	Bacteria carrying capacity
a	1.1980	0.9822	Contact rate
H	-1.1905	-0.9623	Half Saturation constant
c	-0.9324	-0.4196	Minimum Infectious Dose
r	-0.2305	-0.5267	Logistic bacteria growth
μ	-5.5e-004	-2.5830 e-004	Human birth/death
ξ	0.2352	0.0636	Shedding rate

Table 2.2: The sensitivity of the magnitude of the peak outbreak to the parameters. Two columns for the initial density of bacteria below or above its carrying capacity K.

The carrying capacity K has the strongest relationship to the magnitude of the outbreak peak. The positive value tells us that a higher carrying capacity would lead to a more severe epidemic. In contrast to the shedding rate ξ which has among the lowest of sensitivity indices, K would thus be an important parameter to control in order to reduce the harm of an outbreak.

A negative relationship between r and the peak magnitude might seem counter intuitive, but the per capita growth rate of bacteria at any given time is $r\left(1-\frac{B}{K}\right)$ and during the peak the bacteria exist over their natural carrying capacity, so the growth rate would be negative and thus there is a negative relationship between r and the peak amplitude.

The sensitivity index with respect to the human birth/death rate μ is very low in comparison to all the others. This makes sense, because the initial peak of an epidemic occurs relatively quickly after the introduction of sick people or introduction of high levels of bacteria and the birth and death of new susceptibles would not be on the same time scale.

A negative relationship between the minimum infectious dose (MID) c and peak amplitude is consistent with our understanding of the disease dynamics, because a larger MID means it would take a higher bacterial density to cause any infections at all. Thus a higher MID would mean less infections and a smaller outbreak peak.

The recovery rate δ has a strong negative relationship to the peak outbreak level as a higher δ leads to few infectives by definition.

2.E.2 Sensitivity of the outbreak peak time

Parameter	Sensitivity B(0)< K	Sensitivity B(0)>K	
δ	0.0772	-6.7542	Recovery Rate
K	0.4392	4.8433	Bacteria carrying capacity
a	-0.2177	-0.3361	Contact Rate
H	0.2159	0.3264	Half Saturation constant
c	0.9319	0.0928	Minimum Infectious Dose
r	-0.6327	3.9216	Logistic Bacteria growth
μ	3.5491e-005	4.3194e-005	Human birth/death
ξ	-0.2269	-0.1425	Shedding rate

Table 2.3: The sensitivity of the time of the outbreak maximum to the parameters.

Once again we see from Table 2.3 that the carrying capacity K has a large influence on the dynamics of the system. It has one of the largest sensitivity indices, being many times greater than that of the shedding rate ξ. This suggests that K is a more important quantity to control to prevent outbreaks. The positive relationship means a smaller carrying capacity would lead to a quicker outbreak as well as a smaller

one as we saw in the last section.

Noticeable is the lack of effect of μ, as with the amplitude of the peak. It has such a negligible effect for the same reasons as outlined previously.

The relationship between contact rate a and the time of the maximum outbreak is a negative relationship, because a higher contact rate causes more new infections and so the timing of the maximum would be attained earlier than otherwise.

The recovery rate δ is interesting because its effect changes sign as well as magnitude considerably with different values of $B(0)$ in relation to carrying capacity. When $B(0) > K$ the effect of δ is greatest and negative. A higher value of δ would mean individuals would be infected, and thus infectious, for less time, so the outbreak should not be as severe and would occur earlier than otherwise. As the magnitude of δ is so small when it is positive, the positive relationship does not yield insight into the relationship of outbreak time and recovery rate.

The per capita growth rate is $r\left(1 - \frac{B}{K}\right)$ and so when $B > K$ this growth rate is negative. If $B(0) < K$ then the growth rate will be positive in the beginning of the outbreak, so a larger r would mean a higher growth rate, and thus the epidemic would peak earlier. This is supported by the negative relationship with r and peak time when $B(0) < K$. If however $B(0) > K$, the per capita growth rate will be negative from the start, and as B will remain above K for all time, the growth rate will always be negative. So a larger r value would mean slower growth, and the epidemic wave would take longer to reach a maximum. This is supported by the strong positive relationship of r and peak time when $B(0) > K$ as can be seen in Table 2.3.

Parameter	Sensitivity of S^*	Sensitivity of I^*	Sensitivity of B^*	
δ	0.0321	-0.9453	-0.0780	Recovery Rate
K	-1.9877	-0.1036	1.0666	Bacteria carrying capacity
a	-1.0314	-0.0611	0.0402	Contact Rate
H	1.0260	0.0606	-0.0399	Half Saturation constant
c	0.9932	0.0225	0.0014	Minimum Infectious Dose
r	0.0323	-0.0329	0.0474	Logistic Bacteria growth
μ	0.8472	0.8177	0.0811	Human birth/death
ξ	-0.0323	0.0123	-0.0179	Shedding rate

Table 2.4: The sensitivity of the components of the endemic equilibrium.

2.E.3 Sensitivity of the endemic steady state

We can look at the sensitivity of one of the interior equilibria E^* with respect to the parameters when E^* exists. Here we only look at $B(0) < K$ as the other case has similar sensitivity results, and we assume the other endemic steady states would yield similar results.

The final size of the susceptible population is most sensitive to the carrying capacity K and contact rate a, with a negative relationship in both cases. This is because a higher contact rate causes more infections and a higher carrying capacity causes more bacteria which indirectly leads to more infections. A higher shedding rate would cause more infections which is confirmed with the negative relationship between S^* and ξ. But S^* is many times less sensitive to ξ than to K which again points to K as the more important parameter to focus on in disease control. The minimal infectious dose (MID) c is nearly as sensitive as the contact rate, but has a positive relationship as a higher MID would lead to fewer infections and a higher S^*. There is a weak relationship with δ but as our model does not allow for reinfection, this

accounts for the small magnitude of the sensitivity.

The endemic level of infective individuals is most sensitive to the recovery rate δ and the birth/death rate μ. The strong negative relationship with δ is because recovery is the main way that infectives leave the infected component of our model. The relationship with μ is complicated in that the birth rate and death rate are the same in our model. So a larger μ means more deaths and thus more infectives leaving the infected component, but also more newly born susceptibles to possibly enter the infected class. The positive relationship means that the positive effect of births is more important to I^* than the negative effect of deaths. The shedding rate ξ has a weak relationship with I^* but the positive relationship is as expected because a larger ξ leads to more infectives and a higher I^* value.

The endemic level of the bacteria population is most sensitive to the bacterial carrying capacity K and has a positive relationship to it as expected. A higher K means more bacteria and as $B^* > K$ (equivalent to $B^* > 1$ in nondimensional form) the relationship is positive. The shedding rate has a small sensitivity which suggests that the logistic part of $\frac{dB}{dt}$ is more important to the endemic level of B^*. As such the relationship with the MID is also minimal. The strong relationship with K and weak one with ξ also again suggests the important of K instead of ξ as a control measure. This could mean, for example, that monitoring the bacterial levels in water reservoirs is more important than simply controlling or restricting access to the water supply to avoid contamination.

2.F Discussion

Cholera has the potential to quickly spread over large areas and can cause many deaths. Thus a full understanding of the dynamics is essential to effectively re-

spond to outbreaks. With the continuing outbreaks there is the opportunity for mathematical modeling to help decipher these dynamics and provide suggestions for governments and health care bodies in effective intervention. An estimate for the basic reproductive number in regions affected by cholera would give important information for controlling future outbreaks and for creating surveillance programs. The potential for amplification in environmental reservoirs and the indirect transmission of the disease make this a nontrivial task. Here we have shown that with $\mathbf{C} = \frac{c}{K} \geq 1$, the disease free equilibrium can be globally asymptotically stable. However as bacteria are existing at a nonzero level, if environmental factors change and alter the carrying capacity enough to make $\mathbf{C} < 1$, then there can be outbreaks. If other parameters are in agreement, an endemic equilibrium is globally asymptotically stable. This change to carrying capacity could be seasonally caused as with different amounts of rain in areas like Bangladesh, or it could be a more permanent change due to natural disasters as in Haiti.

An important thing to note about the relationship between c and K is that if $c < K$ ie) the minimum infectious dose is less than the carrying capacity, then the unique endemic equilibrium can be globally stable. It is globally stable for any nonzero value of the shedding parameter ξ. If however, the minimum infectious dose is greater than the natural carrying capacity, if ξ is low enough, causing the nondimensional ζ to be sufficiently small, then the disease free equilibria becomes globally stable. This highlights the importance of being aware of the value of the natural carrying capacity, because decreasing the shedding rate can eliminate the possibility of an endemic steady state, if the MID is larger than the carrying capacity. If the MID was less than the carrying capacity, the unique endemic steady state could be globally asymptotically stable for the same shedding rate. So ideally, efforts need to be taken to reduce both shedding, and in conjunction with this, the bacteria levels in the reservoir.

Our sensitivity analysis suggests that control measures influencing the carrying capacity K will be more effective in minimizing the epidemic than those concentrating on influencing the shedding rate. While improving the sanitation infrastructure of an area is the obvious step to take to control outbreaks, monitoring and controlling the bacterial levels in the water itself is more important. Improving the infrastructure would surely help control the bacteria levels in the water by decreasing the amount of human contamination, but *V.cholerae* exist independently of humans and so other factors that influence the natural levels of bacteria in the water need to be considered as well in intervention strategies. As mentioned above, controlling both parameters is important and likely to be the most effective, but the carrying capacity K is the more influential of the two on its own.

The original paper of the iSIR model [36] provided some preliminary mathematical results. This analysis adds on to that work, and demonstrates the local stability for most equilibria analytically. In addition, we present the results of dissipativity and determine conditions for global stability.

Further steps to take with this model would be to refine the condition on the global stability of the endemic equilibrium. The condition imposed might not be required, and a biological explanation is in order. Also, a seasonal carrying capacity could be included to simulate the cycles of cholera which occur in regions like Bangladesh. Further altering the model to include bacteriophage is another possibility, with the idea being that the cycles observed in the human population are caused by cycles in the micro scale of bacteria and bacteriophage as has been suggested by Faruque et al. [21] and others.

Chapter 3

The iSIBP Model

3.A Introduction

Cholera has long been associated with water sources, and recently the ecological dynamics of *V.cholerae* have begun to be considered as important to the epidemiology of cholera. Previously, *V.cholerae* was difficult to detect in the aquatic environment, due to the existence of a viable but not culturable state (VBNC or VNC), but modern detection techniques suggest that in endemic areas *V.cholerae* exist naturally even in interepidemic times, and that monitoring natural *V.cholerae* levels can be a useful tool in predicting outbreaks [24, 47].

It has been suggested that it is important to acknowledge the role of bacteriophage when considering *V.cholerae* ecology [21, 22, 54, 81]. The general understanding is that bacteriophage (phage) and bacteria exist in a predator-prey relationship, so cycles that are naturally generated by the relationship could account for the cyclical outbreaks of cholera in endemic regions. In 2006, Jensen et al. [35] created a mathematical model which included a phage component and were able to demonstrate that

bacteriophage are capable of ending outbreaks of cholera by decreasing *V.cholerae* levels, among other results. We will integrate the transmission term from the previous chapter which explicitly accounts for the minimum infectious dose (MID), and focus more on the existence and role of limit cycles in the epidemiology of cholera in our alteration of the model created by Jensen et al. [35].

We will demonstrate the importance of the relationship between the minimum infectious dose and the carrying capacity in relation to the existence of these cycles and endemic equilibria; that the cycles are driven by the bacteria-phage system and not the other way around; and we will demonstrate the existence of a chaotic region in parameter space, which could account for the different nature of outbreaks observed around the world.

In this chapter the iSIBP model is derived, and a forwardly invariant domain is calculated. The system is considered with no shedding present, and a local analysis is performed and limit cycles are located. Then shedding is included and a similar analysis is performed. Lastly, the existence of chaos is explored, followed by a discussion of the mathematical results and their biological significance.

3.B Derivation of the iSIBP Model

Bacteria and bacteriophage exist in a predator-prey relationship. We capture this dynamic by using a Holling II predation term $\gamma \frac{B}{K_1+B} P$, where γ is the maximum predation rate, B and P represent bacteria and phage densities respectively, and K_1 is the half saturation constant of predation (the bacterial level at which predation occurs at half of the maximum rate). We assume that the bacteria population experiences logistic growth in the absence of predation and human influence, with carrying capacity K and maximum growth rate r as in the previous chapter. This

motivates the following model, which assumes no infection-derived immunity for simplicity

$$\frac{dS}{dt} = -\alpha(B)S + \mu I, \tag{3.1a}$$
$$\frac{dI}{dt} = \alpha(B)S - \mu I, \tag{3.1b}$$
$$\frac{dB}{dt} = rB\left(1 - \frac{B}{K}\right) - \gamma\frac{B}{K_1 + B}P + \xi I, \tag{3.1c}$$
$$\frac{dP}{dt} = \beta\gamma\frac{B}{K_1 + B}P - \delta P + \phi\xi I, \tag{3.1d}$$
$$N = S + I. \tag{3.1e}$$

The incidence term we use is $\alpha(B)S$ where $\alpha(B)$ is the bacterial density dependent component. The 'indirect' part of the incidence term $\alpha(B)$ is defined

$$\alpha(B) = \begin{cases} 0, & B < c \\ \frac{a(B-c)}{(B-c)+H}, & B \geq c. \end{cases}$$

Unlike in larger scale predator prey dynamics, where β would be a measure of the conversion rate of prey into predators, often less than unity, β here represent a 'burst size', as each predated bacteria cell will give rise to many new phage cells.

Human contamination of the water supply through infected feces contributes to both bacteria and phage levels and is called 'shedding.' Bacteria and phage shedding rates need not be the same so the rate for bacteria is ξ and for phage it is $\phi\xi$ where ϕ is some constant.

In the absence of predators and humans, bacteria will exist at their carrying capacity K. We assume that phage and bacteria can live naturally without human interference, as in interepidemic times, and so it is assumed that $\beta\gamma > \delta$. If this is not so, phage would die out in the absence of human shedding. This maximum predation

rate γ is difficult to measure, and for numerical solutions is chosen to satisfy this inequality. The half saturation constant for the predation term, K_1, was assumed to be less than the natural carrying capacity K so that predation does not always occur near the maximal rate. For numerical simulations, parameters are taken from the literature and the ranges are given in Table 3.1.

Parameter	Values	Description	Units
r	0.3-14.3	Maximum per capita pathogen growth efficiency	day $^{-1}$
K	10^6	Pathogen carrying capacity	cell liter $^{-1}$
H	$10^6 - 10^8$	Half-saturation pathogen density	cell liter $^{-1}$
a	0.1	Maximum rate of infection	day $^{-1}$
ξ	10 - 100	Pathogen shed rate	cell liter $^{-1}$ day $^{-1}$
μ	0.1	Human recovery rate	day $^{-1}$
N	10^6	Total Population	persons
c	$\approx 10^6$	MID	cell liter $^{-1}$
β	80-100	Phage burst size	virions day $^{-1}$
γ	–	Phage absorption rate	liter virion $^{-1}$ day $^{-1}$
δ	0.5-7.9	Phage death rate	virions day $^{-1}$
ϕ	$10^{-6} - 1$	Mean phage shed rate	virions cell $^{-1}$
K_1	–	Half saturation bacteria predation density	cell

Table 3.1: Parameter values from Jensen et al. [35] and Cash et al. [10]

3.C Forward Invariance

We would like to define a forwardly invariant set in which solutions of (3.1) will be bounded. From the first two equations of (3.1) we see that $\dot{S}(S = 0) = \mu I$ but as $S + I = N$, we can write $\dot{S}(S = 0) = \mu N > 0$. Thus $S(t) > 0$ for $t > 0$. Even though there is no birth or death in this system, if the entire population were to be infected then there would be people recovering and moving back into the susceptible category.

Similarly, $\dot{I}(I=0) = \alpha(B)S \geq 0$ as we just saw that $S(t) > 0$ for $t > 0$ and $\alpha(B) \geq 0$ by definition. As $S > 0$ and $I \geq 0$, then as there are only two compartments for humans, $S \leq N$ and $I < N$.

The BP subsystem is more complicated as for upper bounds, but first note that $\dot{B}(B=0) = \xi I$ thus $B(t) \geq 0$. Similar to the previous section

$$\begin{aligned}\dot{B} =& rB\left(1-\frac{B}{K}\right) - \gamma\frac{B}{K_1+B}P + \xi I,\\ <& rB\left(1-\frac{B}{K}\right) + \xi N\end{aligned}$$

and so we can define

$$B_{max} = \frac{rK + K\sqrt{r^2 + \frac{4r}{K}\xi N}}{2r}$$

where if $B(0) \in [0, B_{max})$ then $B(t) \in [0, B_{max})$ for $t \geq 0$.

Lastly, consider $\dot{P}(P=0) = \phi\xi I \geq 0$ and so $P(t) \geq 0$ for all $t > 0$. The upper bound of $P(t)$ requires the following lemma.

Lemma 6: Define positive constants u and v such that $\frac{((r+u)\beta)^2 K}{4r\beta} < v$. Then for all values of B, the following is true

$$0 < \frac{r}{K}\beta B^2 - ((r+u)\beta)B + v.$$

Proof. Defining constants u and v as above, we see that

$$\begin{aligned}&\frac{((r+u)\beta)^2 K}{4r\beta} < v,\\ \Longleftrightarrow&((r+u)\beta)^2 - \frac{4r}{K}\beta v < 0,\\ \Longleftrightarrow&0 < \frac{r}{K}\beta B^2 - ((r+u)\beta)B + v.\end{aligned}$$

The last two lines are equivalent as the coefficients of the quadratic in the latter are simply arranged as an expression for the discriminant of the quadratic in the former line. □

We can now show that B and P are bounded above, although it was already demonstrated that B is bounded. Consider

$$\begin{aligned}\frac{d}{dt}(\beta B + P) &= r\beta B - \frac{r}{K}B^2\beta + \beta\xi I - \omega P + \phi\xi I, \\ &< r\beta B - \frac{r}{K}B^2\beta - \omega P + (\beta + \phi)\xi N.\end{aligned}$$

And by invoking Lemma 6, we see further that

$$\begin{aligned}\frac{d}{dt}(\beta B + P) &< -u\beta B - \omega P + (\beta + \phi)\xi N + v, \\ &< -d(\beta B + P) + (\beta + \phi)\xi N + v,\end{aligned}$$

where $U := \min\{u, \omega\}$, which implies that $\beta B + P$ is bounded. Defining $V := (\beta + \phi)\xi N + v$, we can write

$$\limsup_{t\to\infty} \beta B(t) + P(t) \leq \frac{U}{V} \quad \text{or} \quad \beta B(t) + P(t) \leq \max\left\{B(0) + P(0), \frac{U}{V}\right\}.$$

We summarize the above results with a proposition

Proposition 5 (Feasible Region): The set

$$\Gamma = \{S, I, B, P \geq 0 : S + I = N, \beta B(t) + P(t) \leq \frac{U}{V}, B < B_{max}\}$$

defines a forwardly invariant region of system (3.1), where $V := (\beta + \phi)\xi N + v$ and $U := \min\{u, \omega\}$, with $u, v > 0$ satisfying $\frac{((r+u)\beta)^2 K}{4r\beta} < v$.

3.D Existence and Stability of Equilibria with no Shedding

3.D.1 Existence of equilibria

In countries with modern sanitation infrastructure, human contamination of the water supply (shedding) is very low; in the ideal case, shedding is completely absent. We can determine the number and stability of steady states of (3.1) without shedding by substituting $\xi = 0$ and further noting that as $S = N - I$, the first equation is not necessary, leaving us with the following

$$\frac{dI}{dt} = \alpha(B)(N - I) - \mu I, \tag{3.2a}$$

$$\frac{dB}{dt} = rB\left(1 - \frac{B}{K}\right) - \gamma\frac{B}{K_1 + B}P, \tag{3.2b}$$

$$\frac{dP}{dt} = \beta\gamma\frac{B}{K_1 + B}P - \delta P. \tag{3.2c}$$

If the bacteria level is below the minimum infectious dose, then $\alpha(B) = 0$. The first equation of (3.2) implies that $I^* = 0$ in this case, and so $S^* = N$ as well. If $I^* = 0$, then equations 2 and 3 of (3.2) at steady state become

$$0 = rB\left(1 - \frac{B}{K}\right) - \gamma\frac{B}{K_1 + B}P \qquad \text{and} \qquad 0 = \left(\beta\gamma\frac{B}{K_1 + B} - \delta\right)P.$$

Equation 2 of (3.2) at steady state can be solved for P, which is a quadratic in B. Define $P = F_1(B) = \frac{r}{\gamma K}(K - B)(K_1 + B)$ having roots $B = K$ and $B = -K_1$. The solution $B = -K_1$ is not biologically relevant and also is not within our invariant region Γ, as defined in the previous section. The other root, $B = K$, of $F_1(B)$ satisfies $\alpha(K) = 0$ only if $K \leq c$. Equation 3 at steady state can be solved as well; either $P = 0$ or $B = B_1 := \frac{\delta K_1}{\beta\gamma - \delta}$; with the latter being relevant only if $B_1 \leq c$

and $\alpha(B_1) = 0$. To satisfy both equations at once, either $(B, P) = (0, 0), (K, 0)$ or (B_1, P_1), where $P_1 = F_1(B_1)$.

Thus when $\alpha(B) = 0$, there are three possible steady states, all of which are disease free. The simplest equilibrium point occurs when $S = N$, $I = 0$, $B = 0$ and $P = 0$. The disease-free, bacteria-free and phage-free equilibrium $E_0 = (N, 0, 0, 0)$ is always an equilibrium of (3.2) for all parameter values. The disease-free, phage-free equilibrium denoted $E_K = (N, 0, K, 0)$ is an equilibrium if $K \leq c$. Similarly, if $B_1 \leq c$ then $\alpha(B_1) = 0$ and the disease-free equilibrium $E_1 = (N, 0, B_1, P_1)$ exists. However, for the positivity of P_1, we require that $B_1 < K$. Note that if $B_1 = K$, then $P_1 = 0$ and E_1 is simply E_K.

The case of equilibria when $\alpha(B) \neq 0$ is more complicated, but it can be shown that there are up to two additional equilibria denoted $E^+_{1,2} = (S^*_{1,2}, I^*_{1,2}, B^*_{1,2}, P^*_{1,2})$ where all of the entries are strictly positive, making $E^+_{1,2}$ the only interior equilibria if they exist. If $\alpha(B^*) \neq 0$, first note that $B^* > c$ by definition. Dropping the asterisk on B, Equation 1 of (3.2) at equilibrium implies

$$\begin{aligned} 0 &= -a\frac{(B-c)}{B-c+H}S + \mu I, \\ 0 &= -a\frac{(B-c)}{B-c+H}(N-I) + \mu I, \\ I^* &= G_1(B^*) := Na\frac{(B-c)}{(a+\mu)(B-c)+\mu H}. \end{aligned}$$

So for each equilibrium value B^* such that $\alpha(B^*) \neq 0$, there exists a unique value $I^* = G_1(B^*)$. To find B^* and P^*, it is of no consequence that $I^* \neq 0$ because with $\xi = 0$, Equations 2 and 3 of (3.2) do not contain terms including I. Thus the nontrivial values of (B, P) that satisfy Equations 2 and 3 at steady state are the same as before: $(B, P) = (K, 0)$ and (B_1, P_1), but now $K > c$ is required so that $\alpha(K) \neq 0$ and $B_1 > c$ so that $\alpha(B_1) \neq 0$. For the positivity of P_1 it is still necessary that $B_1 < K$.

Summarizing, there are up to two endemic equilibria of (3.2), $E_K^* = (S_K^*, I_K^*, K, 0)$ and $E_1^* = (S_1^*, I_1^*, B_1, P_1)$, where $I_K^* = G(K)$, $I_1^* = G_1(B_1)$ and $S_i^* = N - I_i^*$ with the condition that $K > c$ and $c < B_1 < K$ for E_K^* and E_1^* to exist, respectively. As in the nonendemic equilibria case, if $B_1 = K$ this would mean $P_1 = 0$ and $E_K^* = E_1^*$, leaving only one endemic equilibrium.

3.D.2 Linearization

Due to the threshold in the infection term, linearization yields two cases, one for $B^* \leq c$ with $\alpha(B^*) = 0$, denoted Jac_1, and one for $B^* > c$ with $\alpha(B^*) \neq 0$, denoted Jac_2. The conditions surrounding the existence of the particular equilibrium point will determine which jacobian to use and there are never cases where both would apply. The jacobians are written:

$$Jac_1(I,B,P) = \begin{pmatrix} -\mu & 0 & 0 \\ 0 & r - 2\frac{r}{K}B - \frac{\gamma K_1}{(K_1+B)^2}P & -\gamma\frac{B}{K_1+B} \\ 0 & \beta\gamma\frac{aH}{(B-c+H)^2}P & \beta\gamma\frac{B}{K_1+B} - \delta \end{pmatrix},$$

and

$$Jac_2(I,B,P) = \begin{pmatrix} -\alpha(B) - \mu & (N-I)\frac{aH}{(B-c+H)^2} & 0 \\ 0 & r - 2\frac{r}{K}B - \frac{\gamma K_1}{(K_1+B)^2}P & -\gamma\frac{B}{K_1+B} \\ 0 & \beta\gamma\frac{aH}{(B-c+H)^2}P & \beta\gamma\frac{B}{K_1+B} - \delta \end{pmatrix}.$$

The differences between Jac_1 and Jac_2 are all within the first row due to the nonzero $\alpha(B)$ in the case of $B^* > c$. On the invariant set Γ the jacobians are both of the

form

$$Jac(I,B,P) = \begin{pmatrix} * & + & + \\ + & * & - \\ + & + & * \end{pmatrix}$$

which is sign stable but not sign symmetric. Thus unlike our model in the previous chapter, the system is not monotone on an invariant set.

3.D.3 Stability of the disease-free, bacteria-free, phage-free equilibrium E_0

Consider Jac_1 for $E_0 = (N, 0, 0, 0)$ as $B_0 = 0 < c$. The result is a diagonal matrix

$$J_1(0,0,0) = \begin{pmatrix} -\mu & 0 & 0 \\ 0 & r & 0 \\ 0 & 0 & -\delta \end{pmatrix},$$

with eigenvalues $\lambda = -\mu, -\delta < 0$ and $r > 0$. This means that the disease-free, bacteria-free and phage-free equilibrium E_0 is a saddlenode equilibrium with a one-dimensional unstable manifold.

3.D.4 Stability of the disease-free, phage-free equilibrium E_K

For the disease-free, phage-free equilibrium $E_K = (N, 0, K, 0)$ to exist, it is necessary that $K \leq c$ so that $\alpha(K) = 0$ and so we use J_1 to consider the local stability, writing

$$Jac_1(0,K,0) = \begin{pmatrix} -\mu & 0 & 0 \\ 0 & -r & -\gamma\frac{K}{K_1+K} \\ 0 & 0 & \beta\gamma\frac{K}{K_1+K} - \delta \end{pmatrix}.$$

Note that as the matrix is triangular, the eigenvalues are

$$\lambda = -\mu, -r, \beta\gamma\frac{K}{K_1 + K} - \delta.$$

If $\beta\gamma\frac{K}{K_1+K} - \delta < 0$, then all eigenvalues are negative and E_K is a stable equilibrium, but if $\beta\gamma\frac{K}{K_1+K} - \delta > 0$, then E_K is a saddlenode equilibrium with a one-dimensional unstable manifold. Rearranging to solve for K

$$E_K \text{ stable} \qquad \iff \qquad K < \frac{\delta K_1}{\beta\gamma - \delta} = B_1.$$

Note that $B_1 < K$ is required for E_1 to exist, so the existence of E_1 and the stability of E_K are contrary notions.

3.D.5 Stability of the disease-free equilibrium E_1

This equilibrium is also a boundary equilibrium but is perhaps more realistic as it has a nonzero phage level. The bacteria level is defined $B_1 = \frac{\delta K_1}{\beta\gamma-\delta}$ and $P_1 = F_1(B_1) = \frac{r}{K}(-B_1 + K)(B_1 + K_1)$. For $E_1 = (N, 0, B_1, P_1)$ to exist, $B_1 \leq c$ to ensure $\alpha(B_1) = 0$ and $B_1 < K$ for $P_1 > 0$. Note that the bacterial level here is less than that of E_K. Here we again use Jac_1, writing

$$Jac_1(0, B_1, P_1) = \begin{pmatrix} -\mu & 0 & 0 \\ 0 & r - 2\frac{r}{K}B_1 - \frac{\gamma K_1}{(K_1+B_1)^2}P_1 & -\gamma\frac{B_1}{B_1+K_1} \\ 0 & \beta\gamma\frac{K_1}{(K_1+B_1)^2}P_1 & \beta\gamma\frac{B_1}{B_1+K_1} - \delta \end{pmatrix}$$

but note that in the last entry of $Jac_1(0, B_1, P_1)$

$$\beta\gamma\frac{B_1}{B_1 + K_1} - \delta = \frac{\beta\gamma\delta K_1}{(\beta\gamma - \delta)K_1 + \delta K_1} - \delta = \frac{\beta\gamma\delta K_1}{\beta\gamma K_1} - \delta = 0$$

so that

$$Jac_1(0, B_1, P_1) = \begin{pmatrix} -\mu & 0 & 0 \\ 0 & r - 2\frac{r}{K}B_1 - \frac{\gamma K_1}{(K_1+B_1)^2}P_1 & -\gamma\frac{B_1}{B_1+K_1} \\ 0 & \beta\gamma\frac{K_1}{(K_1+B_1)^2}P_1 & 0 \end{pmatrix}.$$

The matrix is slightly more complicated, so we will use a lemma from McCluskey and van den Driessche [48] with regard to three-dimensional matrices.

Lemma 7 (Lemma 3, McCluskey and van den Driessche (2003)): Let A by a 3×3 matrix with real entries. If $tr(A)$, $\det A$ and $\det A^{[2]}$ are all negative, then all of the eigenvalues of A have negative real part.

The converse of Lemma 7 is also true, which is apparent if you note that the eigenvalues of the second additive compound matrix $A^{[2]}$, for a 3×3 matrix A, are just $\sum \lambda_i + \lambda_j$ for $i < j$ with λ_i being the eigenvalues of A.

Defining $J(2,2) = r - 2\frac{r}{K}B_1 - \gamma\frac{K_1}{(K_1+B_1)^2}P_1$, the second additive compound of Jac_1 at E_1 is

$$Jac_1^{[2]}(0, B_1, P_1) = \begin{pmatrix} -\mu + J(2,2) & -\gamma\frac{B_1}{B_1+K_1} & 0 \\ \beta\gamma\frac{K_1}{(K_1+B_1)^2}P_1 & -\mu & 0 \\ 0 & 0 & J(2,2) \end{pmatrix}.$$

The determinant of $Jac_1(E_1)$ is

$$\begin{aligned} \det Jac_1(E_1) &= -\mu \det \begin{bmatrix} J(2,2) & -\gamma\frac{B_1}{B_1+K_1} \\ \beta\gamma\frac{K_1}{(K_1+B_1)^2}P_1 & 0 \end{bmatrix}, \\ &= -\mu\gamma\frac{B_1}{B_1+K_1}\beta\gamma\frac{K_1}{(K_1+B_1)^2}P_1, \\ &< 0, \end{aligned}$$

so it will always satisfy its role in the antecedent of Lemma 7. The trace is given

$$tr(Jac_1(0, B_1, P_1)) = -\mu + J(2,2),$$

and consider

$$\begin{aligned}
J(2,2) &= r - 2\frac{r}{K}B_1 - \gamma\frac{K_1}{(K_1+B_1)^2}P_1 \\
&= r - 2\frac{r}{K}B_1 - \gamma\frac{K_1}{(K_1+B_1)^2}\frac{r}{\gamma K}(-B_1+K)(B_1+K_1) \\
&= r - 2\frac{r}{K}B_1 - r\frac{K_1}{(K_1+B_1)}\frac{K-B_1}{K} \\
&= r\left(1 - 2\frac{B_1}{K} - \frac{K_1}{(K_1+B_1)}\frac{K-B_1}{K}\right) \\
&= r\left(\frac{K(K_1+B_1) - 2B_1(K_1+B_1) - K_1(K-B_1}{K(K_1+B_1)}\right) \\
&= \frac{rB_1}{K(K_1+B_1}(K-(K_1+2B_1)).
\end{aligned}$$

Thus $sgn(J(2,2)) = sgn(K-(K_1+2B_1))$, where

$$\begin{aligned}
K-(K_1+2B_1) &= K - \left(K_1 + \frac{2\delta K_1}{\beta\gamma-\delta}\right) \\
&= K - K_1\left(\frac{\beta\gamma+\delta}{\beta\gamma-\delta}\right).
\end{aligned}$$

We conclude about the trace that

$$\begin{aligned}
J(2,2) < 0 \qquad &\Rightarrow \qquad tr(Jac_1) < 0, \\
J(2,2) > 0, -\mu + J(2,2) < 0 \qquad &\Rightarrow \qquad tr(Jac_1) < 0, \\
J(2,2) > 0, -\mu + J(2,2) > 0 \qquad &\Rightarrow \qquad tr(Jac_1) > 0.
\end{aligned}$$

Lastly we need to consider the sign of $\det Jac_1^{[2]}(E_1)$, which is written

$$\begin{aligned}\det Jac_1^{[2]}(E_1) &= J(2,2)\det\begin{bmatrix} -\mu + J(2,2) & -\gamma\frac{B_1}{B_1+K_1}, \\ \beta\gamma\frac{K_1}{(K_1+B_1)^2}P_1 & -\mu \end{bmatrix} \\ &= J(2,2)\left\{[-\mu J(2,2)][-\mu] + \left(\beta\gamma\frac{K_1}{(K_1+B_1)^2}P_1\right)\left(\gamma\frac{B_1}{B_1+K_1}\right)\right\}.\end{aligned}$$

We can see that if $J(2,2) < 0$, then $\det Jac_1^{[2]} < 0$ and if $J(2,2) > 0$ but $J(2,2) - \mu < 0$, then $\det Jac_1^{[2]} > 0$. The last case of $J(2,2) > 0$ and $J(2,2) - \mu > 0$ is not necessary for our purposes. To summarize about the trace and determinant of the second additive compound matrix

$$\begin{aligned} J(2,2) < 0 \quad &\Rightarrow \quad trJac_1(E_1) < 0 \\ &\quad \text{and} \quad \det Jac_1^{[2]}(E_1) < 0, \\ J(2,2) > 0 \quad &\Rightarrow \quad trJac_1(E_1) > 0 \\ &\quad \text{or} \quad \det Jac_1^{[2]}(E_1) > 0 \end{aligned}$$

and because $\det Jac_1(0, B_1, P_1) < 0$ all the time, by Lemma 7

$$\begin{aligned} E_1 \text{ is stable} \quad &\iff \quad J(2,2) < 0 \\ &\iff \quad K < \frac{\beta\gamma+\delta}{\beta\gamma-\delta}K_1 = B_1 + \beta\gamma\frac{K_1}{\beta\gamma-\delta}. \end{aligned}$$

Define $B_3 := B_1 + \beta\gamma\frac{K_1}{\beta\gamma-\delta}$ and note that as we assume $\beta\gamma > \delta$ it follows that $B_3 > 2B_1$.

3.D.6 Stability of the phage-free endemic equilibrium E_K^*

Consider $E_K^* = (S_K^*, I_K^*, K, 0)$ where $K > c$. Thus we need to use Jac_2 unlike the previous cases, but we again make use of the McCluskey and van den Driessche [48]

Lemma which requires the use of the jacobian itself, namely

$$Jac_2(I_K^*, K, 0) = \begin{pmatrix} -\alpha(K) - \mu & (N - I_K^*)\frac{aH}{(B-c+H)^2} & 0 \\ 0 & -r & -\gamma\frac{K}{K_1+K} \\ 0 & 0 & \beta\gamma\frac{K}{K_1+K} - \delta \end{pmatrix}$$

and

$$Jac_2^{[2]}(E_K^*) = \begin{pmatrix} -\alpha(K) - \mu - r & -\gamma\frac{K}{K_1+K} & 0 \\ 0 & -\alpha(K) - \mu + \left(\beta\gamma\frac{K}{K+K_1} - \delta\right) & (N - I^*)\frac{aH}{(K-c+H)^2} \\ 0 & 0 & -r + \left(\beta\gamma\frac{K}{K+K_1} - \delta\right) \end{pmatrix}.$$

We can compute the trace and determinant of Jac_2 and the determinant of $Jac_2^{[2]}$ evaluated at E_K^* to determine the stability of E_K^*, finding that

$$tr(Jac_2(E_K^*)) = -\alpha(K) - \mu + \left(\beta\gamma\frac{K}{K+K_1} - \delta\right)$$

with

$$\begin{aligned} \det Jac_2(E_K^*) =& [-\alpha(K) - \mu] \det \begin{bmatrix} -r & -\gamma\frac{K}{K_1+K} \\ 0 & \beta\gamma\frac{K}{K_1+K} - \delta \end{bmatrix} \\ & - (N - I_1^*)\frac{aH}{(K-c+H)^2} \det \begin{bmatrix} 0 & -\gamma\frac{K}{K_1+K} \\ 0 & \beta\gamma\frac{K}{K_1+K} - \delta \end{bmatrix} \\ =& [-\alpha(K) - \mu][-r]\left[\beta\gamma\frac{K}{K_1+K} - \delta\right] \end{aligned}$$

and

$$\begin{aligned}\det Jac_2^{[2]}(E_K^*) =&[-\alpha(K)-\mu-r]\det\begin{bmatrix}-\alpha(K)-\mu+\beta\gamma\frac{K}{K_1+K}-\delta & (N-I_1^*)\frac{aH}{(K-c+H)^2}\\ 0 & -r+\beta\gamma\frac{K}{K_1+K}-\delta\end{bmatrix}\\ &+\gamma\frac{K}{K_1+K}\det\begin{bmatrix}0 & (N-I_1^*)\frac{aH}{(K-c+H)^2}\\ 0 & -r+\beta\gamma\frac{K}{K_1+K}-\delta\end{bmatrix}\\ =&[-\alpha(K)-\mu-r]\left[-\alpha(K)-\mu+\beta\gamma\frac{K}{K+K_1}-\delta\right]\left[-r+\beta\gamma\frac{K}{K_1+K}-\delta\right].\end{aligned}$$

Common to all three expressions is that if $\beta\gamma\frac{K}{K+K_1}-\delta<0$, then they are each negative. And if $\beta\gamma\frac{K}{K+K_1}-\delta>0$, then $\det Jac_2$ at E_K^* is positive. Solving for K, we see that

$$\beta\gamma\frac{K}{K+K_1}-\delta \qquad \Longleftrightarrow \qquad K<B_1$$

and so

$$E_K^* \text{ is stable} \qquad \Longleftrightarrow \qquad K<B_1.$$

Note that the stability condition of E_K^* is contrary to the existence condition for E_1^* and so there can only ever be at most one locally stable endemic equilibrium point at a time.

3.D.7 Stability of the interior endemic equilibrium E_1^*

Lastly, consider the local stability of interior endemic equilibrium $E_1^*=(I_1^*,B_1,P_1)$ which exists if $c<B_1<K$. Because $B_1>c$, again Jac_2 is used to evaluate the local

stability. We write

$$Jac_2(I_1^*, B_1, P_1) = \begin{pmatrix} -\alpha(B_1) - \mu & (N - I^*)\frac{aH}{(B_1 - c + H)^2} & 0 \\ 0 & r - 2\frac{r}{K}B_1 - \gamma\frac{K_1}{(K_1+B_1)^2}P_1 & -\gamma\frac{B_1}{K_1+B_1} \\ 0 & \beta\gamma\frac{K_1}{(K_1+B_1)^2}P_1 & \beta\gamma\frac{B_1}{B_1+K_1} - \delta \end{pmatrix}$$

and note that as previously demonstrated $\beta\gamma\frac{B_1}{B_1+K_1} - \delta = 0$ and we can write $J(2,2) = r - 2\frac{r}{K}B_1 - \gamma\frac{K_1}{(K_1+B_1)^2}P_1$. Thus the Jac_2 and its second additive compound are

$$Jac_2(I_1^*, B_1, P_1) = \begin{pmatrix} -\alpha(B_1) - \mu & (N - I^*)\frac{aH}{(B_1 - c + H)^2} & 0 \\ 0 & J(2,2) & -\gamma\frac{B_1}{K_1+B_1} \\ 0 & \beta\gamma\frac{K_1}{(K_1+B_1)^2}P_1 & 0 \end{pmatrix}$$

and

$$Jac_2^{[2]}(I_1^*, B_1, P_1) = \begin{pmatrix} -\alpha(B_1) - \mu + J(2,2) & -\gamma\frac{B_1}{K_1+B_1} & 0 \\ \beta\gamma\frac{K_1}{(K_1+B_1)^2}P_1 & -\alpha(B_1) - \mu & (N - I^*)\frac{aH}{(B_1 - c + H)^2} \\ 0 & 0 & J(2,2) \end{pmatrix}.$$

The trace and determinant are straightforward to compute, with

$$tr(Jac_2(I_1^*, B_1, P_1)) = -\alpha(B_1) - \mu + J(2,2)$$

and

$$\begin{aligned}\det Jac_2(I_1^*, B_1, P_1) =&(-\alpha(B_1) - \mu) \det \begin{bmatrix} J(2,2) & -\gamma\frac{B_1}{B_1+K_1} \\ \beta\gamma\frac{K_1}{(K_1+B_1)^2}P_1 & 0 \end{bmatrix} \\ &- (N - I_1^*)\frac{aH}{(B_1 - c + H)^2} \det \begin{bmatrix} 0 & -\gamma\frac{B_1}{B_1+K_1} \\ 0 & 0 \end{bmatrix} \\ =&[-\alpha(B_1) - \mu]\gamma\frac{B_1}{B_1 + K_1}\beta\gamma\frac{K_1}{(K_1 + B_1)^2}P_1 < 0.\end{aligned}$$

So the determinant is always negative, and the trace can be negative if $J(2,2) < 0$. Lastly, consider

$$\begin{aligned}\det Jac_2^{[2]}(I_1^*, B_1, P_1) =&J(2,2) \det \begin{bmatrix} -\alpha(B_1) - \mu + J(2,2) & -\gamma\frac{B_1}{B_1+K_1} \\ \beta\gamma\frac{K_1}{(K_1+B_1)^2}P_1 & -\alpha(B_1) - \mu \end{bmatrix} \\ &-(N - I_1^*)\frac{aH}{(B_1 - c + H)^2} \det \begin{bmatrix} -\alpha(B_1) - \mu + J(2,2) & -\gamma\frac{B_1}{B_1+K_1} \\ 0 & 0 \end{bmatrix} \\ =&J(2,2)\Big\{[-\alpha(B_1) - \mu + J(2,2)][-\alpha(B_1) - \mu] \\ &+ \beta\gamma\frac{K_1}{(K_1 + B_1)^2}P_1\gamma\frac{B_1}{B_1 + K_1}\Big\},\end{aligned}$$

which appears complicated but the important part is that $J(2,2) < 0$ implies that it is negative. Furthermore, $0 < J(2,2) < \alpha(B_1) + \mu$ implies that $\det Jac_2^{[2]}(E_1^*) > 0$, and $J(2,2) > \alpha(B_1) + \mu$ implies that both $\det Jac_2^{[2]}(E_1^*) > 0$ and $tr(E_1) > 0$. We saw previously that $J(2,2) < 0$ is equivalent to $B_1 < B_3$, thus

$$E_1^* \text{ is stable} \qquad \Longleftrightarrow \qquad B_1 < B_3 = B_1 + \frac{\beta\gamma}{\beta\gamma - \delta}.$$

3.D.8 Local stability summary, bifurcation diagrams and numerical simulations

Noting that there are at most 2 equilibria that exist at any one time other than E_0, and writing 'un' for 'locally unstable' and 's' for 'locally asympototically stable', we can summarize the preceding local stability results with a proposition.

Proposition 6 (Local stability of the non-shedding case): E_0 always exists and is locally stable for all parameter values.

If $c < K$	and $c \geq B_1$
	$B_3 \leq K$ implies E_1(un) and E_K^*(un) exist,
	$K < B_3$ implies E_1(s) and E_K^*(un) exist
	and $c < B_1$
	$K < B_1$ implies E_K^*(s) exists
	$B_1 < K < B_3$ implies E_K^*(un) and E_1^*(s) exist
	$B_3 \leq K$ implies E_K^*(un) and E_1^*(un) exist.
If $c \geq K$	and $c \geq B_1$
	$K < B_1$ implies E_K(s) exists
	$B_1 < K < B_3$ implies E_K(un) and E_1(s) exist
	$B_3 \leq K$ implies E_K(un) and E_1(un) exist
	and $c < B_1$
	as $B_1 < B_3$ then E_K(s) exists.

The results of Proposition 6 are perhaps better understood as a bifurcation diagram. Figure 3.1 demonstrates the changes in stability as the carrying capacity K is varied. The upper diagram is for the case when the minimum infectious dose c is greater

than B_1, which means that only E_1 can exist, and not E_1^*. The lower figure has $c < B_1$, which reverses the situation.

If $K = B_3$, implying $J(2,2) = 0$, then computing $\det[\lambda I - Jac_1(E_1)]$ we find,

$$\det \begin{pmatrix} \lambda + \alpha(B_1) + \mu & 0 & 0 \\ 0 & \lambda & -\gamma \frac{B_1}{B_1+K_1} \\ 0 & \beta\gamma \frac{K_1}{(K_1+B_1)^2} P_1 & \lambda \end{pmatrix}$$
$$= (\lambda + \alpha(B_1) + \mu) \left\{ \lambda^2 + \beta\gamma \frac{K_1}{(B_1+K_1)^2} P_1 \frac{\gamma B_1}{B_1+K_1} \right\},$$

which has one real negative and two purely imaginary roots. We conclude that E_1 undergoes a Hopf bifurcation as K passes B_1, and E_1 changes from locally stable to unstable. In Figure 3.2, we demonstrate the existence of limit cycles occuring as a result of the unstable E_1.

The stability conditions for the endemic equilibrium E_1^* are the same as for E_1 and it also undergoes a Hopf bifurcation when it exists and K increases passed B_3. The only difference in the calculation of the eigenvalues of $Jac_2(E_1^*)$ is that the second entry in Jac_2 is nonzero, but as $\xi = 0$, the zeros in the first column reduce the calculation of the eigenvalues of $Jac_2(E_1^*)$ to that shown above.

When E_1 or E_1^* is unstable and the carrying capacity K is less than the MID (c), cycles are observed numerically in the bacteria-phage system (BP) but not the susceptible-infected (SI) system. If K is sufficiently larger than c, implying that the MID is at a level such that bacteria at carrying capacity would cause infections, the cycles exist in both the SI and BP systems with the infected population peaking 4 days after and the phage population 8 days after in Figure 3.2. While these cycles are far too short to match real world situations, as the infected class peaks occurred after the bacteria class, and because with shedding at zero the BP system influences the SI system unidirectionally, their existence does support the idea that cycles

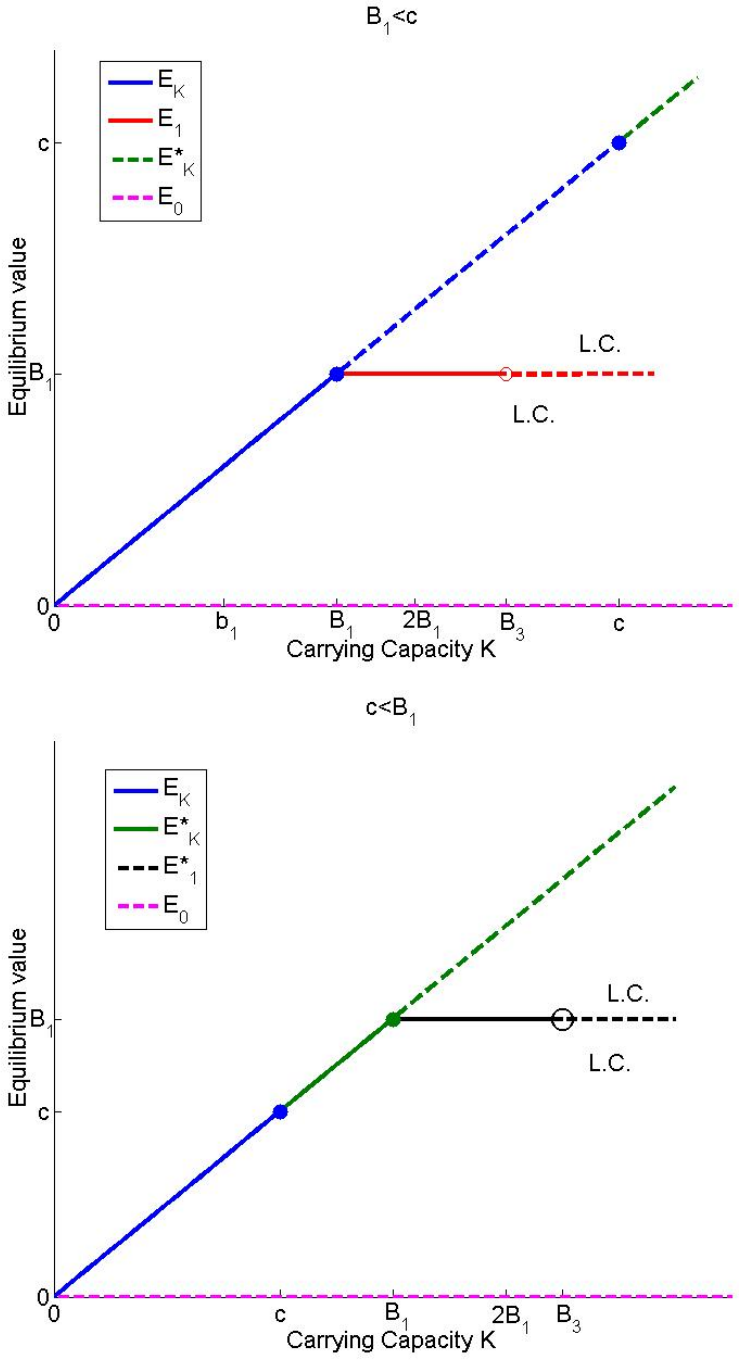

Figure 3.1: Bifurcation diagrams when $\xi = 0$ and there is no shedding. Limit cycles exist when E_1 and E_1^* undergo Hopf bifurcations, and are denoted L.C.

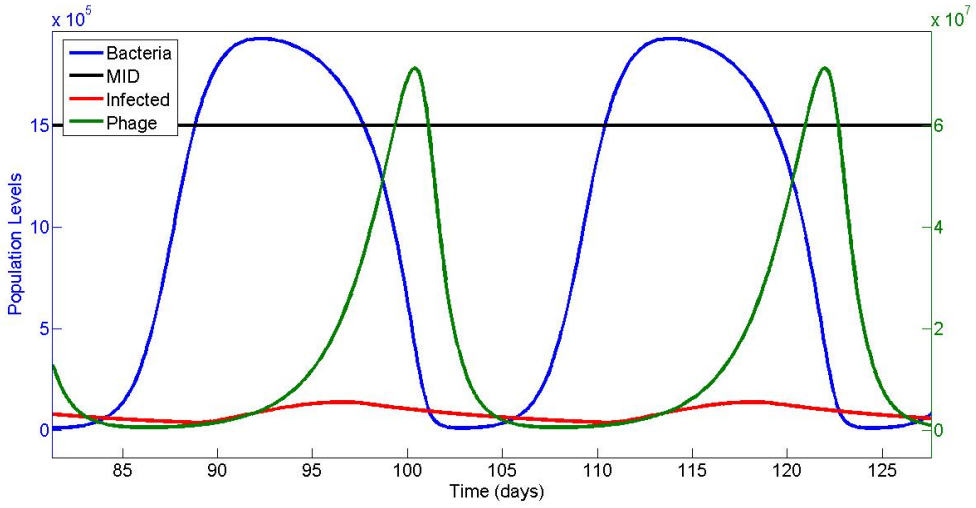

Figure 3.2: Cycles in Phage, Bacteria and Infected populations. The Bacteria peak ends first, followed by the Infected 4 days later and Phage 8 days later. Parameters are $r = 3, K = 7.3e6, \gamma = 0.02, K_1 = 1.6e6, \beta = 80, \delta = 1, \xi = 0, a = 0.1, c = 7.1e6, \mu = 0.1$ and $H = 1e6$.

that naturally occur are bottom-up and not top-down in cause. When shedding is included, the cycles lengthen to relevant levels as we shall see in the next section.

3.E Existence and Stability of Equilibria with Shedding

3.E.1 Existence of equilibria

The complete absence of human contamination of the water supply is the ideal, but it is certainly not the reality anywhere and particularly not in places where the disease is endemic. Noting that the first equation of (3.1) is not necessary as

$S + I = N$, we can rewrite it as follows

$$\begin{aligned}
\frac{dI}{dt} =& \alpha(B)(N - I) - \mu I, \\
\frac{dB}{dt} =& rB\left(1 - \frac{B}{K}\right) - \gamma\frac{B}{K_1 + B}P + \xi I, \\
\frac{dP}{dt} =& \beta\gamma\frac{B}{K_1 + B}P - \delta P + \alpha\xi I.
\end{aligned} \tag{3.3}$$

From Equation 1, at a steady state if $\alpha(B) = 0$ then $I^* = 0$. In this case equations 2 and 3 become the same as in the last section, meaning that

$$\begin{aligned}
0 &= \beta\gamma\frac{B}{K_1 + B}P - \delta P \\
0 &= \left(\beta\gamma\frac{B}{K_1 + B} - \delta\right)P.
\end{aligned}$$

Thus, the same endemic equilibria $E_0 = (N, 0, 0, 0)$, $E_K = (N, 0, K, 0$ and $E_1 = (N, 0, B_1, P_1)$ exist as before, with the same conditions. Namely that $K \leq c$ for E_K to exist, and $B_1 \leq c$ with $B_1 < K$ for E_1 to exist.

As ξ is not in Equation 1 of (3.3), it is then identical to its analogue in (3.2). So if $\alpha(B) \neq 0$ at steady state, then $I^* = G_1(B^*) = Na\frac{(B^*-c)}{(a+\mu)(B^*-c)+\mu H}$. Equations 2 and 3 of (3.3) become

$$\begin{aligned}
0 &= \beta\gamma\frac{B}{K_1 + B}P - \delta P + \alpha\xi I^* \\
0 &= \left(\beta\gamma\frac{B}{K_1 + B} - \delta\right)P + \alpha\xi I^*
\end{aligned}$$

and the latter can be solved to attain a P^* value, writing $G_1(B^*)$ for I^*

$$\begin{aligned} P^* &= \frac{-\alpha\xi I^*}{\beta\gamma\frac{B}{K_1+B}-\delta} = \frac{-\alpha\xi G_1(B^*)}{\beta\gamma\frac{B}{K_1+B}-\delta} \\ &= \frac{-\alpha\xi G(B^*)(K_1+B)}{\beta\gamma B^* - \delta(K_1+B^*)}. \end{aligned}$$

This expression for P^* provides a condition for B^* as the denominator must be strictly negative in order to have a well defined and positive value for P^*. We see that

$$\begin{aligned} &\beta\gamma\frac{B}{K_1+B} - \delta < 0 \\ \Rightarrow &B^* < (K_1+B^*)\frac{\delta}{\beta\gamma} = K_1\frac{\delta}{\beta\gamma} + B^*\frac{\delta}{\beta\gamma}, \\ &\left(1-\frac{\delta}{\beta\gamma}\right)B^* < K_1\frac{\delta}{\beta\gamma}, \\ &B^* < \frac{K_1\delta}{\beta\gamma-\delta} = B_1 \end{aligned}$$

is another condition for any equilibrium with $\alpha(B^*) \neq 0$. So we have an expression that gives a unique P^* for each value of B^*. Solving Equation 2 of (3.3) at equilibrium for B^* will then possibly lead to endemic equilibria E^* . Dropping the asterisks on B^* for convenience,

$$\begin{aligned} 0 &= rB\left(1-\frac{B}{K}\right) + \xi I^* - \gamma\frac{B}{K_1+B}P^* \\ 0 &= rB\left(1-\frac{B}{K}\right) + \xi G(B) + \gamma\frac{B}{K_1+B}\frac{\phi\xi G(B)(K_1+B)}{\beta\gamma B - \delta(K_1+B)} \\ 0 &= rB\left(1-\frac{B}{K}\right) + \xi G(B) + \gamma B\frac{\phi\xi G(B)}{\beta\gamma B - \delta(K_1+B)} \\ 0 &= rB\left(1-\frac{B}{K}\right) + \left[1+\gamma\phi\frac{B}{(\beta\gamma-\delta B-\delta K_1)}\right]\xi\frac{Na(B-c)}{(a+\mu)(B-c)+\mu H} \\ 0 &= F(B) + G(B) \end{aligned} \tag{1.4}$$

where

$$F(B) = rB\left(1 - \frac{B}{K}\right)[(a+\mu)(B-c) + \mu H][(\beta\gamma - \delta)B - \delta K_1)]$$
$$G(B) = Na\xi[\gamma(\phi+\beta)B - \delta K_1](B-c).$$

Note that $F(B)$ is a quartic with roots 0, K, $B_2 := c - \frac{\mu H}{a+\mu}$ and B_1, which was defined previously as $B_1 = \frac{\delta K_1}{\beta\gamma - \delta}$, that opens downwards. The three roots of 0, B_1 and K are nonnegative, but B_2 could be negative or zero with realistic parameters. To find solutions to $0 = F(B) + G(B)$ we will plot $F(B)$ and $-G(B)$ to look for intersections. As such note that $-G(B)$ is a downward opening parabola, with roots c and $b_1 := \frac{\delta K_1}{\gamma(\phi+\beta) - \delta}$.

The roots of the two functions have some obvious relationships which limit the number of possibilities we need to consider when plotting them. Consider b_1 and B_1 which are clearly related. We assume $\beta\gamma - \delta > 0$ and as $\phi > 0$, being part of the shedding term for the phage population $\phi\xi$, it is clear that $0 < b_1 < B_1$. Also $B_2 < c$ as all parameter values are positive. Previously we found that $c < B^* < B_1$ to ensure $P^* > 0$ and $\alpha(B^*) > 0$, so this imples $c < B_1$ is a condition for any B^* to exist.

Between the third and fourth roots of F, we see that $F(B) > 0$, whatever those roots may be. If the largest root is B_1, then we find a problem if c is the next largest of $\{b_1, c, K, B_1, B_2\}$. As $-G(c) = 0$ with $-G(B) < 0$ for $B \geq c$, and $F(c) > 0$, then clearly no intersections can occur until $B > B_1$ when $F(B)$ is no longer nonnegative. Any such intersection would be inadmissible as $B^* > B_1$ for that B^*. Also, any intersections between F and $-G$ with $B < c$ are also inadmissible as we require $B^* > c$. Hence, if $c < B_1$ and $\{c, B_1\}$ are the largest of $\{b_1, c, K, B_1, B_2\}$ then there will be no endemic equilibria.

Case	Subcase	Ordering
Ia)		
$0 < B_2 < B_1 < K$	i)$B_2 < b_1 < B_1$	$B_2 < b_1 < c < B_1$
		$B_2 < c < b_1 < B_1$
	ii)$0 < b_1 < B_2$	$b_1 < B_2 < c < B_1$
Ib)		
$0 < B_2 < K < B_1$	i) $b_1 > K$	$K < c < b_1 < B_1$
		$c < K < b_1 < B_1$
	ii) $B_2 < b_1 < K$	$B_2 < b_1 < c < K$
		$B_2 < c < b_1 < K$
	iii) $b_1 < B_2$	$b_1 < B_2 < c < K < B_1$
I c)		
$K < B_2 < B_1$	i) $B_2 < b_1 < B_1$	$B_2 < c < b_1 < B_1$
II a)		
$B_2 < 0 < B_1 < K$	i) $b_1 < B_1$	$b_1 < c < B_1 < K$
		$c < b_1 < B_1 < K$
II b)		
$B_2 < 0 < K < B_1$	i)$K < b_1$	$K < c < b_1 < B_1$
		$c < K < b_1 < B_1$
	ii) $b_1 < K$	$b_1 < c < K < B_1$
		$c < b_1 < K < B_1$

Table 3.2: Possible ordering of $\{B_2, B_1, K, b_1, c\}$. The first column determines the order of $\{B_2, B_1, K\}$, the second places b_1 in that ordering, and the third column places c within the ordering.

The possible orderings of $\{B_2, B_1, K, b_1, c\}$ are outline in Table 3.2. There are only 9 combinations of $\{B_2, B_1, K, b_1\}$ and 15 orderings of all of the roots of F and G when all of the restrictions are considered. From this we can plot all possible configurations of F and G as in Figures 3.3 and 3.4. There can be up to 4 equilibria at one time depending on the relationships among the parameters. From Figures 3.3 and 3.4, we see that when there are two internal equilibria, the values of $B^*_{1,2}$ are between the second and third entries in the ordering of $\{c, K, b_1, B_1\}$. Also, note that E_1 and $E^+_{1,2}$ cannot exist at the same time as their conditions for existence are contrary.

We can summarize these results with a proposition.

Proposition 7 (Existence of Equilibria): The equilibrium $E_0 = (N, 0, 0, 0)$ always exists.

If $c \geq K$ and $B_1 \leq c$,

if also $B_1 > K$, then only E_K exists.

if $B_1 \leq K$ then E_K and E_1 exist.

and $B_1 > c$,

if $c < b_1$ then there are up to $B^*_{1,2} \in (c, b_1)$ and E_K.

if $c > b_1$ then there are no internal equilibria but E_K exists.

If $c < K$ and $B_1 > c$

then B^* exists between the second and third

in the ordering of $\{c, K, b_1, B_1\}$.

and $B_1 \leq c$

there are no internal equilibria and E_1 is an equilibrium.

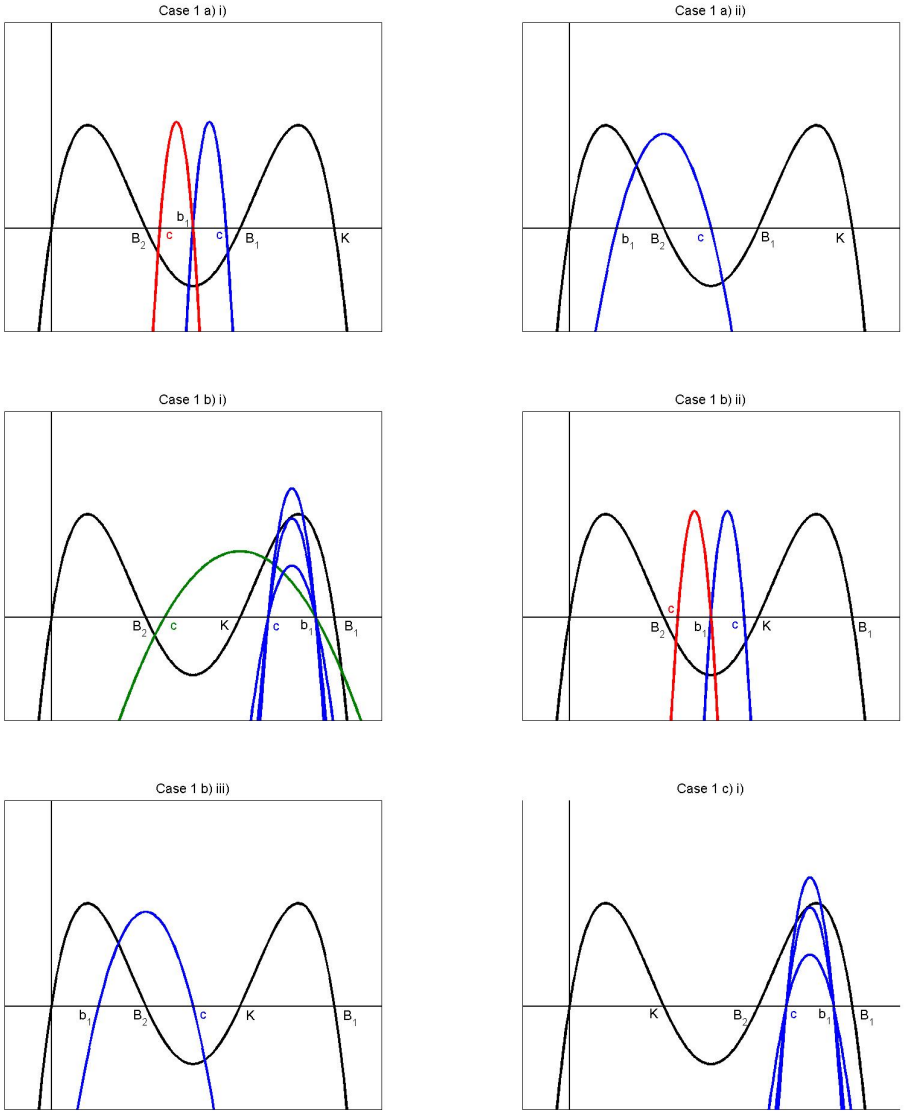

Figure 3.3: In each graph above there are at most two intersections between the quartic (in black) and the quadratics (in red, blue or green). Relevant intersections need to be greater than c, but less than B_1.

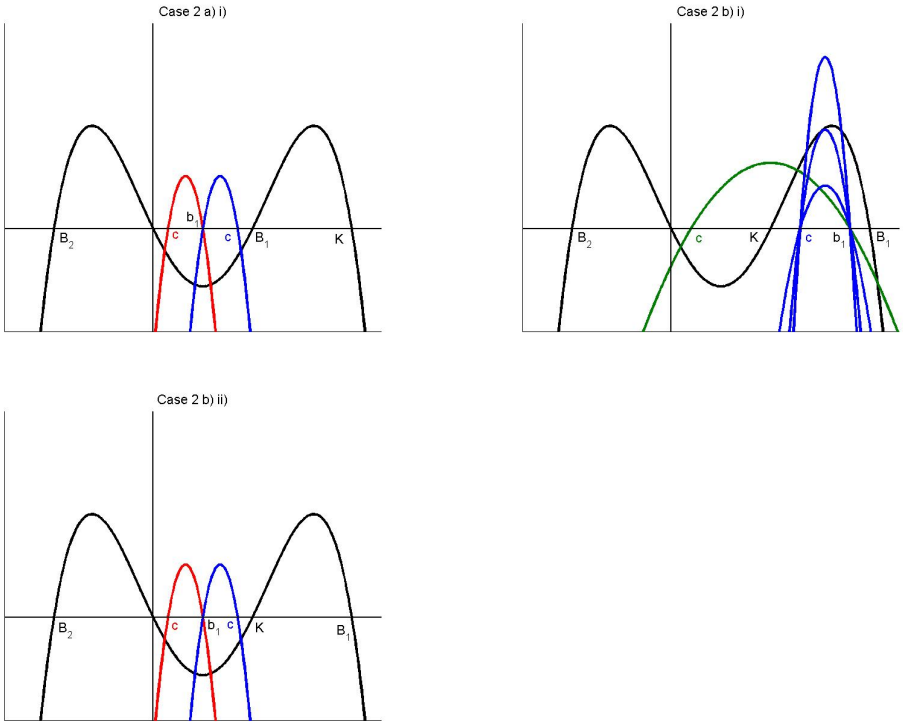

Figure 3.4: The cases where B_2 is negative and in each graph above there are at most two intersections between the quartic (in black) and the quadratics (in red, blue or green). Relevant intersections need to be greater than c, but less than B_1.

3.E.2 Linearization

Due to the threshold in $\alpha(B)$, we will have two linearizations of (3.3) with the first having $\alpha(B) = 0$ denoted J_1

$$J_1(I,B,P) = \begin{pmatrix} -\mu & 0 & 0 \\ \xi & r - 2\frac{r}{K}B - \frac{\gamma K_1}{(K_1+B)^2}P & -\gamma\frac{B}{K_1+B} \\ \phi\xi & \beta\gamma\frac{aH}{(B-c+H)^2}P & \beta\gamma\frac{B}{K_1+B} - \delta \end{pmatrix},$$

and the second linearization applies when $\alpha(B) \neq 0$, denoted J_2

$$J_2(I,B,P) = \begin{pmatrix} -\alpha(B) - \mu & (N-I)\frac{aH}{(B-c+H)^2} & 0 \\ \xi & r - 2\frac{r}{K}B - \frac{\gamma K_1}{(K_1+B)^2}P & -\gamma\frac{B}{K_1+B} \\ \alpha\xi & \beta\gamma\frac{aH}{(B-c+H)^2}P & \beta\gamma\frac{B}{K_1+B} - \delta \end{pmatrix}.$$

3.E.3 Stability of disease-free, bacteria-free, phage-free equilibrium E_0

Consider J_1 for $E_0 = (N, 0, 0, 0)$ as $B_0 = 0 < c$. The result is a triangular matrix

$$J_1(0,0,0) = \begin{pmatrix} -\mu & 0 & 0 \\ \xi & r & 0 \\ \alpha\xi & 0 & -\delta \end{pmatrix},$$

with eigenvalues $-\mu, -\delta < 0$ and $r > 0$. This means that the disease free, bacteria free and phage free equilibrium E_0 is a saddlenode equilibrium with a one-dimensional unstable manifold.

3.E.4 Stability of the disease-free phage-free equilibrium E_K

For the boundary (or disease-free, phage-free) equilibrium $E_K = (N, 0, K, 0)$ to exist, it is necessary that $K \leq c$ so that $\alpha(K) = 0$, and so we only have to use J_1 to consider the local stability. So consider

$$J_1(0, K, 0) = \begin{pmatrix} -\mu & 0 & 0 \\ \xi & -r & -\gamma\frac{K}{K_1+K} \\ \alpha\xi & 0 & \beta\gamma\frac{K}{K_1+K} - \delta \end{pmatrix}$$

and

$$J_1^{[2]}(0, K, 0) = \begin{pmatrix} -\mu - r & \left(-\gamma\frac{K}{K_1+K}\right) & 0 \\ 0 & -\mu + \beta\gamma\frac{K}{K_1+K} - \delta & 0 \\ -\alpha\xi & \xi & -r + \left(\beta\gamma\frac{K}{K_1+K} - \delta\right) \end{pmatrix}$$

and note that

$$\begin{aligned} tr(J_1(0, K, 0)) &= -\mu - r + \left(\beta\gamma\frac{K}{K_1 + K} - \delta\right), \\ \det J_1(0, K, 0) &= \mu r \left(\beta\gamma\frac{K}{K_1 + K} - \delta\right), \\ \det J_1^{[2]} &= (-\mu - r)\left(-\mu + \beta\gamma\frac{K}{K_1 + K} - \delta\right)\left(-r + \beta\gamma\frac{K}{K_1 + K} - \delta\right). \end{aligned}$$

If $\beta\gamma\frac{K}{K_1+K} - \delta < 0$ this implies that $tr(J_1)$, $\det J_1$ and $\det J_1^{[2]}$ are all negative, but if $\beta\gamma\frac{K}{K_1+K} - \delta > 0$ then $\det J_1 > 0$. By Lemma 7 this means that E_K is stable if, and only if $\beta\gamma\frac{K}{K_1+K} < 0$. Rearranging to solve for K,

$$E_K \text{ is stable} \qquad \iff \qquad K < \frac{\delta K_1}{\beta\gamma - \delta} = B_1.$$

Note that $B_1 < K$ is required for E_1 to exist, so the existence of E_1 and the stability of E_K are contrary notions.

3.E.5 Stability of the disease-free equilibrium E_1

This equilibrium is also a boundary equilibrium but is perhaps more realistic as it has a nonzero phage level. The bacteria level is defined $B_1 = \frac{\delta K_1}{\beta\gamma - \delta}$ and $P_1 = F_1(B_1) = \frac{r}{K}(-B_1 + K)(B_1 + K_1)$. For $E_1 = (N, 0, B_1, P_1)$ to exist, $B_1 \leq c$ to ensure $\alpha(B_1) = 0$, and $B_1 < K$ for $P_1 > 0$. Note that the bacterial level here is less than in the E_K equilibrium and recall that if $B_1 = K$ then $P_1 = 0$ and E_1 is simply E_K. Here we again use J_1

$$J_1(0, B_1, P_1) = \begin{pmatrix} -\mu & 0 & 0 \\ \xi & r - 2\frac{r}{K}B_1 - \frac{\gamma K_1}{(K_1+B_1)^2}P_1 & -\gamma\frac{B_1}{B_1+K_1} \\ \alpha\xi & \beta\gamma\frac{K_1}{(K_1+B_1)^2}P_1 & \beta\gamma\frac{B_1}{B_1+K_1} - \delta \end{pmatrix}$$

but note that in the last entry of J_1

$$\beta\gamma\frac{B_1}{B_1 + K_1} - \delta = \frac{\beta\gamma\delta K_1}{(\beta\gamma - \delta)K_1 + \delta K_1} - \delta = \frac{\beta\gamma\delta K_1}{\beta\gamma K_1} - \delta = 0$$

so that

$$J_1(0, B_1, P_1) = \begin{pmatrix} -\mu & 0 & 0 \\ \xi & r - 2\frac{r}{K}B_1 - \frac{\gamma K_1}{(K_1+B_1)^2}P_1 & -\gamma\frac{B_1}{B_1+K_1} \\ \alpha\xi & \beta\gamma\frac{K_1}{(K_1+B_1)^2}P_1 & 0 \end{pmatrix}.$$

Defining $J(2,2) = r - 2\frac{r}{K}B_1 - \gamma\frac{K_1}{(K_1+B_1)^2}P_1$ again as in the previous non-shedding case, the second additive compound matrix of J_1 is

$$J_1^{[2]}(0, B_1, P_1) = \begin{pmatrix} -\mu + J(2,2) & -\gamma\frac{B_1}{B_1+K_1} & 0 \\ \beta\gamma\frac{K_1}{(K_1+B_1)^2}P_1 & -\mu & 0 \\ -\alpha\xi & \xi & J(2,2) \end{pmatrix}.$$

The determinant of J_1 is

$$\begin{aligned}\det J_1(0, B_1, P_1) &= -\mu \det \begin{bmatrix} J(2,2) & -\gamma \frac{B_1}{B_1+K_1} \\ \beta\gamma \frac{K_1}{(K_1+B_1)^2} P_1 & 0 \end{bmatrix} \\ &= -\mu\gamma \frac{B_1}{B_1+K_1} \beta\gamma \frac{K_1}{(K_1+B_1)^2} P_1 \\ &< 0\end{aligned}$$

so it will always satisfy the antecedent of Lemma 7. The trace is given

$$tr(J_1(0, B_1, P_1)) = -\mu + J(2,2)$$

As before $J(2,2) < 0$ if, and only if, $K < B_3 = B_1 + \frac{\beta\gamma K_1}{\beta\gamma - \delta}$. Thus we can conclude about the trace that

$$\begin{aligned} J(2,2) < 0 \qquad &\Rightarrow \qquad tr(J_1) < 0, \\ J(2,2) > 0, -\mu + J(2,2) < 0 \qquad &\Rightarrow \qquad tr(J_1) < 0, \\ J(2,2) > 0, -\mu + J(2,2) > 0 \qquad &\Rightarrow \qquad tr(J_1) > 0. \end{aligned}$$

Lastly consider the sign of $\det J_1^{[2]}$

$$\begin{aligned}\det J_1^{[2]}(0, B_1, P_1) &= J(2,2) \det \begin{bmatrix} -\mu + J(2,2) & -\gamma \frac{B_1}{B_1+K_1} \\ \beta\gamma \frac{K_1}{(K_1+B_1)^2} P_1 & -\mu \end{bmatrix} \\ &= J(2,2) \left\{ [-\mu + J(2,2)][-\mu] + \left(\beta\gamma \frac{K_1}{(K_1+B_1)^2} P_1 \right) \left(\gamma \frac{B_1}{B_1+K_1} \right) \right\},\end{aligned}$$

where it is clear that if $J(2,2) < 0$ then $\det J_1^{[2]} < 0$ and if $J(2,2) > 0$ but $J(2,2) - \mu < 0$ then $\det J_1^{[2]} > 0$. The last case of $J(2,2) > 0$ and $J(2,2) - \mu > 0$ is not necessary for our purposes. To summarize about the trace and determinant of the

second additive compound matrix

$$\begin{aligned} J(2,2) < 0 \quad &\Rightarrow \quad tr J_1(0, B_1, P_1) < 0 \\ &\text{and} \quad \det J_1^{[2]}(0, B_1, P_1) < 0, \\ J(2,2) > 0 \quad &\Rightarrow \quad tr J_1(0, B_1, P_1) > 0 \\ &\text{or} \quad \det J_1^{[2]}(0, B_1, P_1) > 0, \end{aligned}$$

and because $\det J_1(0, B_1, P_1) < 0$ all the time, by Lemma 7

$$\begin{aligned} E_1 \text{ is stable} \quad &\iff \quad J(2,2) < 0 \\ &\iff \quad K < \frac{\beta\gamma + \delta}{\beta\gamma - \delta} K_1 = B_1 + \beta\gamma \frac{K_1}{\beta\gamma - \delta} \end{aligned}$$

writing as previously $B_3 = B_1 + \beta\gamma \frac{K_1}{\beta\gamma - \delta}$.

3.E.6 Stability of endemic equilibria E^* and $E^*_{1,2}$

The stability of the endemic steady states was found numerically. If $c > b_1$ and $c < B_1$, there is a unique endemic equilibrium, E^*. Using parameter values $r = 1, \gamma = 0.02, K_1 = 3.6e5, \beta = 80, \delta = 1, \xi = 50, \phi = 1, a = 0.1, H = 1e6, C = 5.9e5$ and $\mu = 0.1$, will achieve such a relationship. If $K = 7e5 > c$ or larger, E_K does not exist and E_0 and E^* are the only equilibria. Limit cycles are observed and if B^* and its eigenvalues are computed numerically, we see that E^* is a saddlenode equilibrium with a two-dimensional unstable manifold.

If $K = 4e5 < c = 5e5$, with all other parameters the same, then $K < c < b_1$ and two endemic equilibria exist, along with E_0 and E_K. In this case they are both saddlenode equilibria, where E_1^* (with the smaller B^* value) has a one-dimensional unstable manifold, and the other has a two-dimensional unstable manifold. If $K =$

$5.9e5 > c$ or greater, there is a unique endemic equilibria and E_K no longer exists. As before, it is a saddlenode with two dimensional unstable manifold.

Lastly, if K_1 is decreased to $K_1 = 1.6e6$, with all other parameters as before, if $c > b_1$ and the endemic equilibrium is unique, it is again a saddlenode with two dimensional unstable manifold. If instead $c < b_1$, then when the two internal equilibria exist, E_1^* (with the smaller B^*) is a saddlenode with one dimensional unstable manifold as before. The larger however, is stable as its eigenvalues all have negative real part. Finally, if $K > c$, for example $K = 2.2e6$ or higher, there is a unique endemic equilibrium E^* which is locally stable as all eigenvalues have negative real part.

3.E.7 Local stability summary, bifurcation diagrams and numerical simulations

We can summarize the local stability results of the previous sections with a proposition, writing 'un' for locally unstable, and 's' for local asymptotic stability.

Proposition 8 (Local Stability): The equilibrium E_0 is always locally unstable.

If $c \geq K$ and $B_1 \leq c$,

if $K > B_3$, then E_1(un) and E_K(un).

if $B_1 < K < B_3$ then E_1(s) and E_K(un).

if $K < B_1$ then E_K(s).

and $B_1 > c$,

if $c < b_1$ then there are up to $E^*_{1,2}$ and E_K(s),

with $B^*_i \in (c, b_1)$.

if $c > b_1$ then there are no internal equilibria but E_K(s).

If $c < K$ and $B_1 > c$,

then E^* exists,

with B^* between the second and third in the ordering of $\{c, K, b_1, B_1\}$.

and $B_1 \leq c$,

if $K > B_3$, then E_1(un).

if $K < B_3$, then E_1(s).

In addition to the disease-free, bacteria-free and phage-free equilibrium E_0, which always exists and is always locally unstable, there are at most three other equilibria for any given set of parameters. Note that E_1 and E_K are never both stable at the same time, as the condition for the local stability of E_K implies that E_1 does not exist. Of the two, E_1 is more realistic as it has the phage population existing at nonzero levels, which is certainly the case during inter-epidemic times. The existence of a stable endemic equilibrium, either when E^* is unique, or when it exists with another, which is unstable, does not match the usual pattern of explosive outbreaks of cholera, but if the B^* level is low enough, perhaps it could be biologically relevant for certain areas. Our main interest is when unstable equilibria exist and cause limit

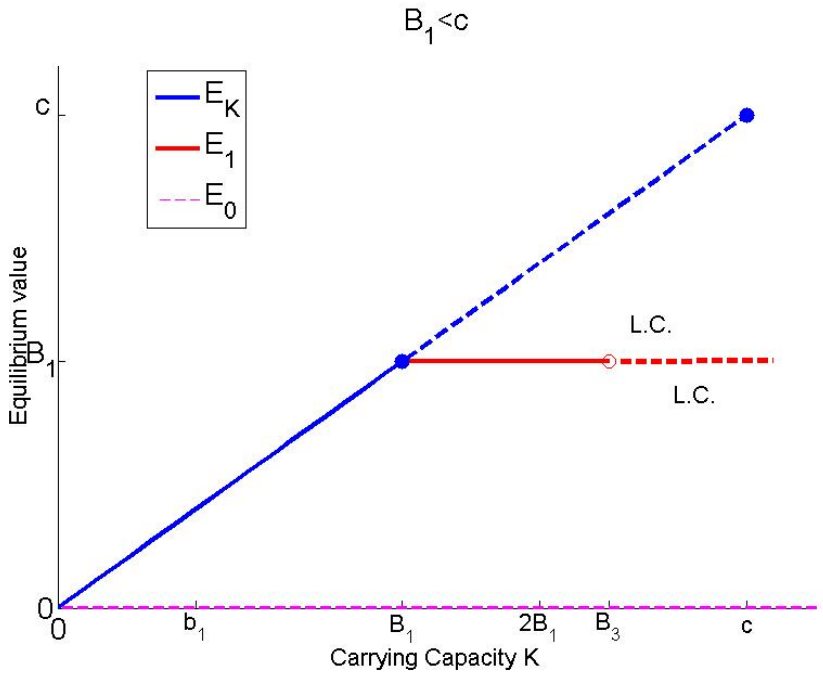

Figure 3.5: Bifurcation diagrams with all parameters positive and $B_1 < c$, which implies only nonendemic equilibria exist. Equilibrium E_1 undergoes a Hopf bifurcation when carrying capacity K increases passed B_3, leading to limit cycles denoted L.C.

cycles, as will be discussed below.

The results of Proposition 8 are perhaps better understood with bifurcation diagrams. Figure 3.5 shows the case when $B_1 < c$, and only nonendemic equilibria are possible. In the figure $B_3 < c$, which means that both E_1 and E_K can be unstable at the same time. If this was reversed and $B_3 > c$, the difference would be that E_1 would be unstable only when E_K did not exist, and the two could not be unstable for the same set of parameters.

Equilibrium E_1 is only present in the upper diagram, and when the carrying capacity

$K = B_3$, we can calculate $\det[\lambda I - J_1(E_1)]$, noting that $J(2,2) = 0$ to see that

$$\begin{aligned}\det[\lambda I - J_1(E_1)] &= \begin{pmatrix} \lambda+\mu & 0 & 0 \\ -\xi & \lambda & \gamma\frac{B_1}{B_1+K_1} \\ -\phi\xi & -\beta\gamma\frac{K_1}{(K_1+B_1)^2}P_1 & \lambda \end{pmatrix} \\ &= (\lambda+\mu)\left\{\lambda^2 + \beta\gamma\frac{K_1}{(K_1+B_1)^2}P_1\gamma\frac{B_1}{B_1+K_1}\right\}\end{aligned}$$

and observe that $J_1(E_1)$ has one negative eigenvalue and two purely imaginary eigenvalues. Thus E_1 undergoes a Hopf bifurcation as K increases passed B_3 and E_1 switches from locally stable to unstable. With parameters in the region where E_1 is unstable, we find limit cycles to exist. If $K < c$, then these cycles exist only in the BP community and do not cause any infections. Figure 3.6 demonstrates such limit cycles, with period of only 14 days, and phage peaking 5 days after the bacteria class does. If $K > c$ by a large enough amount, meaning that the minimum infectious dose is less than the normal carrying capacity of bacteria, the cycles enter the human population as well and increase greatly in period. Unlike the case with $\xi = 0$, the period of these cycles can even be approximately 180 days, which could correspond to the biannual outbreaks observed in some endemic areas. Figure 3.7 is an example of of such cycles with period of 181 days. The bacteria are the first to peak, followed by the human infected population 3 days later, and the phage 1 day after the infected class. As these cycles can exist at low levels and only enter the human population when the bacteria levels increase passed the MID, and because the bacteria peak before the infected human population, we conclude that the BP system is 'driving' these limit cycles.

Figure 3.8 contains bifurcation diagrams for the cases of endemic equilibria. The upper diagram is for when E^* is unique, and numerically it is found to always be unstable and causing limit cycles. The lower diagram is very similar, except up to two $E^*_{1,2}$ can exist. These are either both unstable, or the equilibrium with the

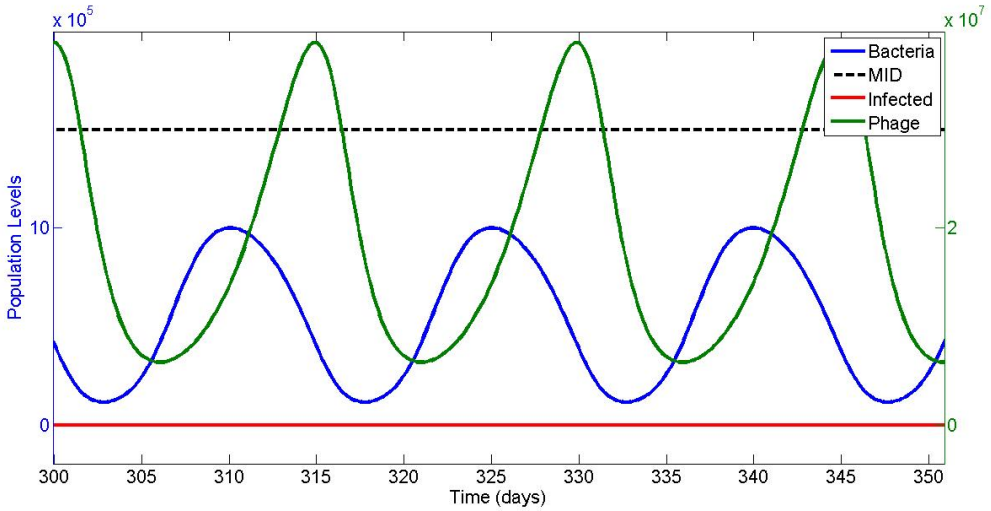

Figure 3.6: The case when E_1 is unstable and $K < c$. When the bacteria levels pass the minimum infectious dose (MID), the cycles spread to the human population as well. The period is approximately 14 days and the Phage peak 4 days the Bacteria. The parameter values used were $r = 1, K = 1.3e6, \gamma = 0.02, K_1 = 2.5e5, \beta = 80, \delta = 1, \xi = 50, \phi = 1, a = 0.1, H = 1e6, C = 1.5e6$ and $\mu = 0.1$.

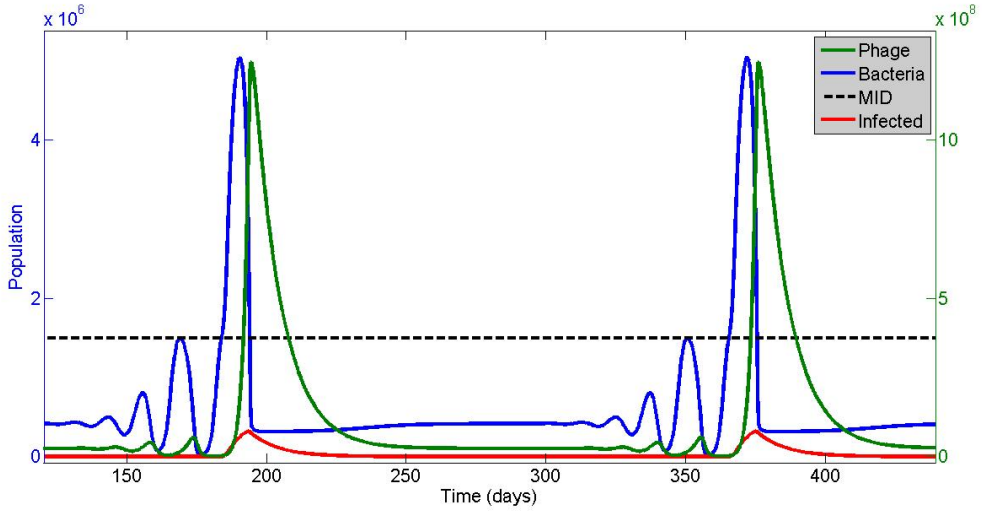

Figure 3.7: The case when E_1 is unstable and $K > c$. When the bacteria levels pass the minimum infectious dose (MID), the cycles spread to the human population as well. The Infected class peaks 3 days after the Bacteria, and the Phage 4 days after. The period is 181 days, which corresponds to biannual outbreaks in endemic areas. The parameter values used were $r = 1, K = 1.8e6, \gamma = 0.02, K_1 = 2.5e5, \beta = 80, \delta = 1, \xi = 50, \phi = 1, a = 0.1, H = 1e6, C = 1.5e6$ and $\mu = 0.1$.

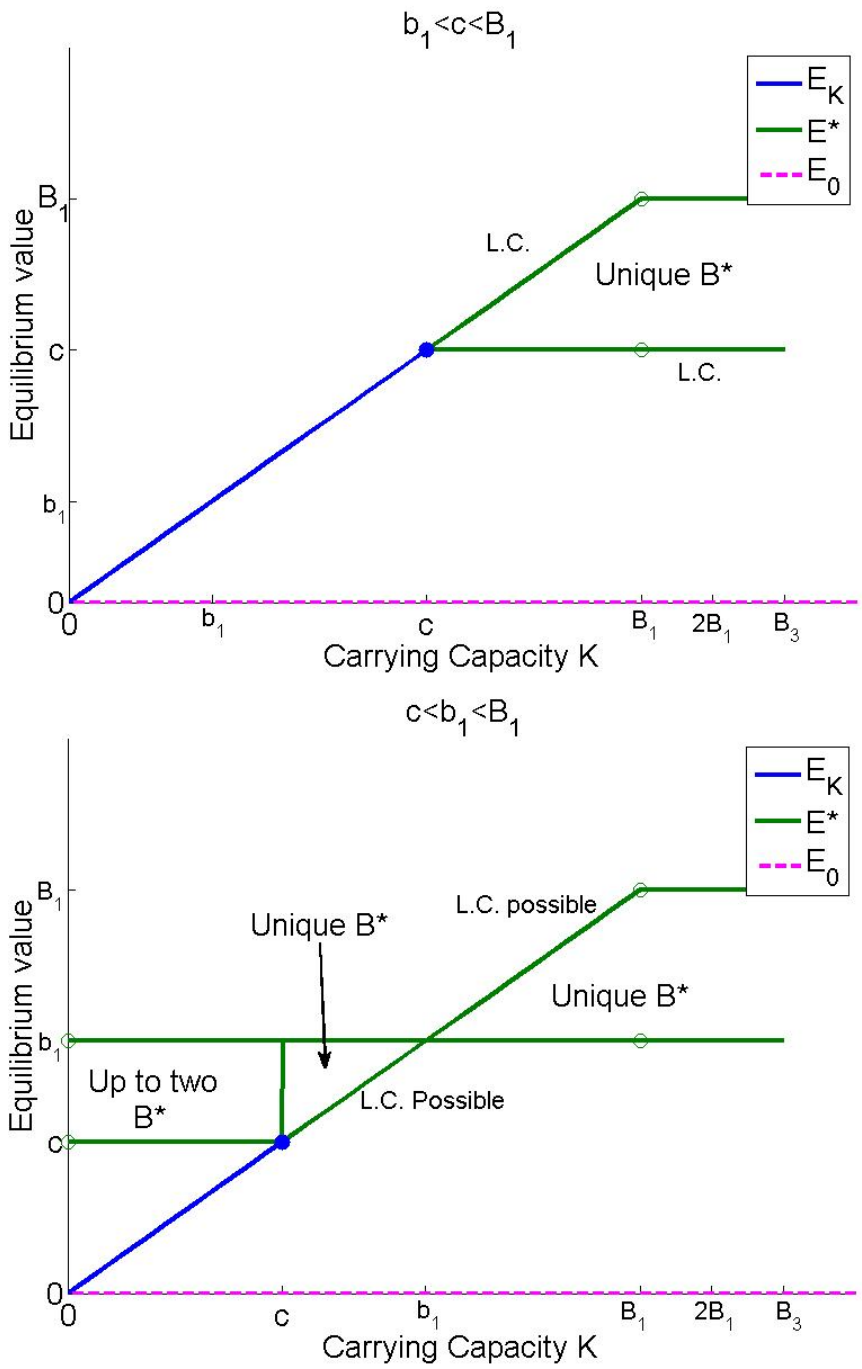

Figure 3.8: Bifurcation diagrams with all parameters positive. Limit cycles exist when E^* is unique and unstable and are denoted L.C. When $c > b_1$, E^* is always unstable and there are cycles. When $c < b_1$, these cycles exist when E^* was unstable, but are absent when it is stable. If there are two equilibria $E^*_{1,2}$, they are either both unstable, or the one with the smaller B^*_i is unstable and the larger is stable. Limit cycles are not observed with parameters in this range.

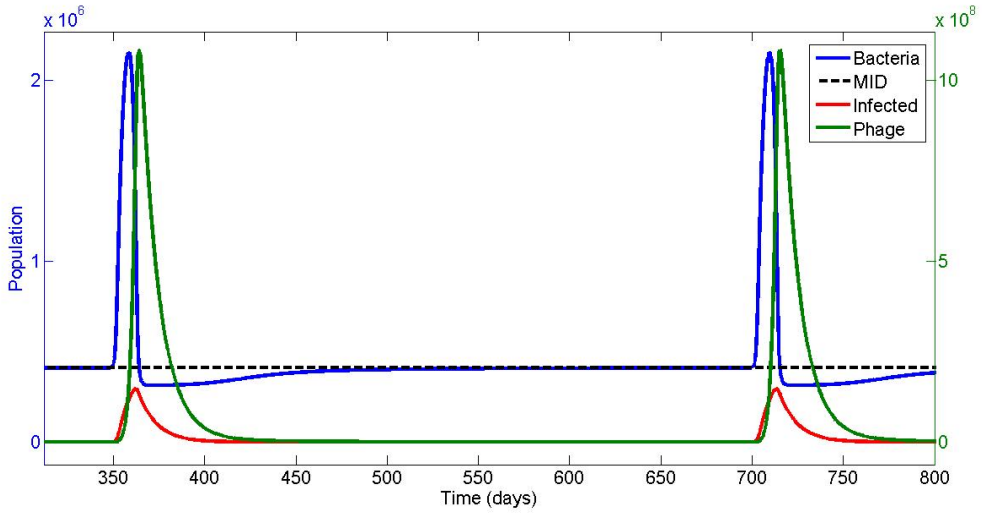

Figure 3.9: The case when E^* is unique and unstable with $K > c$. When the bacteria levels pass the minimum infectious dose (MID), the cycles spread to the human population as well. The Infected class peaks 3 days after the Bacteria, and the Phage 6 days after. The period is 350 days, which corresponds to annual outbreaks in endemic areas. The parameter values used were $r = 1, K = 4.12e5, \gamma = 0.02, K_1 = 2.5e5, \beta = 80, \delta = 1, \xi = 50, \phi = 1, a = 0.1, H = 1e6, C = 4.1e5$ and $\mu = 0.1$.

smaller B_i^* value is unstable and the larger is stable. The unique E^* in the lower diagram could be either stable or unstable for realistic parameter values, and when it is unstable, limit cycles are found to exist. These cycles range in period, but can be found with periods of approximately 360 days, as in Figure 3.9, which correspond to the annual outbreaks observed in some endemic areas.

3.F Chaos

In many countries that experience endemic cholera, there are annual cholera outbreaks which appear to be periodic. However, in countries with similar sanitation infrastructure, the outbreaks are much more frequent and lack an overwhelmingly periodic structure. The general trend is that countries closer to the equator have higher levels of outbreaks with greater frequency, while countries that are further

from the equator typically have seasonal outbreaks [18]. An explanation for this difference in outbreak type may lie in the existence of chaotic behaviour in (3.1) for certain values of the shedding parameters ξ and ϕ in relation to the temperature related parameter r.

The maximal growth rate of bacteria r is proportional to the values ξ_c and ϕ_c where chaos first occurs. If this value of r is itself proportional to average temperatures, and thus inverse to the distance from the equator, then warmer countries with a higher r value could have chaotic behaviour of bacterial levels, and thus outbreaks, with the same values of ξ and ϕ. A positive relationship between bacteria proliferation and average temperature is known to exist, so this explanation is plausible [69].

Figure 3.10 demonstrates different trends in cholera outbreaks for countries at different latitudes. Malaysia for example is the closest to the equator of the four countries shown, at a latitude of 4^o, and has a somewhat uniform distribution of monthly outbreaks when summed over 32 years. The other three countries of Romania, Iran and Zambia, which are at a distance of at least $\pm 13^o$ from the equator, have much stronger trends in what month cholera outbreaks typically occur. For Romania and Iran, which are both in the Northern Hemisphere, outbreaks typically occur between August and November. In Zambia, which is in the Southern Hemisphere, outbreaks occur most often between February and May. A larger value of the maximal bacterial growth rate r for countries closer to the equator, which also corresponds to a lower value of ξ_c and ϕ_c, could explain why the outbreaks in warmer countries occur less seasonally than in countries further away from the equator.

In Figures 3.11 and 3.12, the shedding parameter ξ is increased and the period of the limit cycles is measured (the other parameters are chosen to make limit cycles exist). In both Figures, it is the unstable E_1 which causes the cycles, but an unstable E^* can also be used. A trajectory is plotted for each set of parameters, and the last

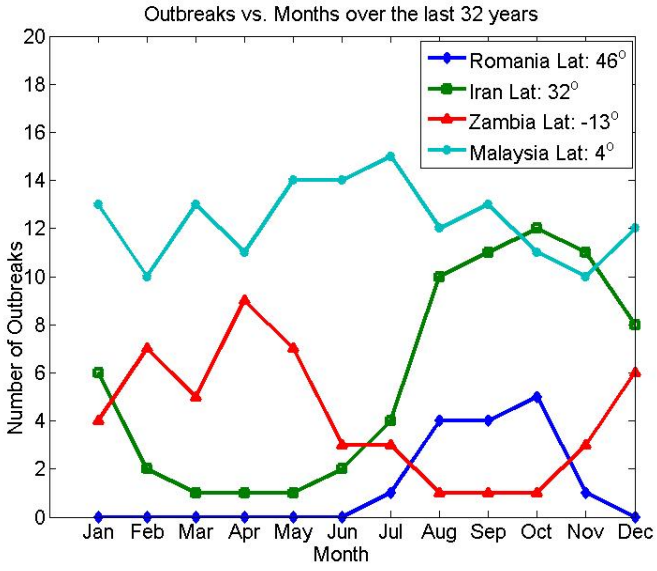

Figure 3.10: Sums of monthly cholera outbreaks over the last 32 years in countries at different latitudes, adapted from Emch et al. [18].

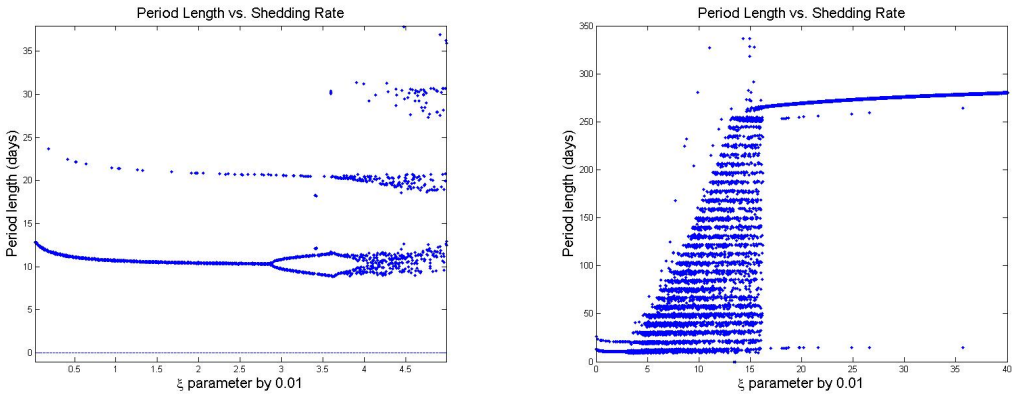

Figure 3.11: Chaotic behaviour with an r value (maximum bacterial growth rate) of 1. On the left is a zoomed in look at the pre-chaos interval of the graph on the right. The remaining parameters are $K = 1e6, \gamma = 0.021, K1 = 1/4K, \beta = 100, \delta = 1, \phi = 0, a = 0.1, C = 5e5, \mu = 0.1, H = 1e6$.

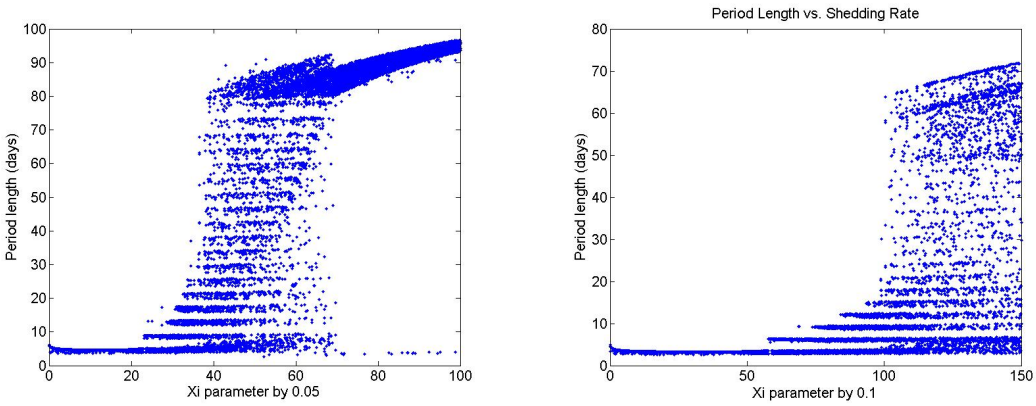

Figure 3.12: Chaotic behaviour with an r value (maximum bacterial growth rate) of 5. The remaining parameters are $K = 1e6, \gamma = 0.021, K1 = 1/4K, \beta = 100, \delta = 1, \phi = 0, a = 0.1, C = 5e5, \mu = 0.1, H = 1e6$.

10 local maximums are found numerically, and used to find the period of the cycle. There are certain intervals for ξ, however, where the trajectory is not periodic, but rapidly oscillates with varying amplitude and period. In these intervals the 'period', has many values for each ξ value. We will show below that these intervals produce chaotic behaviour.

In Figure 3.11, the maximal growth rate is comparatively low, and the chaotic interval occurs for lower values of ξ. When the ξ value is small, the limit cycles initially decrease in amplitude (not shown) as well as period length, as pictured. There is a certain value where period doubling first appears, and the populations go through cycles with the a similar period as previously, but alternating in height. When the shedding rate is increased further passed a threshold ξ_c, chaotic behaviour emerges. With a higher value of r, the chaotic window is shifted to the right as in Figure 3.12 where $r = 5$ on the left and $r = 10$ on the right, both being values within the range suggested in the literature [35]. Thus the same values of ξ and ϕ could cause chaotic or periodic trajectories for different values of r.

From Figure 3.11 and 3.12, the erratic behaviour of the period lengths suggest

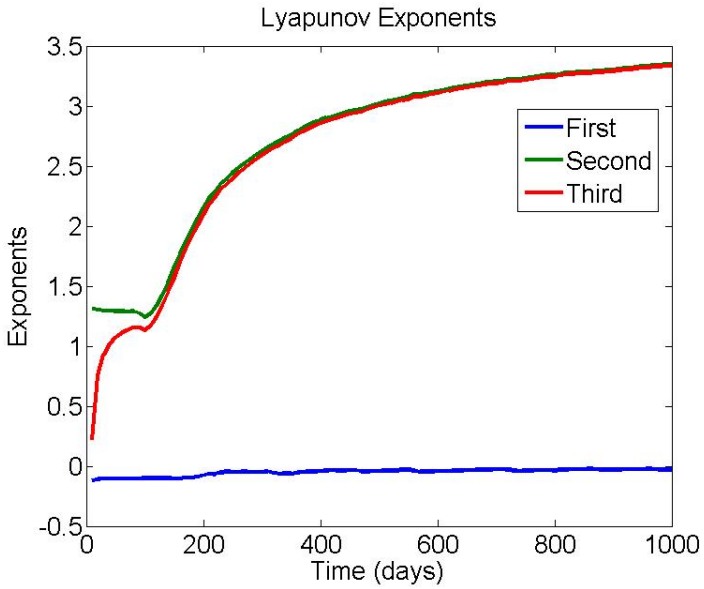

Figure 3.13: Lyapunov Exponents for (3.1). The shedding rate ξ was chosen from the interval [5,15] with all parameters as in Figure 3.11. The largest is positive which is enough to determine the trajectory is chaotic.

chaos, which can further be confirmed by looking at the trajectories. If the ξ value is taken from this erratic interval (about (3.6-16) in Figure 3.11) the trajectories rapidly oscillate with varying period and amplitude as time increases, lacking any clear pattern. This however is not enough to determine if the behaviour is chaotic: we should consider the Lyapunov Exponents. When there is chaos, trajectories with very close starting points will not remain close together as time is increased. In Figure 3.13, we see that, due to the positivity of the largest Lyapunov exponent, the behaviour is in fact chaotic.

3.G Discussion

We have presented a model, the iSIBP model, which is an alteration of the one in Jensen et al. [35]. This model explicitly includes the dynamics of bacteriophage

and bacteria and also contains a new indirect infection term which accounts for a minimum infectious dose of the pathogen *V.cholerae*. Unlike Jensen et al. [35] we focused on the existence of stable limit cycles, in order to account for the periodicity observed in outbreaks of cholera in endemic areas. As these cycles exist in the absence of human contribution to the bacteria and phage levels, and because the bacteria cycles peak before the human cycles when they exist in both systems, we conclude that it is the bacteria and phage which are driving the cycles, and not the reverse situation. If the minimum infectious dose was less than the carrying capacity of the bacteria, we observed that the bacteria cycles usually failed to surpass the minimum infectious dose, so there were no new infections and the system was disease free. However, if the natural carrying capacity was sufficiently larger than the minimum infectious dose, these cycles were able to enter the human population, which highlights the importance of understanding the relationship between the two. Additionally, if the phage levels could be enhanced in some way to keep the bacteria below this minimum infectious dose, then the cycles would remain in the bacteria and phage system alone. This idea links back to the 1930s when the use of injections of bacteriophage was explored as a treatment of cholera by limiting *V.cholerae* levels within the human host [4, 60].

Additionally, a chaotic region in the parameter space was identified. The existence of chaotic behaviour could explain the lack of clear periodicity in some endemic areas, with seasonal or other factors increasing the height of these chaotic peaks annually or biannually and creating a pseudo-periodic pattern. The exact role of these external factors would be difficult to determine, given the sensitivity of such a system. As the existence of this chaotic parameter region can be positively correlated with the proliferation rate of *V.cholerae* and overall climate, it could also explain the unpredictable nature of outbreaks in countries nearer the equator.

Future work on the iSIBP model could be to explicitly include the role of infection-

derived immunity through the use of a recovered class, even though immunity is somewhat accounted for in the value of the minimum infectious dose. Exact conditions for the existence of limit cycles would be valuable as well as a definitive relationship between the amplitude and period of the cycles to other parameters in the system. This would be useful in establishing useful connections between simulations and the data. Furthermore, including a second disease-causing serogroup of *V.cholerae* would increase the realism of the model for use in regions where outbreaks caused by serogroups O1 and O139 occur simultaneously.

Chapter 4

Discussion and Further Directions

4.A Discussion

In this thesis, two models for cholera dynamics were presented that utilized a new infection term specifically suited to indirectly transmitted diseases. The complicated life cycle of *Vibrio cholerae*, the causative agent of cholera, merits an explicit consideration of its natural aquatic environment when considering the epidemiology of the disease. The relationship between the minimum infectious dose, which is at the heart of the indirect infection term, and the natural carrying capacity of the bacteria in its aquatic environment, is demonstrated to be of the utmost importance. Mathematical and numerical investigations have revealed a number of biologically and mathematically significant results.

Investigation of the iSIR model reveals the existence of globally stable endemic and disease-free equilibria, determined through the relationship between the minimum infectious dose, c, the carrying capacity of the bacteria, K, and the shedding rate ξ. Should the average health and immune system capabilities of the population

be sufficient to tolerate bacterially contaminated water, and the shedding rate be sufficiently small, the human and bacteria populations will exist independently of each other. This case reflects both interepidemic periods where cholera outbreaks are common, and also the situation in regions where cholera outbreaks are not experienced. Should however the carrying capacity be sufficiently high (enough to overwhelm the average immune response of the human population), an endemic steady state will exist that can be globally stable. If this situation is only temporary, the iSIR model can thus account for isolated outbreaks of cholera, and if it persists, the model is suitable for regions where cholera cases are constant occurrences.

Sensitivity analyses suggest the effectiveness of reducing the carrying capacity K to lessen the severity of cholera outbreaks, when they occur, and this reduction was found to be more influential than simply decreasing human contamination of the water supply alone. This raises an interesting point for discussions of disease control in that alternative measures of outbreak reduction that do not necessarily restrict access to the water supply should also be considered.

The existence of stable bacteria- and phage-driven limit cycles in the iSIBP model demonstrates the importance of bacteriophage to cholera outbreaks. These cycles can exist exclusively in the bacteria and phage system without causing infections, as is likely the case in interepidemic times. It is only when the bacteria cycles cross the minimum infectious dose threshold that infections are caused and the cycles enter the human population as well. It appears to be necessary that the carrying capacity be greater than the MID in order for this to occur, again highlighting the importance in understanding the relationship between the two quantities. Further, these cycles can be annual or biannual in their period length, matching the observed dynamics of cholera in different regions. This would provide support for disease control measures designed to enhance phage levels in some way in order to keep the bacteria levels below this minimum infectious dose threshold.

A chaotic region in the parameter space of the iSIBP model could explain the differences in the interannual patterns of outbreaks of cholera in some endemic areas, and the lack of any sort of annual pattern in other areas. The sensitivity of a system with chaotic behaviour also accounts for the difficulty in definitely determining the role of seasonal factors, which has been an ongoing problem in the study of cholera epidemiology.

4.B Further Questions

Given the importance of the ordering of c and K to the disease dynamics, it is crucial to experimentally find more accurate values for these quantities. Seasonal parameter values could be included into the iSIR model in order to increase the length of the time interval that the system can represent. Similarly, relaxing the assumption of permanent immunity to temporary immunity through an explicit delay term, or some simple route from the recovered category back to the susceptible one, would also make the model more realistic and extend the time interval it could be used to represent.

Besides the obvious refinement of the local stability analysis, the addition of a recovered category to the iSIBP model to explicitly include some form of disease derived-immunity is a first step in making the model more useful. The minimum infectious dose implicitly incorporates an idea of immunity, but does so in a nondynamic way. Including a second serogroup of *V.cholerae* would greatly complicate the system with the required addition of at least one new compartment, but could prove useful in simulating outbreaks where both serogroups are simultaneously active. Alternate forms of phage predation could also be included, as when bacterial cells are not destroyed outright in the creation of new phage cells, but instead infected and left alive to less rapidly produce more phage. With a higher dimensional system, we

can expect more mathematically complicated dynamics that could possibly reveal new insights into the epidemiology.

Bibliography

[1] Abd H, A Weintraub, and G Sandstrom. Intracellular survival and replication of *Vibrio cholerae* O139 in aquatic free-living amoebae. Environ. Microbiol. 7, 1003–1008, 2005.

[2] Alam M, NA Hasan, A Sadique, NA Bhuiyan, KU Ahmed, S Nusrin, GB Nair, AK Siddique, RB Sack, DA Sack, A Huq, and RR Colwell. Seasonal Cholera Caused by *Vibrio cholerae* Serogroups O1 and O139 in the Coastal Aquatic Environment of Bangladesh. Appl. Environ. Microbiol. 72(6): 4096–4104, 2006.

[3] Alam M, M Sultana, GB Nair, AK Siddique, NA Hasan, RB Sack, DA Sack, KU Ahmed, A Sadique, H Watanabe, CJ Grim, A Huq and RR Colwell. Viable but nonculturable *Vibrio cholerae* O1 in biofilms in the aquatic environment and their role in cholera transmission. Proc. Natl Acad. Sci. USA 104, 17801–17806, 2007.

[4] Asheshov I and Lahiri MN. The treatment of cholera with bacteriophage. Ind. Med. Gaz. 66:179–184, 1931.

[5] Baker RM, FL Singleton, and MA Hood. Effects of nutrient deprivation on Vibrio cholerae. Appl. Environ. Microbiol. 46:930-940, 1983.

[6] Basu A, P Garg, S Datta, S Chakraborty, T Bhattacharya, A Khan, T Ramamurthy, SK Bhattacharya, S Yamasaki, Y Takeda, and GB Nair. *Vibrio cholerae* O139 in Calcutta, 1992-1998: Incidence, antibiograms, and genotypes. Emerg. Infect. Dis. 6:139-148, 2000.

[7] Bertuzzo E, S Azaele, A Maritan, M Gatto, I Rodriguez-Iturbe, and A Rinaldo. On the space-time evolution of a cholera epidemic. Water Resources Research, Vol.44, W01424, 8 pp.,doi:10.1029/2007WR006211, 2008.

[8] Bouma MJ and M Pascual. Seasonal and interannual cycles of endemic cholera in Bengal 1891-1940 in relation to climate and geography. Hydrobiologia 460: 147–156, 2001.

[9] Capasso V and SL Paveri-Fontana. A mathematical model for the 1973 cholera epidemic in the European Mediterranean region. Rev. Epidemiol. Sante Publique. 27(2):121-32,1979.

[10] Cash, R.A., S.I. Music, J.P. Libonati, M.J. Snyder, R.P. Wenzel, and R.B. Hornick. Response of man to infection with *Vibrio cholerae*. I. Clinical., serologic, and bacteriologic responses to a known inoculum. J. Infect. Dis. 129:45-52, 1974.

[11] Chitsulo L, D Engles, A Montresor, and L Savioli. The global status of schistosomiasis and its control. Acta Trop. 77: 41–51, 2000.

[12] Cholera Working Group, ICDRRB. Large epidemic of cholera like disase in Bangladesh caused by *Vibrio cholerae* O139 synonym Bengal. Lancet. 342:387-390, 1993.

[13] Codeço CT. 2001. Endemic and epidemic dynamics of cholera: The role of the aquatic resevoir BMC Infect. Dis. 1(1):1, 2001.

[14] Colwell RR, J Kaper, and SW Joseph. *Vibrio cholerae*, *Vibrio parahaemolyticus*, and other vibrios: occurrence and distribution in Chesapeake Bay. Science. 198: 394-396, 1977.

[15] Colwell RR, PR Brayton, DJ Grimes, DB Roszak, SA Huq, and LM Palmer. Viable but non-culturable *Vibrio cholerae* and related pathogens in the environment: implications for release of genetically engineered microorganisms. Nature Biotech. 3: 817–820, 1985.

[16] Colwell RR, and A Huq. Environmental reservoir of *Vibrio cholerae*. The causative agent of cholera. Ann. N. Y. Acad. Sci. 740:44– 54.154, 1994.

[17] Colwell RR, P Brayton, D Herrington, B Tall, A Huq, and MM Levine. Viable but nonculturable *Vibrio cholerae* O1 revert to a cultivable state in the human intestine. World J. Microbiol. Biotechnol. 12: 28-31, 1996.

[18] Emch M, Feldacker C, Islam M S, Ali M. Seasonality of cholera from 1974 to 2005: a review of global patterns. International Journal of Health Geographics 2008, 7:31 doi:10.1186/1476-072X-7-31

[19] Estes MK, EL Palmer, and JF Obijeski. Rotavirus: a review. Curr. Top. Microbiol. Immunol. 105: 123–184, 1983.

[20] Faruque SM, MJ Albert, and JJ Mekalanos. Epidemiology, genetics, and ecology of toxigenic *Vibrio cholerae*. Microbiol. Mol. Biol. Rev. 62:1301-1314, 1998.

[21] Faruque SM, IB Naser, MJ Islam, ASG Faruque, AN Ghosh, GB Nair, DA Sack, and JJ Mekalanos. Seasonal epidemics of cholera inversely correlate with the prevalence of environmental cholera phages. PNAS 102(5): 1702-1707, 2005.

[22] Faruque SM, MJ Islam, QS Ahmad, ASG Faruque, DA Sack, GB Nair, and JJ Mekalanos. Self-limiting nature of seasonal cholera epidemics: Role of host-mediated amplification of phage. PNAS 102(17): 6119-6124, 2005.

[23] Fields BS, RF Benson, RE Besser. *Legionella* and legionnaires' disease: 25 years of investigation. Clin. Microbiol. Rev. 15(3): 506–526, 2002.

[24] Franco A, AD Fix, A Prada, E Paredes, JC Palomino, AC Wright, JA Johnson, R McCarter, H Guerra, and JG Morris. Cholera in Lima, Peru correlates with prior isolation of *Vibrio cholerae* from the environment. Am. J. Epidemiol. 146(12):1067–1075, 1997.

[25] Glass RI, S Becker, MI Huq, BJ Stoll, MU Khan, MH Merson,JV Lee, and RE Black, 1982. Endemic cholera in rural Bangladesh. 1966-1980. Am. J. Epidemiol. 116(6): 959-970, 1982.

[26] Guckert JB, MA Hood, and DC White. Phospholipid ester-linked fatty acid profile changes during nutrient deprivation of Vibrio cholerae: increases in the translcis ratio and proportions of cyclopropyl fatty acids. Appl. Environ. Microbiol. 52(4):794-801, 1986.

[27] Halpern M,YB Broza, S Mittler, E Arakawa, and M Broza. Chironomid egg masses as a natural reservoir of *Vibrio cholerae* non-O1 and non-O139 in freshwater habitats. Microb. Ecol. 47(4): 341–349, 2004.

[28] Hartley DM, Morris JG Jr, Smith DL. Hyperinfectivity: A critical element in the ability of V. cholerae to cause epidemics? PLoS Med 3(1): e7, 2006.

[29] Hood MA, JB Guckert, DC White, and F Deck. Effect of nutrient deprivation on lipid, carbohydrate, DNA, RNA, and protein levels in Vibrio cholerae. Appl. Environ. Microbiol. 52(4):788-793, 1986.

[30] Hornick RB, SI Music, and R Wenzel. The Broad Street pump revisited: response of volunteers to ingested cholera Vibrio. Bull. N. Y. Acad. Med. 47(10):1181–1191, 1971.

[31] Huq A, RR Colwell, R Rahman, A Ali, MAR Chowdhury,l S Pareveen, DA Sack, and E Ruseek-Cohen. Detection of *Vibrio cholerae* 01 in the Aquatic Environment by Fluorescent-Monoclonal Antibody and Culture Methods Appl. Environ. Microbiol. 1990, 56(8):2370, 1990.

[32] Huq A, ING Rivera, and RR Colwell. Epidemiological significance of viable but nonculturable microorganisms. In: Colwell RR and Grimes DJ (Eds). *Nonculturable microorganisms in the environment*. Washington, DC: American Society of Microbiology Press, 2000.

[33] Islam MS, BS Drasar, and RB Sack. The aquatic environment as a reservoir of *Vibrio cholerae*: a review. J Diarrhoeal Dis Res 12(2): 87–96, 1993.

[34] Islam MS, BS Drasar, and B Sack. Probable Role of Blue-green Algae in Maintaining Endemicity and Seasonality of Cholera in Bangladesh: a Hypothesis. J Diarrhoeal Dis Res, 12(4): 245-256, 1994

[35] Jensen MA, SM Faruque, JJ Mekalanos, and BR Levin. Modeling the role of bacteriophage in the control of cholera outbreaks. PNAS 103(12): 4652-4657, 2006.

[36] Joh RI, H Wang, H Weiss, JS Weitz. Dynamics of Indirectly Transmitted Infectious Diseases with Immunological Threshold. Bull Math Biol 71: 845-862, 2009

[37] Johnson JA, CA Salles, P Panigrahi, MJ Albert, AC Wright, RJ Johnson, and JG Morris, Jr. *Vibrio cholerae* O139 Synonym Bengal is closely related to *Vibrio cholerae* El Tor but has important differences. Infect. Immun. 62(5):2108-2110, 1994.

[38] Kaper JB, JG Morris Jr, and MM Levine. Cholera. Clin. Microbiol. Rev. 8(1): 48–86, 1995.

[39] Kermack WO and AG McKendrick. Contributions to the Mathematical Theory of Epidemics - I. Proceedings of the Royal Society, 115A, 1927.

[40] Koelle K, X Rodo, M Pascual, M Yunus, and G Mostafa. Refractory periods and climate forcing in cholera dynamics. Nature, 436:696-700, DOI:10.1038/nature03820, 2005.

[41] Levine MM, RE Black, ML Clements, DR Nalin, L Cisneros, RA Finkelstein. Volunteer studies in development of vaccines against cholera and enterotoxigenic *escherichia coli*: a review. In: Holme, T., Holmgren, J., Merson, M.H., Mollby, R. (Eds.), Acute Enteric Infections in Children. New Prospects for Treatment and Prevention, pp. 443–459. Elsevier/North-Holland Biomedical Press, Amsterdam, 1981.

[42] Li MY, JS Muldowney. Global stability for the SEIR model in epidemiology. Math. Biosci. 125(2), 155-164, 1995.

[43] Li MY, L Wang. Global stability in some SEIR epidemic models. IMA Math. Appl, 126, 295-311, Springer, New York, 2000.

[44] Lipp EK, A Huq, and RR Colwell. 2002. Effects of Global Climate on Infectious Disease: the Cholera Model. Clin. Microbiol. Rev. 15(4):757-770, 2002. DOI: 10.1128/CMR.15.4.757-770.2002.

[45] Lobitz B, L Beck, A Huq, B Wood, G Fuchs, ASG Faruque and R Colwell. Climate and infectious disease: Use of remote sensing for detection of *Vibrio cholerae* by indirect measurement. PNAS, 97(4): 1438-1443, 2000.

[46] Longini IM Jr et al. Epidemic and endemic cholera trends over a 33-year period in Bangladesh. J. Infect. Dis. 186(2): 246–251, 2002.

[47] Madico G, W Checkley, RH Gilman, N Bravo, L Cabrera, M Calderon, and A Ceballos. Active surveillance for *Vibrio cholerae* O1 and vibriophages in

sewage water as a potential tool to predict cholera outbreaks. J. Clin. Microbiol. 34(12):2968–2972, 1996.

[48] McCluskey CC and P van den Driessche. Global Analysis of Two Tuberculosis Models. Journal of Dynamics and Differential Equations, 16(1):139-166, 2004.

[49] Merrell DS, SM Butler, F Qadri, NA Dolganov, A Alam, MB Cohen, SB Calderwood, GK Schoolnik, and A Camilli. Host-induced epidemic spread of the cholera bacterium Nature, 417(6889): 642–645. doi:10.1038/nature00778, 2002.

[50] Mukandavire Z, S Liao, J Wang, H Gaff, DL Smith, JG Morris Jr. Estimating the reproductive numbers for the 2008-2009 cholera outbreaks in Zimbabwe. PNAS, 108(21): 8767-8772, 2011.

[51] Mukhopadhyay AK, S Garg, R Mitra, A Basu, K Rajendran, D Dutta, SK Bhattacharya, T Shimada, T Takeda, and Y Takeda. Temporal shifts in traits of Vibrio cholerae strains isolated from hospitalized patients in Calcutta: a 3-year (1993-1995) analysis. J. Clin. Microbiol. 34: 2537-2543, 1996.

[52] Murphy KM, P Travers, M Walport. Janeway's Immunobiology, 7th edn. Garland Science, 2007.

[53] Murray J, DA McFarland, and RJ Waldman. Cost-effectiveness of oral cholera vaccine in a stable refugee population at risk for epidemic cholera and in a population with endemic cholera. Bulletin of the World Health Organization, 76(4): 343-352, 1998.

[54] Nelson EJ, A Chowdhury, J Flynn, S Schild, L Bourassa, Y Shao, RC LaRocque, SB Calderwood, F Qadri, A Camilli. Transmission of *Vibrio cholerae* is antagonized by lytic phage and entry into the aquatic environment. PLoS Pathog. 4(10), e1000187 ,2008.

[55] Nelson EJ, JB Harris, JG Morris Jr, SB Calderwood and A Camilli. Cholera transmission: the host, pathogen and bacteriophage dynamic. Nature Reviews. 7: 693-702, 2009.

[56] Norris HT. Cholera, p. 160–188. In D. Barua and W. Burrows (eds.), The pathology of cholera. The W. B. Saunders Co., Philadelphia, Pa. 1974.

[57] Oliver JD, and WF Stringer. Lipid composition of psychrophilic marine Vibrio sp. during starvation-induced morphogenesis. Appl. Environ. Microbiol. 47(3):461-466, 1984.

[58] Oliver JD. The viable but nonculturable state in bacteria. J. Microbiol. 43(S): 93–100, 2005.

[59] Pacini, F. 1854. Observazioni microscopiche e deduzioni patologiche sul cholera asiatico. Gaz. Med. Ital. 6:405–412, 1854.

[60] Pasricha CL, de Monte AJH, and O'Flynn EG. Bacteriophage in the treatment of cholera. Ind. Med. Gaz. 71: 61–68, 1936.

[61] Pascual M, X Rodo, S Ellner, R Colwell, and M Bouma. Cholera Dynamics and El Nino-Southern Oscillation. Science, 289(5485): 1766–1769,2000.

[62] Rodo X, M Pascual, G Fuchs and ASG Faruque. ENSO and cholera: A nonstationary link related to climate change? PNAS, 99(20): 12901-12906, 2002.

[63] Rose JB. Environmental ecology of *crptosporidium* and public health implications. Annu. Rev. Public Health 18: 135–161, 1997.

[64] Rosenbert CE. The cholera years. The University of Chicago Press, Chicago, Ill., 1962.

[65] Sack DA, Sack RB and Chaignat, CL. Getting serious about cholera. N. Engl. J. Med. 355: 649–651, 2006.

[66] Sanchez LA. Dynamics of the modified Michaelis-Menten system. J. Math. Anal. Appl. 317(1): 71-79, 2006.

[67] Shukla BN, DV Singh, and SC Sanyal. Attachment of non-culturable toxigenic *Vibrio cholerae* O1 and non-O1 and *Aeromonas* spp. to the aquatic arthropod *Gerris spinolae* and plants in the River Ganga, Varanasi. FEMS Immunol. Med. Microbiol. 12(2): 113–120, 1995.

[68] Siddique AK, K Akram, K Zaman, P Mutsuddy, A Eusof, and RB Sack. *Vibrio cholerae* O139: how great is the threat of a pandemic? Trop. Med. Int. Health. 1:393-398, 1996.

[69] Singleton FL, RW Atwell, MS Jangi, and RR Colwell. Effects of temperature and salinity on *Vibrio cholerae* growth. Appl. Environ. Microbiol. 44(5): 1047–1058, 1982.

[70] Smith H. Monotone Dynamcial Systems: An Introduction to the Theory of Competitive and Cooperative Systems. Math. Surveys Monogr. 41, AMS, Providence, RI, 1995.

[71] Suttle, CA. Viruses in the sea. Nature, 437:356–361, 2005.

[72] Tamplin ML, AL Gauzens, A Huq, DA Sack, and RR Colwell. Attachment of *Vibrio cholerae* serogroup O1 to zooplankton and phytoplankton of Bangladesh waters. Appl. Environ. Microbiol. 56(6):1977, 1990.

[73] Tian JP and Wang J. Global stability for cholera epidemic models Mathematical Biosciences 232: 31–41, 2011.

[74] Tien JH, DJD Earn. Multiple Transmission Pathways and Disease Dynamics in a Waterborne Pathogen Mode. Bulletin of Mathematical Biology, 72: 1506-1533, 2010

[75] Wachsmuth IK, Blake PA, and Olsvik Ø (eds) in Vibrio cholerae and Cholera: Molecular to Global Perspectives. ASM, Washington DC,1994.

[76] Waldor MK, and JJ Mekalanos. Lysogenic conversion by a filamentous phage encoding cholera toxin. Science 272(5270):1910–1914, 1996.

[77] Weintraub A, G Widmalm, P Jansson, M Jansson, K Hultenby, and MJ Albert. *Vibrio cholerae* O139 Bengal possesses a capsular polysaccharide which may confer increased virulence. Microb. Path. 16:235- 241, 1994.

[78] Wolfe MS. Giardiasis. Clin. Microbiol. 5(1): 93–100, 1992.

[79] Wolfe ND, CP Dunovan, and J Diamond. Origins of major human infectious diseases. Nature 447: 279–283, 2007.

[80] WHO Scientific Working Group. 1980. Cholera and other Vibrio-associated diarrhoeas. Bull. W. H. O. 58:353–374.

[81] Zahid MSH, SMN Udden, ASG Faruque, SB Calderwood, JJ Mekalanos, and SM Faruque. Effect of phage on the infectivity of *Vibrio cholerae* and emergence of genetic variants. Infect. Immun. 76: 5266–5273, 2008.

[82] Zaki SR, PW Greer, LM Coffield, CS Goldsmith, KB Nolte, K Foucar, RM Feddersen, RE Zumwalt, GL Miller, AS Khan, PE Rollin, TG Ksiazek, ST Nichol, BWJ Mahy and CJ Peters. Hantavirus pulmonary syndrome—pathogenesis of an emerging infectious disease. Am. J. Pathol. 146: 552–579, 1995.